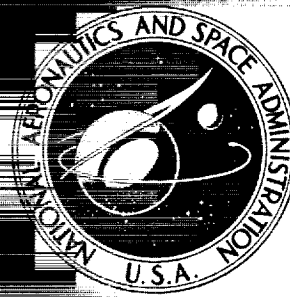


N72-27991

**NASA CONTRACTOR
REPORT**



NASA CR-2067

NASA CR-2067

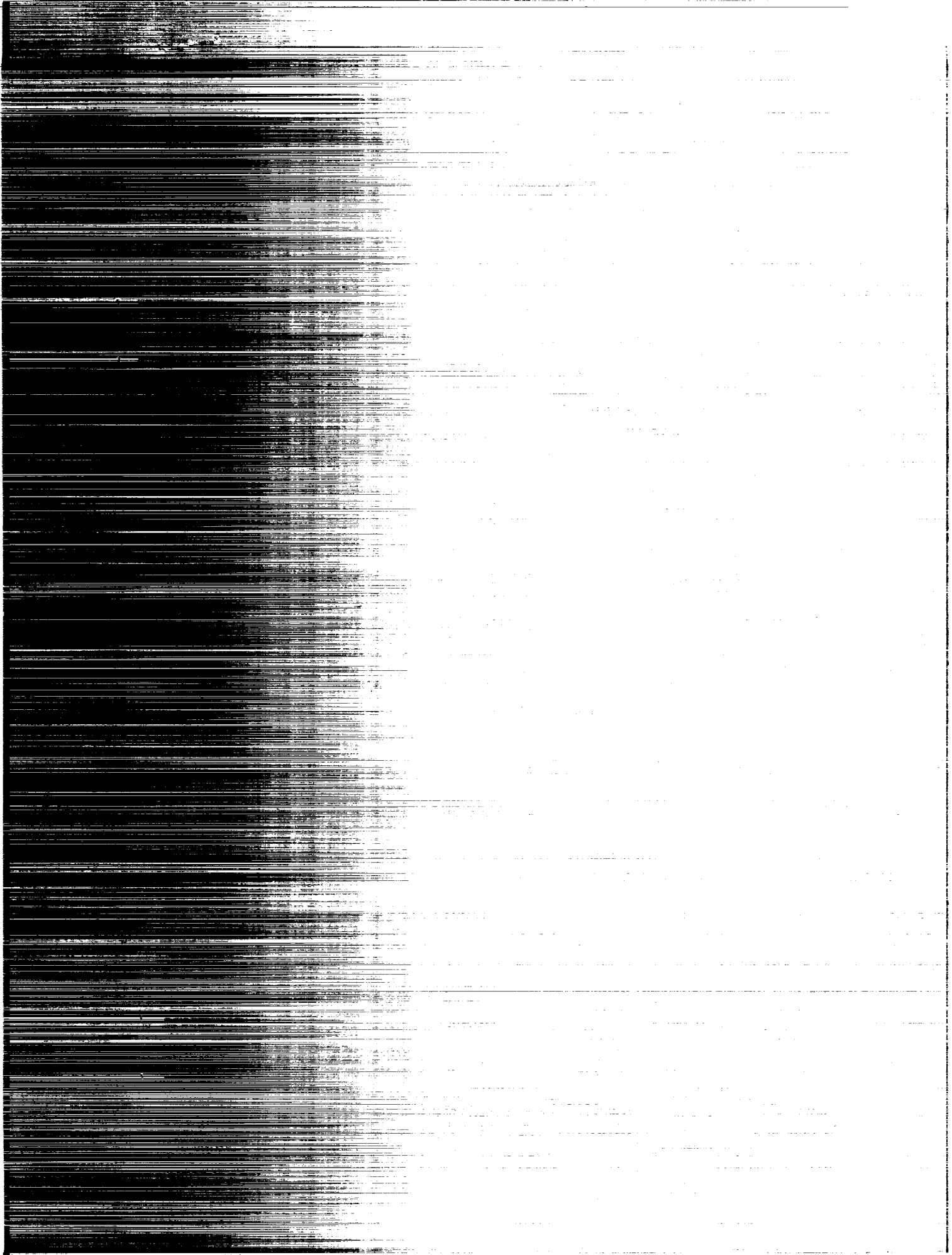
**CASE FILE
COPY**

**ANALYSIS AND TESTING OF
HIGH ENTRAINMENT SINGLE-NOZZLE
JET PUMPS WITH
VARIABLE-AREA MIXING TUBES**

*by Kenneth E. Hickman, Philip G. Hill,
and Gerald B. Gilbert*

*Prepared by
DYNATECH R/D COMPANY
Cambridge, Mass.
for Ames Research Center*

NATIONAL AERONAUTICS AND SPACE ADMINISTRATION • WASHINGTON, D. C. • JUNE 1972



1. Report No. NASA CR-2067		2. Government Accession No.		3. Recipient's Catalog No.	
4. Title and Subtitle Analysis and Testing of High Entrainment Single-Nozzle Jet Pumps with Variable-Area Mixing Tubes"				5. Report Date June 1972	
				6. Performing Organization Code	
7. Author(s) Kenneth E. Hickman, Philip G. Hill, and Gerald B. Gilbert				8. Performing Organization Report No.	
				10. Work Unit No.	
9. Performing Organization Name and Address Dynatech R/D Company Cambridge, Massachusetts				11. Contract or Grant No. NAS 2-5845	
				13. Type of Report and Period Covered Contractor Report	
12. Sponsoring Agency Name and Address National Aeronautics & Space Administration Washington, D.C.				14. Sponsoring Agency Code	
15. Supplementary Notes					
16. Abstract <p>In this investigation, an analytical model was developed to predict the performance characteristics of axisymmetric single-nozzle jet pumps with variable area mixing tubes. The primary flow may be subsonic or supersonic. The computer program presented in this report uses integral techniques to calculate the velocity profiles and the wall static pressures that result from the mixing of the supersonic primary jet and the subsonic secondary flow.</p> <p>An experimental program was conducted to measure mixing tube wall static pressure variations, velocity profiles, and temperature profiles in a variable area mixing tube with a supersonic ($M = 2.72$) primary jet. Static pressure variations were measured at four different secondary flow rates. These test results were used to evaluate the analytical model. The analytical results compared well to the experimental data. Therefore, the analysis is believed to be ready for use to relate jet pump performance characteristics to mixing tube design.</p>					
17. Key Words (Suggested by Author(s)) jet-pump, ejector, compressible flow, supersonic nozzle, computer program				18. Distribution Statement UNCLASSIFIED-UNLIMITED	
19. Security Classif. (of this report) Unclassified		20. Security Classif. (of this page) Unclassified		21. No. of Pages 137	
				22. Price* 3.00	

TABLE OF CONTENTS

<u>Section</u>		
	SUMMARY	1
1.	INTRODUCTION	3
	1.1 Background	3
	1.2 Previous Work	3
	1.3 Objectives of This Investigation	5
2.	SYMBOLS	6
3.	ANALYSIS	9
	3.1 Purpose	9
	3.2 General Description of the Analytical Model	9
	3.3 Transition Zone Analysis	15
	3.4 Flow Analysis Upstream of Jet Attachment (Part 1)	22
	3.5 Flow Analysis Downstream of Jet Attachment (Part 2)	25
4.	TEST PROGRAM	29
	4.1 Test Arrangement	29
	4.2 Instrumentation and Data Reduction Procedures	32
	4.2.1 Instrumentation	32
	4.2.2 Data Reduction Procedures	32
	4.2.3 Suction Duct Losses	33
	4.3 Test Results	34
5.	COMPARISON OF ANALYTICAL AND EXPERIMENTAL RESULTS	37
	5.1 Mixing Tube Wall Static Pressure Variations	37
	5.2 Velocity and Temperature Profiles	38
6.	CONCLUSIONS	41
	APPENDIX A - Equations for the Flow	43
	A1 Upstream of Jet Attachment	43
	A2 Downstream of Jet Attachment	44

TABLE OF CONTENTS (Continued)

Section

APPENDIX B - The Computer Program	77
B1 General Description	77
B2 Input Data Format	79
B3 Listing	85
B4 Typical Sets of Input and Output Data	112
REFERENCES	116
TABLES	117
FIGURES	121

ANALYSIS AND TESTING OF HIGH ENTRAINMENT SINGLE-NOZZLE JET PUMPS WITH VARIABLE-AREA MIXING TUBES

By Kenneth E. Hickman, Philip G. Hill, and Gerald B. Gilbert

SUMMARY

The use of jet pumps is of increasing interest for boundary layer control or control force augmentation in V/STOL aircraft. In typical applications, a small mass flow of primary air at pressures up to 400 psia can be used to entrain a much larger mass flow of secondary air at ambient conditions. The primary nozzle flow is supersonic while the secondary flow is subsonic. The jet pump system design objectives may be maximum entrainment, maximum thrust augmentation, or some combination of the two. Little information is available in the literature to guide the designer of jet pumps for such applications.

In this investigation, an analytical model was developed to predict the performance characteristics of axisymmetric single-nozzle jet pumps with variable area mixing tubes. The primary flow may be subsonic or supersonic. In the region upstream of the section where the central jet reaches the wall, the analysis is based upon the hypothesis that the mixing phenomenon is fundamentally similar to the mixing of a free turbulent jet with the surrounding fluid. The eddy viscosity values used in the analysis are adjusted to allow for the effect of the duct walls on the mixing process. Integral techniques are employed in a computer program to solve the continuity, momentum, and energy equations to determine the variation of flow properties along the mixing tube. Wall boundary layer effects are included in the analysis.

Downstream of the section where the jet reaches the wall, the velocity profile is assumed to approach asymptotically the profile for fully developed turbulent flow in a pipe. Viscous forces are present throughout the flow so no distinct boundary layer analysis is employed. The eddy viscosity is assumed to approach the fully-developed flow value asymptotically. Wall friction forces are calculated from the fully-developed pipe flow friction coefficient. Integral techniques are employed as before to determine the variation of flow properties along the mixing tube.

An experimental program was conducted to measure mixing tube wall static pressure variations, velocity profiles, and temperature profiles in a variable area mixing tube with a supersonic ($M = 2.72$) primary jet. Static pressure variations were measured at four different secondary flow rates. These test results were used to evaluate the analytical model.

The analytical model yields good predictions of wall static pressure distributions, velocity profiles, and temperature profiles along the mixing tube. Therefore, the analysis is believed to be ready for use to relate jet pump performance characteristics to mixing tube design.

Section 1

INTRODUCTION

1.1 Background

A number of STOL aircraft boundary layer control systems now under consideration employ jet pumps to entrain large flows of secondary air and direct them over deflected flaps to achieve lift augmentation. Some proposed VTOL aircraft systems also employ jet pumps for direct lift or control force augmentation. The primary, high-pressure flow for the jet pumps can be provided either by bleed from main engine compressors or by an auxiliary power unit.

The use of jet pumps as primary components of V/STOL aircraft systems makes necessary the development of new design techniques for these devices. In aircraft applications, it is essential to be able to minimize the size of jet pumps for particular primary and secondary flow conditions. Jet pumps for boundary layer control systems generally must have high entrainment ratios--the secondary flow often must be over 10 times larger than the primary flow--but pressure rises of only a few psf are needed. The primary flow may be highly supersonic. Thus, design procedures which have been developed in the past for the more conventional low-entrainment, high-pressure rise industrial jet pumps are not suitable for V/STOL aircraft jet pump design.

1.2 Previous Work

In an earlier program, Dynatech R/D Company carried out an analytical and experimental investigation of high-entrainment ratio air-to-air jet pumps for the Ames Research Center of NASA (reference 1). This investigation was limited to jet pumps with constant-diameter mixing tubes. An analytical procedure and a computer program were developed to predict the performance of such a jet pump over a range of operating conditions. The accuracy of the analysis was confirmed by comparing predicted performance to test results for a number

of multiple-nozzle jet pump configurations at different primary flow pressure and temperature levels. Procedures were demonstrated for matching a jet pump to its duct system for maximum entrainment or thrust augmentation.

The selection of the constant-diameter mixing tube configuration allowed considerable simplification of the analysis, design, and construction of the jet pump. However, it is unlikely that constant-area jet pumps give the best performance for all applications. Almost no information is available to indicate the extent of performance improvements which can be achieved with other mixing tube configurations.

A method for predicting the flow behavior in jet pumps with arbitrary mixing tube shapes and incompressible flows was reported by P.G. Hill (reference 2). The method is based upon the hypothesis that the mixing phenomenon in a jet pump has a fundamental similarity to the mixing of a free turbulent jet with the surrounding fluid. Therefore, as in a free jet, the turbulent Reynolds number--

$$Re_T = \frac{\text{jet velocity} \times \text{duct radius}}{\text{eddy viscosity}}$$

--will remain constant with distance as mixing occurs. This is a rather gross simplifying assumption but the resulting flow predictions are good. Static pressure variations and velocity profiles computed on this basis agreed well with test data for Helmbold's converging-diverging mixing tube. Once the static pressure distribution is known, the jet pump performance can be predicted without further difficulty.

The analytical methods of reference 2 are limited in application to incompressible flow in axisymmetric jet pumps having a single primary jet. These analytical methods must be modified to include compressible flow effects if the methods are to be useful for the designer of V/STOL aircraft jet pump systems.

1.3 Objectives of This Investigation

The specific objectives of this investigation are as follows:

- to develop an analytical procedure for predicting the performance of high-entrainment-ratio compressible flow jet pumps with arbitrary mixing tube geometry.
- to obtain test results with jet pumps having variable-area mixing tubes so that the analytical methods can be checked.

The analytical procedure is formulated to allow prediction of the performance of a particular jet pump nozzle and mixing tube combination over a range of primary and secondary flow conditions. To select the best jet pump design for a particular application, the analysis can be used to predict the performance for a number of different mixing tube shapes. Comparison of the performance characteristics will show which geometry is best. The off-design performance of the jet pump can be determined by using the same analytical procedures.

Section 2

SYMBOLS

A	area, ft ²
b	diameter of jet at which $U = U_0 + \frac{U_j}{2}$, ft
C _f	wall friction coefficient
C _w	nozzle flow coefficient
E	dimensionless eddy viscosity = $\frac{\epsilon}{UR}$
f ₀	free jet profile value = f ₀ (η); equation (1)
f ₂ (η)	velocity profile at the end of Part 1, equation (7)
g ₀	dimensional constant = 32.2, lbm-ft/lbf-sec ²
g ₂ (η)	auxiliary velocity profile, equation (7)
gg (η)	velocity profile for fully-developed flow in a pipe
H	boundary layer shape factor
k	specific heat ratio
K _L	suction duct loss coefficient
m	entrainment ratio = W ₀ /W ₁
n _g	number of equal-radial-increment annuli used in integral analyses, equation (36)
p	static pressure, lbf/ft ²
P	stagnation pressure, lbf/ft ²
P ₀₂	secondary flow stagnation pressure after correction for suction duct losses, lbf/ft ²
R	tube radius, ft
R ₀	radius at nozzle exit section, ft
R _g	gas constant x g ₀ , ft ² /sec ² -° R

Re_m	Reynolds number based on mean velocity; equation (50)
Re_T	turbulent Reynolds number
R_θ	momentum thickness Reynolds number
S_{oo}, S_{20}	parameters defined by equations (29) and (30)
T_o	stagnation temperature at any radius in mixing zone, ° R
T_{oj}	relative stagnation temperature at centerline of jet, ° R
T_{oo}	stagnation temperature of flow adjacent to the duct, ° R
ΔT_o	difference between stagnation temperature at any radius in the jet and the stagnation temperature of the surrounding flow, ° R
T	temperature ratio = T_{oj}/T_{oo}
U	velocity, ft/sec
U_c	velocity at centerline of jet, ft/sec
U_j	velocity at centerline of jet relative to U_o , ft/sec
U_{jo}	relative velocity at centerline of jet at end of transition section, ft/sec
U_{joo}	relative velocity at centerline of jet at beginning of transition section, ft/sec
U_o	velocity of outer stream, ft/sec
U_r	velocity ratio for transition zone = U_{jo}/U_{joo}
$V(J)$	terms in equation (37)
W_o	mass flow rate, secondary flow, lbm/sec
W_1	mass flow rate, primary flow, lbm/sec
$W(J,K)$	coefficient matrix; equation (37)
x	axial position along mixing tube, ft
x_{core}	length of the transition zone, ft

y	radius, ft
$Y(K)$	derivatives in equation (37)
γ	velocity profile shape parameter
δ	width of shear layer, ft
δ^*	boundary layer displacement thickness, ft
ϵ	eddy kinematic viscosity, ft ² /sec
η	dimensionless radius = y/δ or y/R
θ	boundary layer momentum thickness, ft
λ	velocity ratio U_o/U_j
ρ	density, lbm/ft ³
τ	shear stress, lbf/ft ²
ν	kinematic viscosity, ft ² /sec

Subscripts

∞	value at top-hat section
1	primary flow
core	dimension at end of transition zone
eff	effective radius or area of mixing tube
m	value at mean area of transition zone
noz	primary nozzle exit area
SD	suction duct upstream of mixing tube

Section 3

ANALYSIS

3.1 Purpose

The purpose of the analysis developed in this section is to predict the performance characteristics of compressible flow jet pumps with variable-area mixing tubes. The jet pumps may have supersonic or subsonic primary flow issuing from a single nozzle located along the axis of an axisymmetric cylindrical mixing tube. The secondary flow and the mixed flow downstream must remain subsonic. The primary and secondary flows are taken to be the same perfect gas.

A particular objective of the analysis is to predict the variation in static pressure along the length of the mixing tube. Knowledge of this pressure variation allows calculation of the thrust augmentation of the jet pump, an essential parameter for jet pump application studies.

3.2 General Description of the Analytical Model

The analysis is based upon the incompressible flow jet pump analytical model developed by Dr. P. G. Hill (reference 2). This analytical model, with its associated computer program, was modified in the present study to account for compressible flow effects. The formulation of the analytical model is described in this section. The computer program which is based upon the compressible flow model is described in Appendix B of this report.

The following initial assumptions are made for the analysis:

1. The primary and secondary flows are the same perfect gas.
2. No heat is transferred across the wall of the jet pump.

3. The jet pump consists of an axisymmetric, cylindrical, variable-area mixing tube with a single primary nozzle located along the axis.
4. The primary and secondary flow conditions and the nozzle geometry are assumed to be such that no normal shocks or moisture condensation shocks occur in the primary flow.
5. The secondary flow and the combined flows after mixing are assumed to remain subsonic throughout the mixing tube.
6. The velocity of the primary jet at the nozzle exit is greater than the velocity of the secondary flow.
7. The static pressure is constant across any section perpendicular to the axis of the jet pump.

Dr. Hill's analysis identifies three distinct flow regimes in a jet pump. These regimes are shown in figure 1; they may be described as follows:

Part 1 - A region in which the jet is approximately self-preserving and is immersed in a potential outer stream which may be accelerating or decelerating, depending on the shape of the duct and the rate of entrainment of mass into the jet.

Recirculation Zone - A possible region in which recirculation occurs, following a deceleration of the outer stream. At the beginning of this zone the "edge" of the jet has not yet diffused to the wall and the secondary fluid recirculates through the jet. The pressure gradient is generally observed to be negligible in this zone.

Part 2 - The region downstream of the point (fairly distinct in many cases) at which the jet attaches to the wall. An adverse pressure gradient is generally established but the relatively high shearing forces near the wall tend to accelerate the fluid against the pressure gradient. If there is a zone of recirculation, it is terminated in a short axial distance by these high shearing forces.

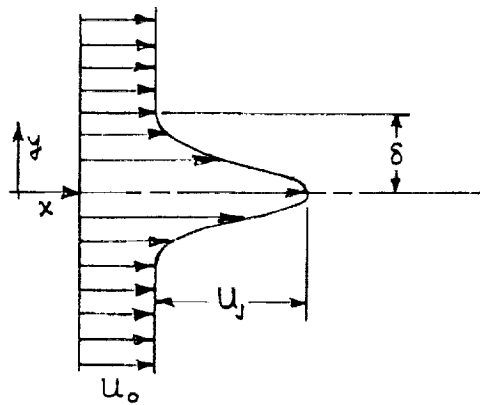
In addition to these three regions, there is a relatively short transition zone between the nozzle exit and the section at which a subsequently self-preserving velocity profile is attained.

In Part (1) the jet velocity profile can be approximated well by

$$\frac{U - U_o}{U_j} = f_o \left(\frac{y}{\delta} \right) \quad \text{at any } x \quad (1)$$

where

U	=	velocity at radius y
U_o	=	outer stream velocity
U_j	=	jet relative velocity at centerline
x	=	axial position along mixing tube
y	=	radius
δ	=	width of shear layer (see sketch)



Velocity Profile at Station x

The functional relationship $f_o(y/\delta)$ is determined quantitatively from velocity profiles measured in axisymmetric jets discharging into free space.

$$f_o(\eta) = 1.0004 - 0.0175\eta - 8.3821\eta^2 + 16.5806\eta^3 - 12.7877\eta^4 + 3.608\eta^5 \quad (2)$$

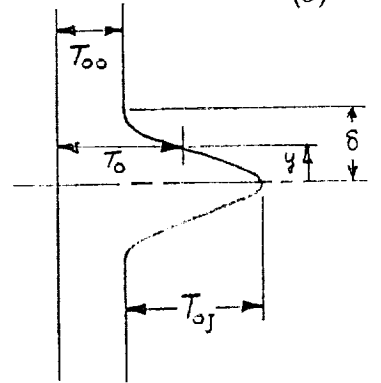
where $\eta = y/\delta$ (Part 1)

The same relationship holds in the recirculation zone but the axial pressure gradient in this region is assumed to be zero.

The relationship above is used to describe the velocity profile at a particular axial station in Part 1 of the mixing tube flow. The continuity, momentum, moment-of-momentum, energy, and boundary layer equations are used to determine the changes in U_j , U_o , δ , temperature, and pressure which occur from station to station along the mixing tube. To solve these equations, the temperature profile must be known so that the density variations across the section can be determined. Following Abramovich (reference 3), the stagnation temperature profile is taken to be the square-root of the velocity profile.

$$\frac{T_o - T_{oo}}{T_{oj}} = f_o^{1/2} \left(\frac{y}{\delta} \right) \quad (3)$$

where T_o = stagnation temperature at any radius in the mixing zone
 T_{oo} = stagnation temperature of surrounding secondary flow
 T_{oj} = relative stagnation temperature at center of jet



The solution of the moment-of-momentum equation requires shear stress values to be known as a function of radius. These values are obtained as follows:

$$\tau = \epsilon \rho \partial U / \partial y \quad (4)$$

where τ = shear stress
 ϵ = eddy kinematic viscosity,
 ρ = density

The value of the turbulent Reynolds number is assumed to remain constant across the flow at any axial station in Part 1. This allows calculation of the eddy viscosity from the following equation:

$$\epsilon = U_j \delta / \text{Re}_T \quad (5)$$

where Re_T = turbulent Reynolds number

At the beginning of Part 1, the jet mixing process is not significantly affected by the presence of the mixing tube walls. Therefore, the value $\text{Re}_{TF} = 147$, from incompressible free jet mixing tests, can be used. Further downstream in Part 1, as the jet approaches the walls, the mixing process is altered from a free jet to a free wake type of mixing. The change in the mixing process is accounted for by using the following equation to determine the eddy viscosity at any station in Part 1:

$$\epsilon = \frac{U_j \delta}{\text{Re}_{TF}} \left[1 + \frac{3}{2} (1 - e^{-1.1\lambda}) \right] \quad (6)$$

where $\lambda = \frac{U_o}{U_j}$

Boundary layer growth must be taken into account in order to predict wall static pressure variations with accuracy. Boundary layer displacement thickness variations are obtained in the analysis by using the methods of Moses (reference 4). The equations used are described in Section 3.4 in this report.

In Part 2, the jet has reached the wall. The free jet mixing velocity profile is no longer appropriate. Instead, the velocity profile is assumed to follow the relationship:

$$U/U_c = f_2(\eta) + \gamma g_2(\eta) \quad (7)$$

where U_c = jet velocity at centerline

$f_2(\eta)$ = velocity profile at the end of Part 1

$\eta = y/R$

R = mixing tube radius at the axial position considered

$\gamma = \gamma(x)$ adjustable shape parameter

$g_2(\eta)$ = auxiliary velocity profile

At the beginning of Part 2, γ is set equal to zero and the velocity profile matches the velocity profile at the end of Part 1. The auxiliary profile $g_2(\eta)$ is chosen so that, as γ approaches 1.0, the U/U_c velocity profile approaches the profile for fully-developed flow in a pipe.

$$g_2(\eta) = gg(\eta) - f_2(\eta) \quad (8)$$

where $gg(\eta)$ = velocity profile for fully-developed flow in a pipe

No boundary layer calculations are made in Part 2. Viscous forces are present throughout the flow so no distinct boundary layer exists. Wall friction forces are calculated from turbulent pipe flow correlations.

The continuity, momentum, moment-of-momentum, and energy equations are used to determine the changes in U_c , γ , temperature, and pressure which occur with distance along the mixing tube in Part 2. The solution of the moment-of-momentum equation requires determination of the eddy viscosity as a function of radius and axial position. Because the flow in Part 2 becomes asymptotic to fully-developed pipe flow, the eddy viscosity must be asymptotic to the fully-developed flow value.

$$\tau / \tau_{\text{wall}} = y/R = \eta \text{ as } \gamma (x) \text{ approaches } 1.0 \quad (9)$$

$$E_{2f} = - \frac{1}{2} \frac{C_{fd} \eta}{\frac{\partial}{\partial \eta} g(\eta)} \quad (10)$$

where $E_{2f} = \epsilon_{2f}/U_c R =$ dimensionless eddy viscosity distribution
 $\epsilon_{2f} =$ eddy kinematic viscosity for fully-developed pipe flow
 $C_{fd} = \frac{\tau_{\text{wall}}}{\frac{1}{2} \rho U_c^2} =$ wall friction coefficient

An arbitrary function is used to make the eddy viscosity distribution in Part 2 continuous with that at the end of Part 1.

$$E_2 = E_1 (1 - \gamma^2) + \gamma^2 E_{2f} \quad (11)$$

where $E_1 =$ dimensionless eddy viscosity at the end of Part 1
calculated from equation (6)

The paragraphs above have described the basic approaches used for the analysis of flow behavior in the variable-area compressible flow jet pump. The fundamental assumptions for the analysis have been identified. The sections which follow present the sets of equations which must be solved in each of the three regions of the flow; the transition zone, the region upstream of jet attachment to the wall (Part 1), and the region downstream of the point of attachment (Part 2).

3.3 Transition Zone Analysis

The transition zone begins at the primary nozzle exit plane and has a length of approximately 20 jet nozzle diameters. At the nozzle exit plane, the static pressure in the supersonic primary flow may be different from the static pressure in the surrounding secondary flow. We assume that before mixing of the two flows begins, the primary jet expands or contracts isentropically until its static pressure matches that of the secondary flow. At the station where this accommodation is complete, the velocity profile is assumed to resemble a "top-hat" as shown in figure 2. Then mixing of the primary and secondary flows begins.

The transition zone continues downstream to the section where the potential core in the jet ends. At this point, the $f_0(y/\delta)$ profile has been attained and the stagnation pressure at the center of the jet begins to fall because of mixing with the secondary flow.

The flow conditions at the end of the transition zone are determined by solving three simultaneous non-linear algebraic equations which are developed from the continuity and momentum equations written for the transition zone as a control volume, and from the condition that the stagnation pressure remains constant along the centerline of the primary jet.

The length of the transition zone is measured from the primary nozzle exit section to the point where the $f_0(y/\delta)$ profile is attained. This length is designated as x_{core} and must be specified as input data for the analysis. For incompressible flow, equation (12) may be used (reference 3).

$$x_{core} = 4.08 \delta_0 \left(1 + \frac{U_{oo}}{U_{joo}} \right) \quad (12)$$

where δ_0 = radius of primary jet at top-hat section

U_{oo} = secondary flow velocity at top-hat section

U_{joo} = primary jet relative velocity

For compressible flow with a supersonic primary jet, the value of x_{core} will depend on whether the jet is under- or over-expanded as it leaves the nozzle. A suitable replacement for equation (12) is not known to be available, so x_{core} was arbitrarily chosen to be equal to the mixing tube inlet diameter. This length is equivalent to about 18 primary nozzle diameters.

The transition from the top-hat profile to the $f_0(y/\delta)$ profile is assumed to occur in a control volume of essentially constant area. The effective mixing tube radius at x_{core} is calculated by taking the boundary layer thickness into account.

$$R_{\text{eff}} = R_{\text{core}} - \Theta H_0 \quad (13)$$

where $\Theta = \Theta_0 + 0.001 x_{\text{core}}$ (14)

R_{eff} = effective radius of mixing tube at x_{core}

R_{core} = radius of mixing tube at x_{core}

Θ = boundary layer momentum thickness at x_{core}

Θ_0 = inlet boundary layer momentum thickness

H_0 = inlet boundary layer shape factor = 1.4 assumed

The flow area available for the secondary flow at the top-hat section is given by equation (15).

$$A_{\text{eff}} = \pi R_{\text{eff}}^2 - A_{\text{noz}} \quad A_{\text{noz}} \cong A_{\text{primary flow}} \quad (15)$$

where A_{eff} = secondary flow area at top-hat section

A_{noz} = area of primary nozzle exit section

The velocity of the secondary flow at the top-hat section is calculated from equation (16).

$$U_{00} = \frac{W_0}{\rho_0 A_{\text{eff}}} \quad (16)$$

where U_{00} = secondary flow velocity at top-hat section

W_0 = mass flow rate of secondary flow

ρ_0 = density of secondary flow

The value of ρ_0 in equation (16) is the density corresponding to the local static pressure and temperature. It is computed by an iterative process using the known values of inlet stagnation pressure and temperature and the appropriate perfect gas relationships. The same calculation yields the value of the local static pressure.

The primary flow conditions at the top-hat section are calculated as follows:

$$T_1 = T_{o1} \left(\frac{p_1}{P_{o1}} \right)^{\frac{k}{k-1}} \quad (17)$$

where T_1 = static temperature in primary flow at top-hat section
 T_{o1} = specified primary flow stagnation temperature
 P_{o1} = specified primary flow stagnation pressure
 p_1 = static pressure from secondary flow calculations

$$U_1 = \sqrt{2 \frac{k}{k-1} R_g (T_{o1} - T_1)} \quad (18)$$

where U_1 = primary flow velocity at top-hat section

$$U_{joo} = U_1 - U_{oo} \quad (19)$$

where U_{joo} = primary jet relative velocity

The flow conditions at the end of the transition zone are computed by using the continuity and momentum relationships and the assumption that the stagnation pressure is unchanged at the center of the jet. The stagnation pressure of the secondary flow outside the mixing region is assumed to remain constant during transition. The stagnation temperature of the secondary flow outside the mixing region, and the stagnation temperature at the center of the primary jet, are assumed to remain constant.

The values of U_{oo} , U_{joo} , p_1 , W_o , and W_1 are known to begin the analysis which determines the velocity profile at the end of the transition zone. The continuity, momentum, and constant centerline pressure equations at the end of the zone may be written as follows on the next page.

$$\text{Continuity: } 2\pi \int_0^{R_{\text{eff}}} \rho U y dy = W_0 + W_1 \quad (20)$$

$$\text{Momentum: } 2\pi \int_0^{R_{\text{eff}}} \frac{\rho U^2}{g_0} y dy + (p - P_{00}) A_m = (p_1 - P_{00}) A_m + \frac{W_1 U_1}{g_0} + \frac{W_0 U_{00}}{g_0} \quad (21)$$

$$\text{Constant Stagnation Pressure Along Centerline: } P_{01} = \text{constant} \quad (22)$$

$$\text{where } A_m = \pi R_{\text{eff}}^2$$

The velocity profile at the end of the transition zone is given by equations (1) and (2). The temperature profile is given by equation (3).

To permit equations (20), (21), and (22) to be solved simultaneously using standard computer subroutines, these equations were rewritten in terms of the following dependent parameters:

$$U_r = \frac{U_{jo}}{U_{j00}} \quad (23)$$

$$\lambda = \frac{U_0}{U_{jo}} \quad (24)$$

$$\frac{\delta}{R_{\text{eff}}} = \frac{\delta}{\sqrt{\frac{A_m}{\pi}}} \quad (25)$$

The continuity, momentum, and constant centerline stagnation pressure equations in final form are as follows:

Continuity:

$$\text{Let } C_{\text{mass}} = \frac{W_o + W_1}{\pi R_{\text{eff}}^2 \rho_{oo} U_{joo}} \quad (26)$$

It can be shown that

$$C_{\text{mass}} = \frac{p}{p_{oo}} \left[U_r \left(\frac{\delta}{R} \right)^2 (Z_1 - S_{20}) + U_r S_{20} \right] \quad (27)$$

where

$$\frac{p}{p_{oo}} = (1 - S_{oo} U_r^2 \lambda^2)^{\frac{k}{k-1}} \quad (28)$$

$$S_{oo} = \frac{k-1}{2} \frac{U_{joo}^2}{k R_g T_{oo}} \quad (29)$$

$$S_{20} = \frac{\lambda}{1 - S_{oo} U_r^2 \lambda^2} \quad (30)$$

$$Z_1 = \int_0^1 \frac{(\lambda + f_o) 2\eta d\eta}{1 + \mathcal{T} f_o^{1/2} - S_{oo} U_r^2 (\lambda + f_o)^2} \quad (31)$$

$$\mathcal{T} = \frac{T_{oj}}{T_{oo}}$$

Momentum:

$$\text{Let } C_{\text{mom}} = \frac{g_o (p - p_{oo}) A_m + W_1 U_1 + W_o U_o}{\pi R_{\text{eff}}^2 \rho_{oo} U_{joo}^2} \quad (32)$$

It can be shown that

$$C_{\text{mom}} = \left(\frac{p}{p_{oo}} - 1 \right) \frac{R_g T_{oo}}{U_{joo}^2} + \left(\frac{p}{p_{oo}} \right) \left[U_r^2 \left(\frac{\delta}{R} \right)^2 (Z_2 - \lambda S_{20}) + U_r^2 \lambda S_{20} \right] \quad (33)$$

where

$$Z_2 = \int_0^1 \frac{(\lambda + f_o)^2 2 \eta d\eta}{1 + \mathbb{T} f_o^{1/2} - S_{oo} U_r^2 (\lambda + f_o)^2} \quad (34)$$

Constant Stagnation Pressure:

$$\frac{1 - S_{oo} U_r^2 \lambda^2}{1 - \frac{S_{oo} T_{oo}}{T_{o1}} U_r^2 (1 + \lambda)^2} = \left(\frac{P_{o1}}{P_{oo} - \Delta P_{SD}} \right)^{\frac{k-1}{k}} \quad (35)$$

where ΔP_{SD} = suction duct losses (see section 4.2.3)

The Z integrals are evaluated by using the following summation:

$$Z_k = \frac{1}{n_s} \sum_{i=1}^{n_s} \left(\frac{N_i}{D_i} \right)_k 2\eta_i \quad (36)$$

where n_s = number of summation strips, each of the same $\Delta\eta$

N_i, D_i are defined as follows:

Equation	K	N_i	D_i
Continuity	1	$\lambda + f_{oi}$	$1 + \mathbb{T} f_{oi}^{1/2} - S_{oo} U_r^2 (\lambda + f_{oi})^2$
Momentum	2	$(\lambda + f_{oi})^2$	same

Equations (27), (33), and (35) are solved simultaneously to yield values of U_r , λ , and δ/R at the end of the transition zone. The value of the static pressure at the end of the zone is then determined from equation (28).

3.4 Flow Analysis Upstream of Jet Attachment

In Part 1, the zone between the end of the transition zone and the section where the jet reaches the wall, seven variables are determined by integral techniques. These dependent variables are U_j , $\lambda = U_o/U_j$, δ , the static pressure p , the relative stagnation temperature at the jet centerline T_{oj} , the boundary layer momentum thickness Θ , and the boundary layer shape factor H .

The values of these variables are obtained by solving seven simultaneous equations of the following general form:

$$\sum_{K=1}^7 W(J,K) \times Y(K) = V(J) \quad (37)$$

where $W(J,K)$ = a coefficient matrix

$Y(K)$ = the derivatives of the dependent variables with respect to x/R_o

$V(J)$ = a set of terms not containing any of the dependent variables, evaluated at the x/R_o station of interest

The Y(K) values are listed below:

$$\left. \begin{aligned}
 Y(1) &= \frac{\partial \left(\frac{U_j}{U_{jo}} \right)}{\partial \left(\frac{x}{R_o} \right)} & Y(5) &= \frac{\partial \left(\frac{T_{oj}}{T_{oo}} \right)}{\partial \left(\frac{x}{R_o} \right)} \\
 Y(2) &= \frac{\partial \lambda}{\partial \left(\frac{x}{R_o} \right)} & Y(6) &= \frac{\partial \left(\frac{\Theta}{R_o} \right)}{\partial \left(\frac{x}{R_o} \right)} \\
 Y(3) &= \frac{\partial \left(\frac{\delta}{R_o} \right)}{\partial \left(\frac{x}{R_o} \right)} & Y(7) &= \frac{\partial H}{\partial \left(\frac{x}{R_o} \right)} \\
 Y(4) &= \frac{\partial \left(\frac{p}{P_{oo}} \right)}{\partial \left(\frac{x}{R_o} \right)}
 \end{aligned} \right\} \quad (38)$$

The J simultaneous equations used to evaluate these derivatives are as follows:

$$\left. \begin{aligned}
 J = 1 : P_{oo} &= \text{stagnation pressure in the flow outside the jet} = \text{constant} \\
 2 : & \text{momentum equation for the complete flow} \\
 3 : & \text{continuity equation} \\
 4 : & \text{energy equation} \\
 5 : & \text{moment-of-momentum equation} \\
 6 : & \text{boundary layer momentum equation} \\
 7 : & \text{boundary layer moment-of-momentum equation}
 \end{aligned} \right\} \quad (39)$$

These equations and the W(J, K) coefficients are given in detail in Appendix A.

The velocity profile for the jet in Part 1 is given by equations (1) and (2), with the distribution function f_o taken from free jet data (reference 5). The jet temperature profile is given by equation (3). In the jet ($0 \leq r \leq \delta$) the shear is obtained from equation (4) with the eddy viscosity given by equation (6).

Outside the jet ($\delta < y < R$), wall shear forces are assumed to be negligible in the momentum equation for the complete flow. The boundary layer momentum thickness Θ and the shape factor H are calculated from the following equations:

$$\frac{d\Theta}{dx} + (2 + H) \frac{\Theta}{U_o} \frac{dU_o}{dx} = \frac{C_f}{2} \quad (40)$$

$$\frac{dH}{dx} = \frac{-H(H+1)(H^2-1)}{2} \frac{1}{U_o} \frac{dU_o}{dx} + \frac{H^2-1}{\Theta} \left[\frac{HC_f}{2} - \frac{0.06(H-1)}{(H+3)R_\Theta^{0.1}} \right] \quad (41)$$

The friction coefficient in these equations is taken from the Ludwig-Tillman skin friction equation (reference 6):

$$C_f = 0.246 R_\Theta^{-0.268} 10^{-.678H} \quad (42)$$

where R_Θ = Reynolds number based on momentum thickness

These equations are based on the assumption that the outer (potential) flow at velocity U_o is incompressible, and use has been made of the relation between the boundary layer and jet mixing parameters given in equation (43):

$$\frac{1}{U_o} \frac{dU_o}{dx} = \frac{1}{\lambda} \frac{d\lambda}{dx} + \frac{1}{U_j} \frac{dU_j}{dx} \quad (43)$$

The equations above allow the boundary layer development to be calculated simultaneously with the main flow mixing. Thus, the boundary layer displacement thickness is taken into account when the momentum, continuity, and energy equations are integrated across the mixing tube cross section.

The seven equations (39) are solved simultaneously to yield the values of the derivatives (38). Then the derivatives are integrated using Runge-Kutta-Merson techniques. This integration yields the desired values of U_j , U_o , δ , p , T_{oj} , Θ , and H at selected values of x/R_o along the mixing tube.

If a region of recirculation is present, the value of U_o becomes negative. The development of an analysis for the flow behavior in a recirculation zone was not included in this investigation.

3.5 Flow Analysis Downstream of Jet Attachment (Part 2)

After the jet reaches the wall, the jet velocity profile is assumed to follow the relationship given in equation (7). At the beginning of Part 2, the value of the shape parameter $\gamma(x)$ is set equal to zero and the velocity profile is given by $f_2(\eta)$. The functional relationship f_2 is defined so as to be identical to the final velocity distribution in Part 1.

$$f_2(\eta) = \frac{f_o(\eta) + \lambda f_{bl}(\eta)}{1 + \lambda} \quad (44)$$

In this equation, $f_{bl}(\eta)$ is the boundary layer profile at the end of Part 1, estimated by using a power law for the boundary layer:

$$u = U_o \left(\frac{y}{\delta_{bl}} \right)^n \quad (45)$$

The exponent n must satisfy the values of momentum and displacement thickness calculated for the boundary layer at the end of Part 1. The resulting equation for f_{bl} follows.

$$f_{bl} = \frac{R (H_1 - 1)}{\Theta_1 H_1 (H_1 + 1)} \left[1 - \eta \right]^{\frac{H_1 - 1}{2}} \quad (46)$$

where Θ_1 = boundary layer momentum thickness at the end of Part 1

H_1 = boundary layer shape factor at the end of Part 1

The velocity profile in Part 2 includes the auxiliary profile $g_2(\eta)$. This profile is defined by equation (8) so that, as γ approaches 1.0, the Part 2 velocity profile asymptotically approaches the profile for fully-developed turbulent flow in a pipe.

In Part 2, the values of five variables are determined by integral techniques. These dependent variables are the velocity profile values U_c and γ , the static pressure p , the temperature ratio T , and the temperature of the flow at the outer radius of the mixing tube, T_{oo} . The values of these variables are obtained by solving six simultaneous equations of the general form given by equation (37). The dependent $Y(K)$ variables are listed below:

$$\begin{aligned} Y(1) &= \frac{\partial \left(\frac{U_c}{U_{jo}} \right)}{\partial \left(\frac{x}{Ro} \right)} & Y(4) &= \frac{\partial \left(\frac{p}{P_{ooi}} \right)}{\partial \left(\frac{x}{Ro} \right)} \\ Y(2) &= \frac{\partial \left(\frac{U_o}{U_c} \right)}{\partial \left(\frac{x}{Ro} \right)} \text{ (not used)} & Y(5) &= \frac{\partial \left(\frac{T_{oi}}{T_{oo}} \right)}{\partial \left(\frac{x}{Ro} \right)} \\ Y(3) &= \frac{\partial \gamma}{\partial \left(\frac{x}{Ro} \right)} & Y(6) &= \frac{\partial \left(\frac{T_{oo}}{T_{ooi}} \right)}{\partial \left(\frac{x}{Ro} \right)} \end{aligned} \quad (47)$$

where P_{ooi} and T_{ooi} are the constant values of P_{oo} and T_{oo} in Part 1. The variable $Y(2)$ above remains zero throughout the Part 2 analysis; this variable is a redundant parameter which remains from an earlier version of the computer program.

The equations used to evaluate these derivatives are as follows:

$$\begin{aligned}
 J = 1 &= \text{continuity equation} \\
 J = 2 &= \text{energy equation} \\
 J = 3 &= \text{momentum equation for the complete flow} \\
 J = 4 &= \text{moment-of-momentum integral equation} \\
 J = 5 &= \text{centerline velocity-temperature relationship} \\
 J = 6 &= \text{wall velocity} = 0
 \end{aligned} \tag{48}$$

These equations and the $W(J, K)$ coefficients are given in detail in Appendix A.

The form of the stagnation temperature profile must be known in order to solve the first four equations (48). For simplicity, the temperature profile was assumed to be the same as in a free jet.

$$\frac{T_o - T_{oo}}{T_{oj}} = \sqrt{f_o(\eta)} \quad \text{in Part 2} \tag{49}$$

This approximation is justified by the test results in Section 4.3 of this report.

Wall shear stresses are included in the momentum equation for the complete flow. The wall friction coefficient used in the analysis is based upon pipe flow correlations which yield equation (50).

$$C_{fd_f} = \frac{\tau_{\text{wall}}}{\frac{1}{2} \rho U_c^2} = 0.048 \left(\frac{\bar{U}}{U_c} \right)^2 Re_m^{-.20} \tag{50}$$

where

$$\begin{aligned}
 Re_m &= \frac{\bar{U} D}{\nu} \quad \text{Reynold's number based on mean velocity} \\
 \bar{U} &= \text{mass-average mean velocity} \\
 U_c &= \text{centerline velocity} \\
 \nu &= \text{kinematic viscosity}
 \end{aligned}$$

This wall friction coefficient is only an approximation to the actual value because the velocity profile near the wall in Part 2 of the jet pump mixing tube is generally not identical to the fully-developed pipe flow velocity profile. Comparison of analytical predictions to measured wall static pressure values indicated that equation (50) gave values of C_{fd} which were too high. Therefore, the analysis now employs an arbitrarily reduced friction factor.

$$C_{fd} = 1/2 C_{fd_f} \quad (51)$$

The moment-of-momentum integral equation includes a term which represents axial shear forces between adjacent stream tubes. These shear forces are determined from the eddy viscosity relationship given in equation (11).

The fifth equation in the set, the centerline velocity-temperature relationship, is based upon the test results obtained during this investigation. As shown in Section 4.3 and Figure 16, the following equation may be used to supplement the energy equation in Part 2.

$$\frac{1}{T_j} \frac{dT_j}{dx} = \frac{1}{U_c} \frac{dU_c}{dx} \quad (52)$$

The sixth equation (48) sets U_o , the velocity of the flow along the mixing tube surface, equal to zero. This equation was added to eliminate $Y(2)$, the redundant variable in equation (47), during the solution of the six simultaneous equations (48). The solution of these equations yields the values of the derivatives (47). The derivatives then are integrated using Runge-Kutta-Merson techniques. This integration yields the desired values of U_c , γ , p , T_{oj} , and T_{oo} at selected values of x/R_o along the mixing tube in the region after the jet reaches the wall.

Section 4

TEST PROGRAM

The objective of the test program was to provide data which could be used to evaluate the analytical model. The test conditions are summarized below:

Primary Flow

stagnation pressure: 348 psia
stagnation temperature: 807° F
nozzle throat area: $1.587 \times 10^{-4} \text{ ft}^2$
nozzle geometry: see figure 3
mass flow rate: 6.76 lbm/min

Secondary Flow

inlet stagnation pressure: laboratory ambient (30.06" Hg)
inlet stagnation temperature: laboratory ambient (92° F)
mixing tube geometry: see figure 4
pressure rise: regulated by discharge throttling device

This section of the report describes the jet pump test arrangement, instrumentation and data reduction procedures, and the results which were obtained.

4.1 Test Arrangement

The jet pump test arrangement is shown in figure 5. The primary flow was supplied by a 2-stage reciprocating compressor. Electrical heaters were used to increase the temperature of the flow up to about 800° F. The primary flow was delivered to a single nozzle directed along the axis of the mixing tube.

The momentum of the primary flow entrains a secondary air flow from the room into the bellmouth inlet and then into the mixing tube. Here, the

two streams mix together and the stagnation pressure of the secondary stream is increased. The flow from the mixing tube passes through a conical diffuser and exhausts to the atmosphere through an adjustable throttling cone.

The individual components of the experimental jet pump are described below:

1. Calibrated bellmouth inlet section

This component consists of a wooden bellmouth, metal connecting tube, and fiberglass primary flow inlet section. The bellmouth differential pressure was calibrated in terms of flow rate by using an orifice and blower available in the laboratory. The calibrated bellmouth permitted direct measurement of secondary mass flow rate for all jet pump tests.

2. Mixing tube

The mixing tube geometry was chosen rather arbitrarily before the computer program became available as a design guide. The basic Helmbold mixing tube geometry (reference 7) was selected because this geometry has been tested thoroughly in the incompressible flow regime. The incompressible results provide a guide to the flow behavior which may be expected in the compressible flow regime.

The Helmbold mixing tube was scaled down so that all dimensions were 0.892 times their original values. This scale was selected so that the mixing tube would match an existing discharge diffuser and the mixing tube throat velocity would remain subsonic for all flow rates expected in the test program. The smooth curving

profile of the Helmbold tube was approximated with cones and cylinders as shown in figure 4 for ease of fabrication.

3. Discharge diffuser

A conical diffuser with an area ratio of about 2.8 and a total included angle of 7.1° was added at the end of the mixing tube to maximize static pressure recovery and allow high entrainment ratios to be achieved. Changes in the axial positioning of the throttle cone in the diffuser exit produced a variable system resistance so that the jet pump could be tested over a range of secondary flow rates.

4. Nozzle geometry

Figure 3 shows the geometry of the converging-diverging primary flow nozzle. The area ratio from throat to exit section is 3.24, the area ratio corresponding to one-dimensional isentropic expansion from 350 psia to 14.7 psia. When the jet pump was assembled, the exit plane of the nozzle was at $x = 0$ where x is defined on the mixing tube drawing, figure 4. The mixing tube diameter at the nozzle exit plane is 5.341 in. The nozzle flow coefficient, according to the definition below, was measured to be 0.929.

$$C_w = \frac{W_1}{W_{1,ideal}} \quad (53)$$

where W_1 = measured nozzle flow rate at design pressure and temperature

$W_{1,ideal}$ = isentropic flow rate through nozzle throat at design pressure and temperature; based upon one-dimensional flow assumption

4.2 Instrumentation and Data Reduction Procedures

4.2.1 Instrumentation

The instrumentation used to determine the performance of the experimental jet pump is shown on figure 6 and described in table 1.

The jet pump inlet bellmouth was calibrated for use as a flowmeter. The calibration was accomplished by connecting the bellmouth and the suction duct to the inlet of a blower by means of an orifice run and throttling arrangement. The bellmouth flow equation follows:

$$W_o = 229.5 \sqrt{\rho_b \Delta h_b} \quad (54)$$

where Δh_b = p_b differential pressure, in. H_2O gage

ρ_b = inlet density, lbm/ft^3

The mixing tube was provided with 21 static pressure taps along its length. Four additional static pressure taps were located in the discharge diffuser. Provision was made for traverse probe measurements at five of the static pressure tap sections. The location of all of these taps is given in table 2. The exact dimensions were measured at several stations in the mixing tube after its construction; these dimensions are also given in table 2.

The Kiel-temperature probe which was traversed to measure the velocity and temperature profiles had a stem diameter of $1/8"$. The probe was small enough so that probe blockage effects were negligible during the traversing.

4.2.2 Data Reduction Procedures

The measured data were used to calculate the following jet pump parameters:

$$m = \frac{W_o}{W_1} \quad - \text{jet pump entrainment ratio}$$

$$U \text{ vs } \left(\frac{y}{R} \right) \quad - \text{velocity profiles}$$

$$T_o \text{ vs } \left(\frac{y}{R} \right) \quad - \text{temperature profiles}$$

$$p \text{ vs } \left(\frac{x}{R_o} \right) \quad - \text{mixing tube static pressure variations}$$

The stagnation pressure and temperature profiles were measured at all traverse locations in a plane perpendicular to the axis of the primary flow feed pipe (see figure 6). At the station in the mixing tube throat ($x/R_o = 9.25$), a traverse also was made in the plane of the feed pipe to confirm that the flow was axisymmetric as desired.

The wall static pressure and the traverse probe stagnation pressure and temperature measurements were used with the appropriate compressible flow equations to allow calculation of the velocity profiles at traverse stations 2 through 6. As a result of a thermocouple failure during the test runs, no temperature data were obtained at traverse station 1. Because the temperature profile is required in order to calculate the velocity profile, it was necessary to prepare an approximate temperature profile for this station. The procedure used is described under Test Results in Section 4.3 of this report.

4.2.3 Suction Duct Losses

Results from previous tests of the bellmouth and suction duct assembly (reference 1) and static pressure data from the present test program indicate that stagnation pressure losses in the suction duct upstream of the mixing tube are of the order of 2 in. H_2O for the tested secondary flow rates. These losses may be

accounted for in the jet pump analysis by using equation (55) to calculate the secondary flow stagnation pressure at the primary nozzle exit section in the mixing tube:

$$P_{o2} = P_{oo} - K_L \frac{\rho_{oo} U_{SD}^2}{2 g_o}$$

or

$$P_{o2} = P_{oo} - K_L \frac{W_o^2}{2 g_o \rho_{oo} A_{SD}^2} \quad (55)$$

- where
- P_{o2} = stagnation pressure at primary nozzle exit plane
 - P_{oo} = stagnation pressure at suction duct inlet (laboratory ambient)
 - K_L = suction duct loss coefficient
 - ρ_{oo} = density corresponding to suction duct inlet stagnation state
 - U_{SD} = suction duct velocity (assumed uniform)
 - A_{SD} = suction duct cross-sectional area

For the suction duct in the experimental jet pump, the value of K_L is 0.33.

4.3 Test Results

The jet pump was tested at four values of entrainment ratio, 17.0, 19.4, 21.0, and 23.6. The corresponding values of primary and secondary mass flow rates are given in table 3. The inlet pressures and temperatures were constant throughout the test and were as listed at the beginning of this Section 4.

Wall static pressure values measured along the mixing tube are listed for all four entrainment ratios on table 3. These values are plotted in figure 7.

The operation of the jet pump was reasonably steady (i.e., wall pressure fluctuations were small) when the entrainment ratio was 21.0. Therefore, this condition was selected for the velocity traverse measurements which require long periods of steady operation. The velocity profiles for traverse stations 2 through 6 are shown in figure 8. The associated temperature profiles are shown in figure 9.

Traverses 4 and 5 were taken at the same station in the constant-area throat section of the mixing tube. The axes of the traverse were 90° apart so that any departures from axial symmetry in the flow could be detected. The slight departures which were observed are due to heating of the secondary flow as it passes over the primary nozzle feed pipe upstream of the mixing tube inlet. These departures have a negligible effect on jet pump performance and will not interfere with our comparison of measured and predicted flow behavior through the jet pump.

Because of a thermocouple failure during testing, no temperature data were obtained at traverse station 1. The stagnation pressure measurements at this section cannot be used to determine the velocity profile unless the temperature profile is available. An approximate velocity profile for traverse station 1 was developed by using the analytically-predicted temperature profile together with the measured stagnation pressure values. The resulting velocity profile is given at the end of the next section of this report.

The mass flow rate through the jet pump as determined by the calibrated inlet bellmouth was compared to the mass flow rate obtained by integration of the velocity profiles for stations 4 and 5. Agreement was within 1% (149.8 lbm/min. from integration vs. 148.8 lbm/min. from the bellmouth). The measured velocity profile at station 6 was used for a similar comparison. Integration of this profile gave a mass flow rate of 158.8 lbm/min., about 7% greater than the bellmouth measurement.

The values of $\frac{U_i}{U_{jo}}$ and $\frac{T_i}{T_{jo}}$ calculated from the measured velocity and temperature profiles are plotted in figure 10 to show how the centerline velocities and temperatures vary with distance along the mixing tube. The velocity and temperature ratios are nearly identical over most of the mixing tube length.

COMPARISON OF ANALYTICAL AND EXPERIMENTAL RESULTS

5.1 Mixing Tube Wall Static Pressure Variations

The mixing tube wall static pressure measurements are the most valuable results for evaluating the accuracy of the analytical model for use in jet pump design. The prediction of this pressure variation is the primary purpose of this investigation because knowledge of this variation permits calculation of the pressure force on the mixing tube wall. This force must be known in order to solve the momentum equation during jet pump system optimization studies.

The analytical predictions of mixing tube static pressure variations are compared to test results for four entrainment ratios in figures 11, 12, and 13. The analyses were carried out with two different values assumed for x_{core} , the length of the transition region at the primary nozzle exit, and for two values of the secondary flow rates for each test; the values determined from the test results using the bellmouth calibration equation (54), and values 2% lower. A key to the three figures follows:

<u>Figure No.</u>	<u>x_{core}/R_o</u>	<u>Secondary Flow Rates</u>
11	2.5	from (54), reduced by 2 %
12	2.5	from (54)
13	2.0	from (54), reduced by 2%

The mass flow rates given by equation (54) and used to prepare figure 12 cause the analytical predictions of static pressure to fall below the measured values in the throat section of the mixing tube ($\frac{x}{R_o}$ from 7.34 to 10.7). The assumption that the secondary flow rates are 2% lower yields better agreement as shown in figures 11 and 13. The choice of x_{core} to be $2.5 R_o$ rather than $2.0 R_o$ causes only a small difference in the predicted static pressure levels. The differences are largest in the diffuser sections downstream of the mixing tube throat.

From these results, it was concluded that further comparisons of analytical and experimental results should be based on the assumption that the true secondary flow rates are 2% lower than the flow rates given by equation (54). An uncertainty of $\pm 2\%$ in flow rate is not unreasonable for the bellmouth calibration. The 2% flow correction brings the analytical predictions very close to the experimental results except for the static pressures downstream of the mixing tube throat.

5.2 Velocity and Temperature Profiles

The variation of predicted centerline velocity with distance along the mixing tube is shown in figure 14 for three alternative values of x_{core} ; 1.0, 2.0, and 2.5. The measured values of centerline velocity at traverse stations 2-6 are also plotted in the figure. A value of x_{core}/R_o between 2.0 and 2.5 appears to make the analytical prediction fit the test data most accurately.

The variation of predicted centerline stagnation temperature with distance along the mixing tube also is shown in figure 14. A value of x_{core}/R_o between 2.0 and 2.5 will make the temperature predictions fit the test data upstream of the throat section of the mixing tube. At traverse stations 4, 5, and 6, the measured temperature levels fall about 30°F below the predicted centerline stagnation temperatures.

The analytical results (U_c , U_o , $\frac{\delta}{R_o}$, f_2 , g_2 , and ν), together with the known free jet profile $f_o(\eta)$, allow direct comparison of the velocity and temperature profiles predicted by the analysis to the velocity and temperature profiles measured during the test program. The velocity profiles are compared in figure 15, and the temperature profiles are compared in figure 16. The predicted velocity profiles agree reasonably well with the measured profiles. The measured and predicted temperature profiles agree well for traverse stations 2 and 3, but the predicted temperatures near the centerline for stations 4, 5, and 6 are somewhat higher than they should be.

Stagnation pressure measurements only were obtained at traverse station 1. These measurements, coupled with the analytical temperature profiles predicted for this station, can be used to develop an approximate velocity profile.

The procedures used were as follows:

1. The stagnation pressure data from the traverse probe, together with the local static pressure tap reading, were used to determine the Mach number and T/T_o ratio at each y/R position in the mixing tube cross-section. This data is given in table 4.
2. From the analytical solution for $x_{core} = 2.5 R_o$, the predicted value of $\frac{\delta}{R_o}$ at the traverse station ($\frac{x}{R} = 2.5$) was found to be 0.2118. The local value of $\frac{R}{R_o}$ is 0.889. These results allow the y/R positions of the traverse probe near the duct centerline to be interpreted in terms of the y/δ values for the free jet velocity profile of equations (1) and (2). Using the analytically predicted values $U_c = 3019$ ft/sec, $U_o = 268$ ft/sec, $T_{oc} = 1267^\circ R$, and $T_{oo} = 552^\circ R$, the free jet velocity and temperature profiles can be used, through equations (1), (2), and (3), to determine the predicted values of velocity and stagnation temperature for each y/R position within the jet mixing region. The corresponding static temperatures can be determined from the T/T_o ratios in table 4. The speed of sound is calculated from the static temperature. The predicted flow velocities and speed of sound values are used to calculate Mach numbers for each y/R position within the jet mixing region. These predicted Mach numbers are compared to the "measured" Mach numbers in table 4. If the predicted and measured numbers agree, the associated velocity and temperature profiles afford a good approximation to the true profiles.
3. The same calculation procedure was followed using the analytical solution for $x_{core} = 2.0 R_o$. The predicted value of $\frac{\delta}{R_o}$ at the traverse station was 0.287. The other predicted values employed in the analysis were as follows:

$$\begin{array}{ll} U_c = 2227 \text{ ft/sec.} & T_{oc} = 1041^\circ R \\ U_o = 261 \text{ ft/sec.} & T_{oo} = 552^\circ R \end{array}$$

The predicted and "measured" Mach number profiles for traverse station 1 are compared in figure 17. The predicted profile based upon the assumption that $x_{\text{core}} = 2.0 R_o$ is closer to the measured profile than the $x_{\text{core}} = 2.5 R_o$ profile although the predicted centerline velocity is too high. The predicted velocity and temperature profiles for both x_{core} assumptions are given in table 4. The predicted values were obtained using a secondary flow rate which was 2% less than the value given by equation (54).

Section 6

CONCLUSIONS

An analytical method has been developed to predict the performance characteristics of axisymmetric single-nozzle compressible flow jet pumps with variable area mixing tubes. The primary flow may be either subsonic or supersonic. The analysis is divided into two parts. In part 1, the region between the primary nozzle exit and the point where the jet reaches the wall, the analysis is based upon the hypothesis that the mixing phenomena in the jet pump is fundamentally similar to the mixing of a free turbulent jet with the surrounding fluid. The eddy viscosity is adjusted to account for the influence of the duct walls as the jet approaches the walls. In part 2, downstream of the point where the jet reaches the wall, the velocity profile is allowed to vary from the free jet profile at the end of part 1 to a profile which asymptotically approaches the fully-developed turbulent flow profile in a pipe. Integral techniques are employed in both part 1 and part 2 to solve the continuity, momentum, moment-of-momentum, and energy equations to determine the variations of flow properties along the mixing tube.

An experimental program was conducted to measure mixing tube wall static pressure variations, velocity profiles, and temperature profiles in a variable area mixing tube with a supersonic ($M = 2.72$) primary jet. Static pressure variations were measured at four different secondary flow rates. These test results were used to evaluate the analytical model.

Analytical predictions of wall static pressure distributions along the mixing tube generally agreed well with the test results for all four entrainment ratios. The predicted wall static pressure values differed slightly from the measured pressures downstream of the constant-area throat section. The velocity profiles along the mixing tube were predicted accurately by the analysis. The analytical temperature profiles were not as accurate; the predicted centerline temperatures downstream of the throat were too high. These discrepancies are considered to be minor in view of the comparatively extreme mixing tube geometry used for the test case. Thus, the analysis is ready for use to calculate the pressure force on the wall of a variable area mixing tube. This permits the momentum equation to be solved accurately in jet pump-duct system optimization and design studies.

The analysis in part 2 of the jet pump makes the assumption that the temperature profiles are similar to free jet temperature profiles. A very simple and approximate form of the energy equation is employed. A more accurate energy equation, perhaps augmented by assumption of a different form for the temperature profile, might lead to greater accuracy in the prediction of wall static pressures and temperature profiles in this region.

APPENDIX A

Equations for the Flow

A1 - Part 1 - Upstream of Jet Attachment

The general form of the flow equations, as described in Section 3.4, is as follows:

$$\sum_{k=1}^7 W(J, K) * Y(K) = V(J)$$

The 7 variables are tabulated below, using the convention that the superscript (') represents

$$\frac{\partial}{\partial \left(\frac{x}{R_o} \right)}.$$

$$K = \quad 1 \quad \quad 2 \quad \quad 3 \quad \quad 4 \quad \quad 5 \quad \quad 6 \quad \quad 7$$

$$Y(K) = \left(\frac{U_j}{U_{jo}} \right)' \quad \lambda' \quad \left(\frac{\delta}{R_o} \right)' \quad \left(\frac{p}{p_{oo}} \right)' \quad \left(\frac{T_{oj}}{T_{oo}} \right)' \quad \left(\frac{\theta}{R_o} \right)' \quad H'$$

The $W(J, K)$ coefficients and $V(J)$ terms are determined in this section.

A1-1 Equation for $J = 1$; Constant stagnation pressure in the flow outside the jet.

$$dp = - \rho \frac{U dU}{g_o}$$

$$R_g T \frac{dp}{p} + \lambda U_j d(\lambda U_j) = 0$$

Normalizing:

$$\frac{R_g T}{U_{jo}^2} \frac{dp}{p} + \lambda \frac{U_j}{U_{jo}} \left(\lambda \frac{dU_j}{U_{jo}} + \frac{U_j}{U_{jo}} d\lambda \right) = 0$$

$$\text{Let } BP = \frac{R_g T_{\infty}}{U_{jo}^2} = \frac{k-1}{2kS_o}$$

$$S_o = \frac{U_{jo}^2}{2 \frac{k}{k-1} R_g T_{\infty}}$$

$$\text{Then } T_o = T_{\infty} \left[1 - S_o \frac{U_j^2}{U_{jo}^2} \lambda^2 \right] = \text{Static temperature in the flow outside the jet}$$

The final values follow:

$$W(1,1) = \lambda^2 \frac{U_j}{U_{jo}} \quad W(1,5) = 0$$

$$W(1,2) = \lambda \left(\frac{U_j}{U_{jo}} \right)^2 \quad W(1,6) = 0$$

$$W(1,3) = 0 \quad W(1,7) = 0$$

$$W(1,4) = \left(1 - S_o \frac{U_j^2}{U_{jo}^2} \lambda^2 \right) \frac{BP}{p} \quad V(1) = 0$$

A1-2 Equation for $J = 2$; Momentum equation for the flow

$$- \pi R^2 \frac{dp}{dx} = \frac{d}{dx} \int_0^R \rho U^2 2\pi y dy$$

$$-R^2 \frac{dp}{dx} = \frac{d}{dx} \left\{ \frac{p}{R_g T_{\infty}} U_j^2 \left[\delta^2 \int_0^1 \frac{(\lambda + f_o)^2 2\eta d\eta}{1 + T_{fo}^{1/2} - S_o \frac{U_j^2}{U_{jo}^2} (\lambda + f_o)^2} + \frac{(R^2 - \delta^2) \lambda^2}{1 - S_o \frac{U_j^2}{U_{jo}^2} \lambda^2} \right] \right\}$$

where $\lambda + f_o = \frac{U}{U_j}$

$$1 + \frac{U_j^2}{U_{jo}^2} \frac{1}{2} - S_o (\lambda + f_o)^2 = \frac{T_\eta}{T_{oo}} = \frac{\text{Static Temperature @ } \eta}{\text{Stagnation Temperature @ } \eta = 1.0}$$

$$1 - S_o \frac{U_j^2}{U_{jo}^2} \lambda^2 = \frac{T_o}{T_{oo}} = \frac{\text{Static Temperature}}{\text{Stagnation Temperature}} \quad \text{at } \eta = 1.0$$

Let

$$Z_{12} = \int_0^1 \frac{(\lambda + f_o)^2 2\eta \, d\eta}{1 + \frac{U_j^2}{U_{jo}^2} \frac{1}{2} - S_o (\lambda + f_o)^2}$$

In the computer analysis, this integration is approximated by a summation across the jet:

Let
$$Z_{1J} = \frac{2}{n_s} \sum_{i=1}^{n_s} \frac{N_{iJ}}{D_{iJ}} \eta_i$$

In this equation N_i and D_i are average values of the numerator and denominator across the i^{th} equal-radius annular segment of the jet. The following additional definitions will be used:

$$Z_{2J} = \frac{2}{n_s} \sum_{i=1}^{n_s} \left(\frac{-N_{iJ}}{D_{iJ}^2} \right) \frac{\partial D_{iJ}}{\partial \left(\frac{U_j}{U_{jo}} \right)} \eta_i$$

$$Z_{3J} = \frac{2}{n_s} \sum_{i=1}^{n_s} \frac{1}{D_{iJ}} \frac{\partial N_{iJ}}{\partial \lambda} \eta_i$$

$$Z_{4J} = \frac{2}{n_s} \sum \left(\frac{-N_{iJ}}{D_{iJ}^2} \right) \frac{\partial D_{iJ}}{\partial \lambda} \eta_i$$

$$Z_{5J} = \frac{2}{n_s} \sum \frac{1}{D_{iJ}} \frac{\partial N_{iJ}}{\partial \overline{U}} \eta_i$$

$$Z_{6J} = \frac{2}{n_s} \sum \frac{-N_{iJ}}{D_{iJ}^2} \frac{\partial D_{iJ}}{\partial \overline{U}} \eta_i$$

Then the relations below may be used:

$$\frac{\partial Z_{1J}}{\partial \left(\frac{U_j}{U_{jo}} \right)} = Z_{2J}$$

$$\frac{\partial Z_{1J}}{\partial \lambda} = Z_{3J} + Z_{4J}$$

$$\frac{\partial Z_{1J}}{\partial \overline{U}} = Z_{5J} + Z_{6J}$$

Additional parameters which simplify the equations are defined as follows:

$$S_2 = \frac{\lambda}{1 - S_o \frac{U_j^2}{U_{jo}^2} \lambda^2}$$

$$\frac{R}{R_o} = \frac{R_{tube}}{R_o} - \frac{\Theta}{R_o} H$$

$$\frac{\delta}{R} = \frac{\delta}{R_o} \frac{R_o}{R}$$

Employing these definitions in the momentum equation, the following expression is obtained after reorganizing, normalizing, and differentiating:

$$\begin{aligned} -\frac{dp}{dx} \frac{R_g T_{\infty}}{p U_j^2} &= \left[\frac{p'}{p} + 2 \frac{U_j'}{U_j} \right] \left[\frac{\delta^2}{R^2} Z_{12} + \left(1 - \frac{\delta^2}{R^2}\right) \lambda S_2 \right] + 2 \frac{\delta}{R} \frac{\delta'}{R} Z_{12} \\ &+ \frac{\delta^2}{R^2} \left[Z_{22} \frac{U_j'}{U_{jo}} + (Z_{32} + Z_{42}) \lambda' + (Z_{52} + Z_{62}) T' \right] \\ &+ \left[\frac{2}{R} (R'_{tube} - \Theta' H - H' \Theta) - 2 \frac{\delta}{R} \frac{\delta'}{R} \right] \lambda S_2 \\ &+ \left(1 - \frac{\delta^2}{R^2}\right) \left(S_2 \lambda' + \lambda \frac{\partial S_2}{\partial \lambda} \lambda' + \lambda \frac{\partial S_2}{\partial U_j} U_j' \right) \end{aligned}$$

The final values follow:

$$W(2,1) = \left(\frac{\delta}{R} \right)^2 \left[\frac{2Z_{12}}{\left(\frac{U_j}{U_{jo}} \right)} + Z_{22} \right] + \left[1 - \frac{\delta^2}{R^2} \right] \left[\frac{2\lambda S_2}{\left(\frac{U_j}{U_{jo}} \right)} + \lambda \frac{\partial S_2}{\partial \left(\frac{U_j}{U_{jo}} \right)} \right]$$

$$W(2,2) = \left(\frac{\delta}{R} \right)^2 (Z_{32} + Z_{42}) + \left(1 - \frac{\delta^2}{R^2} \right) \left(S_2 + \lambda \frac{\partial S_2}{\partial \lambda} \right)$$

$$W(2,3) = 2 \frac{\delta}{R} (Z_{12} - \lambda S_2)$$

$$W(2,4) = \frac{P_{oo}}{p} \left[\frac{\delta^2}{R^2} Z_{12} + \left(1 - \frac{\delta^2}{R^2}\right) \lambda S_2 \right] + \frac{BP * P_{oo}}{p \left(\frac{U_j}{U_{jo}}\right)^2}$$

$$W(2,5) = \frac{\delta^2}{R^2} (Z_{52} + Z_{62})$$

$$W(2,6) = -2 \frac{H}{R} S_2 \lambda$$

$$W(2,7) = -2 \frac{\Theta}{R} S_2 \lambda$$

$$V(2) = -2 \frac{R'_{tube}}{R} S_2 \lambda$$

Table A1 lists the values of N_i , D_i , and their derivatives which are required to evaluate the Z parameters in the previous equations.

A1.3 Equation for $J = 3$; Continuity equation

$$W_o + W_1 = 2\pi \int_o^R \rho U y dy \text{ where } R = (\text{Local Duct Radius} - \Theta H)$$

$$W_o + W_1 = \frac{p \pi}{R_g T_{oo}} U_j \left[\delta^2 \int_o^1 \frac{(\lambda + f_o) d\eta^2}{1 + \sqrt{f_o}^{1/2} - S_o \left(\frac{U_j}{U_{jo}}\right)^2 (\lambda + f_o)^2} + \frac{(R^2 - \delta^2) \lambda}{1 - S_o \left(\frac{U_j}{U_{jo}}\right)^2 \lambda^2} \right]$$

or

$$W_o + W_1 = \frac{p \pi}{R_g T_{oo}} U_j \left[\delta^2 Z_{13} + (R^2 - \delta^2) S_2 \right]$$

where

$$Z_{13} = \int_o^1 \frac{(\lambda + f_o) 2\eta d\eta}{1 + \sqrt{f_o}^{1/2} - S_o \left(\frac{U_j}{U_{jo}}\right)^2 (\lambda + f_o)^2}$$

The continuity equation is normalized as follows:

$$\frac{W_o + W_1}{\pi R_o^2 U_{jo}} \frac{R_g T_{oo}}{P_{oo}} = \frac{U_i}{U_{jo}} \left[\left(\frac{\delta}{R_o} \right)^2 Z_{13} + \left(\frac{R^2}{R_o^2} - \frac{\delta^2}{R_o^2} \right) S_2 \right] \frac{p}{P_{oo}}$$

Taking the derivative with respect to $\frac{x}{R_o}$;

$$\begin{aligned} 0 = & \left(\frac{U_i}{U_{jo}} \right) \frac{p}{P_{oo}} \left[\left(\frac{\delta}{R_o} \right)^2 Z_{13} + \left(\frac{R^2}{R_o^2} - \frac{\delta^2}{R_o^2} \right) S_2 \right] + \left(\frac{p}{P_{oo}} \right) \frac{U_i}{U_{jo}} \left[\left(\frac{\delta}{R_o} \right)^2 Z_{13} + \left(\frac{R^2}{R_o^2} - \frac{\delta^2}{R_o^2} \right) S_2 \right] \\ & + \left(\frac{\delta}{R_o} \right)' \left[2 \frac{\delta}{R_o} (Z_{13} - S_2) \right] \frac{U_i}{U_{jo}} \frac{p}{P_{oo}} \\ & + \frac{U_i}{U_{jo}} \frac{p}{P_{oo}} \frac{\delta^2}{R_o^2} \left[Z_{23} \left(\frac{U_i}{U_{jo}} \right)' + (Z_{33} + Z_{43}) \lambda' + (Z_{53} + Z_{63}) \mathbf{r}' \right] \end{aligned}$$

$$\begin{aligned} + \frac{U_i}{U_{jo}} \frac{p}{P_{oo}} \left(\frac{R^2}{R_o^2} - \frac{\delta^2}{R_o^2} \right) \frac{\lambda' (1 - S_o (U_i^2/U_{jo}^2) \lambda^2) + \lambda S_o \left[2 \lambda \lambda' (U_i^2/U_{jo}^2) + 2 \lambda^2 (U_i/U_{jo}) (U_i/U_{jo})' \right]}{\left[1 - S_o \left(\frac{U_i}{U_{jo}} \right)^2 \lambda^2 \right]^2} \\ + 2 \frac{R}{R_o} \frac{U_i}{U_{jo}} \frac{p}{P_{oo}} S_2 \left(\frac{R'_{tube}}{R_o} - \frac{\theta}{R_o} \frac{H}{H'} - \frac{H}{R_o} \theta' \right) \end{aligned}$$

Collecting terms and dividing each by $\left(\frac{R}{R_o}\right)^2 \frac{U_j}{U_{jo}} \frac{p}{p_{oo}} ;$

$$W(3,1) = \frac{U_{jo}}{U_j} \frac{R_o^2}{R^2} \left(\frac{\delta}{R_o}\right)^2 Z_{13} + \left(1 - \frac{R_o^2}{R^2} \frac{\delta^2}{R_o^2}\right) S_2 \frac{U_{jo}}{U_j} + Z_{23} \frac{R_o^2}{R^2} \frac{\delta^2}{R_o^2} \\ + \left(\frac{U_j}{U_{jo}}\right)^{2\lambda} S_2^2 S_o \left(1 - \frac{R_o^2}{R^2} \frac{\delta^2}{R_o^2}\right)$$

$$W(3,2) = \frac{R_o^2}{R^2} \frac{\delta^2}{R_o^2} (Z_{33} + Z_{43}) + \left(1 - \frac{R_o^2}{R^2} \frac{\delta^2}{R_o^2}\right) \frac{1 + S_o \frac{U_j^2}{U_{jo}^2} \lambda^2}{\left(1 - S_o \frac{U_j^2}{U_{jo}^2} \lambda^2\right)^2}$$

$$W(3,3) = 2 \frac{\delta}{R_o} (Z_{13} - S_2) \frac{R_o^2}{R^2}$$

$$W(3,4) = \frac{p_{oo}}{p} \left[\frac{\delta^2}{R_o^2} \frac{R_o^2}{R^2} Z_{13} + \left(1 - \frac{R_o^2}{R^2} \frac{\delta^2}{R_o^2}\right) S_2 \right]$$

$$W(3,5) = \frac{R_o^2}{R^2} \frac{\delta^2}{R_o^2} (Z_{53} + Z_{63})$$

$$W(3,6) = -2S_2 \frac{R_o}{R} H$$

$$W(3, 7) = -2 S_2 \frac{R_o}{R} \frac{\Theta}{R_o}$$

$$V(3) = -2 \frac{R_o}{R} \left(\frac{R}{R_o} \right)' S_2$$

Table A1 lists the values of N_i , D_i , and their derivatives which are required to evaluate the Z parameters in the equations above.

A1-4 Equation for $J = 4$; Energy Equation

$$W_o C_p T_{oo} + W_1 C_p T_{oj} = 2\pi \int_0^R \rho U C_p T_o y dy \text{ where } R = (\text{local duct radius} - \Theta H)$$

or

$$W_o T_{oo} + W_1 T_{oj} = 2\pi \int_0^R \rho U T_o y dy$$

$$W_o T_{oo} + W_1 T_{oj} = \pi \frac{p}{R_g} U_j \left[\delta^2 \int_0^1 \frac{(\lambda + f_o) (1 + T_{fo}^{1/2}) 2\eta d\eta}{1 + T_{fo}^{1/2} - S_o \left(\frac{U_j}{U_{jo}} \right)^2 (\lambda + f_o)^2} + (R^2 - \delta^2) S_2 - 2S_2 \Theta H R \right]$$

Let

$$Z_{14} = \int_0^1 \frac{(\lambda + f_o) (1 + T_{fo}^{1/2}) 2\eta d\eta}{1 + T_{fo}^{1/2} - S_o \left(\frac{U_j}{U_{jo}} \right)^2 (\lambda + f_o)^2}$$

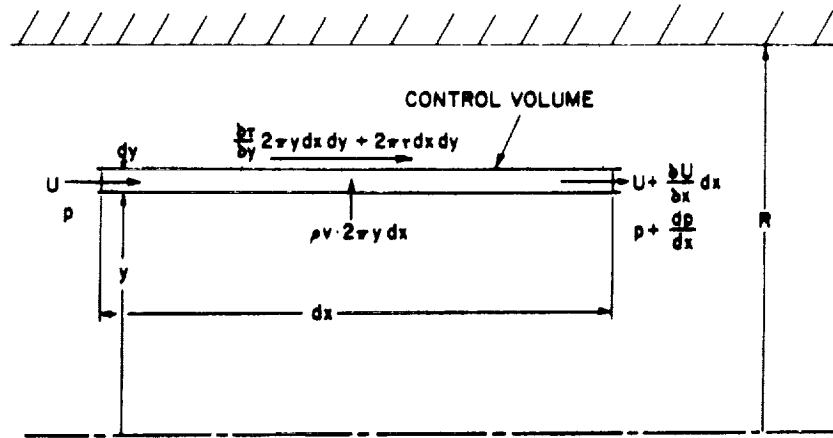
Then, the normalized energy equation may be written as follows:

$$\frac{(W_o T_{oo} + W_1 T_{oj})}{\pi R_o^2 U_{jo}} \frac{R_g}{P_{oo}} = \frac{p}{P_{oo}} \frac{U_j}{U_{jo}} \left[\frac{\delta^2}{R_o^2} Z_{14} + \left(\frac{R^2}{R_o^2} - \frac{\delta^2}{R_o^2} \right) S_2 - 2S_2 \frac{\theta}{R_o} \frac{R}{R_o} H \right]$$

If this equation is compared to the normalized continuity equation in Section A1-3, it is seen that the right-hand sides are identical except for the substitution of Z_{14} for Z_{13} . This means that all of the $W(4,K)$ coefficients are identical to the $W(3,K)$ coefficients except for the substitution of Z_{14} for Z_{13} in all expressions. Table A1 lists the values of N_i , D_i , and their derivatives which are required to evaluate the Z_{14} parameters.

A1-5 Equation for $J = 5$; Moment-of-Momentum Integral Equation

The momentum equation for an annular section of the jet can be derived as follows.



$$\tau 2\pi dy dx - \frac{dp}{dx} dx (2\pi y dy) + 2\pi y \frac{\partial \tau}{\partial y} dy dx = \rho \frac{\partial u}{\partial x} dx u \cdot 2\pi y dy + \rho v 2\pi y dx \frac{\partial u}{\partial y} dy$$

or

$$\tau - \frac{dp}{dx} y + y \frac{\partial \tau}{\partial y} = \rho \frac{\partial u}{\partial x} uy + \rho v y \frac{\partial u}{\partial y}$$

To derive the moment-of momentum integral equation, this momentum equation is multiplied by ydy and integrated across the jet:

$$\int_0^{\delta} \rho u y \frac{\partial u}{\partial x} y dy + \int_0^{\delta} \rho v y \frac{\partial u}{\partial y} y dy = \int_0^{\delta} \frac{\partial (\tau y)}{\partial y} y dy - \int_0^{\delta} \frac{dp}{dx} y^2 dy$$

Noting that $u = U_j(\lambda + f_o)$:

$$\frac{\partial u}{\partial x} = \frac{1}{R_o} U_j'(\lambda + f_o) + \frac{U_j}{R_o} \left[\lambda' + \frac{\partial f_o}{\partial \eta} \left(-\frac{\eta \delta'}{\delta} \right) \right]$$

$$\frac{\partial u}{\partial y} = \frac{U_j}{\delta} \frac{\partial f_o}{\partial \eta}$$

then

$$\begin{aligned} \int_0^{\delta} \rho u y \frac{\partial u}{\partial x} y dy &= \int_0^1 \frac{p}{R_g T_{\infty}} \frac{U_j(\lambda + f_o) \frac{\partial u}{\partial x}}{1 + \Gamma f_o^{1/2} - S_o \frac{U_j^2}{U_{jo}^2} (\lambda + f_o)^2} \delta^3 \eta^2 d\eta \\ &= \frac{p U_j^2 \delta^2}{R_g T_{\infty}} \int_0^1 \frac{\frac{1}{U_j} (\lambda + f_o) \frac{\partial u}{\partial x} \eta^2 d\eta}{1 + \Gamma f_o^{1/2} - S_o \frac{U_j^2}{U_{jo}^2} (\lambda + f_o)^2} \\ &= \frac{p U_j^2 \delta^3}{R_g T_{\infty} R_o} \left[\frac{U_j'}{U_j} Q_1 + \lambda' Q_2 + \frac{\delta'}{\delta} Q_3 \right] \end{aligned}$$

in which

$$\begin{aligned} Q_1 &= \int_0^1 \frac{(\lambda + f_o)^2 \eta^2 d\eta}{D} \\ Q_2 &= \int_0^1 \frac{(\lambda + f_o) \eta^2 d\eta}{D} \\ Q_3 &= - \int_0^1 \frac{\frac{\partial f_o}{\partial \eta} (\lambda + f_o) \eta^3 d\eta}{D} \\ D &= 1 + \Gamma f_o^{1/2} - S_o \frac{U_j^2}{U_{jo}^2} (\lambda + f_o)^2 \end{aligned}$$

In order to evaluate the radial velocity, v , it is necessary to use the continuity relation. Employing a control volume of radius y and length dx , the continuity equation may be written as follows:

$$\begin{aligned}
 \rho v 2 \pi y dx &= - \int_0^y \frac{\partial}{\partial x} (\rho u 2 \pi y dy) dx \\
 \text{so} \quad \rho v y &= - \int_0^y \frac{\partial}{\partial x} (\rho u y) dy \\
 &= - \int_0^y \frac{\partial}{\partial x} \left[\frac{p}{R_g T_{\infty}} \frac{U_j (\lambda + f_o)}{D} \right] y dy \\
 \rho v y &= - \int_0^{\eta} \frac{\delta^2}{R_o R_g T_{\infty}} \left\{ \left[\frac{p' U_j (\lambda + f_o)}{D} + \frac{p U_j' (\lambda + f_o)}{D} + \frac{p U_j}{D} \left(\lambda' - \frac{\partial f_o}{\partial \eta} \eta \frac{\delta'}{\delta} \right) \right] \right. \\
 &\quad \left. - \frac{p U_j (\lambda + f_o)}{D^2} \left[U' \frac{\partial D}{\partial U} + U_j' \frac{\partial D}{\partial U_j} + \lambda' \frac{\partial D}{\partial \lambda} - \eta \frac{\delta'}{\delta} \frac{\partial D}{\partial \eta} \right] \right\} \eta d\eta \\
 - \frac{\rho v y}{\frac{p}{R_g T_{\infty}} U_j \frac{\delta^2}{R_o}} &= \left[\begin{aligned} &\frac{U_j'}{U_j} \int_0^{\eta} \left[\frac{(\lambda + f_o)}{D} - \frac{(\lambda + f_o)}{D^2} \frac{\partial D}{\partial (\frac{U_j}{U_{j_o}})} \frac{U_j}{U_{j_o}} \right] \eta d\eta \\ &+ \lambda' \int_0^{\eta} \left[\frac{1}{D} - \frac{(\lambda + f_o)}{D^2} \frac{\partial D}{\partial \lambda} \right] \eta d\eta \\ &+ \frac{\delta'}{\delta} \int_0^{\eta} \left[-\frac{1}{D} \frac{\partial f_o}{\partial \eta} \eta + \frac{(\lambda + f_o)}{D^2} \eta \frac{\partial D}{\partial \eta} \right] \eta d\eta \\ &+ \frac{p'}{p} \int_0^{\eta} \frac{(\lambda + f_o)}{D} \eta d\eta \\ &+ U' \int_0^{\eta} -\frac{(\lambda + f_o)}{D^2} \frac{\partial D}{\partial U} \eta d\eta \end{aligned} \right] \left[\begin{aligned} &\frac{U_j'}{U_j} \left[V_1 + V_2 \frac{U_j}{U_{j_o}} \right] \\ &+ \lambda' [V_3 + V_4] \\ &+ \frac{\delta'}{\delta} [-V_{10} - V_{11}] \\ &+ \frac{p'}{p} [V_1] \\ &+ U' [V_5 + V_6] \end{aligned} \right]
 \end{aligned}$$

$$\begin{aligned}
\text{in which } V_1 &= \int_0^\eta \frac{(\lambda + f_o)}{D} \eta d\eta & V_5 &= 0 \\
V_2 &= \int_0^\eta - \frac{(\lambda + f_o)}{D^2} \frac{\partial D}{\partial \left(\frac{U_j}{U_{jo}} \right)} \eta d\eta & V_6 &= \int_0^\eta - \frac{(\lambda + f_o)}{D^2} \frac{\partial D}{\partial \eta} \eta d\eta \\
V_3 &= \int_0^\eta \frac{1}{D} \eta d\eta & V_{10} &= \int_0^\eta \frac{1}{D} \frac{\partial f_o}{\partial \eta} \eta^2 d\eta \\
V_4 &= \int_0^\eta - \frac{(\lambda + f_o)}{D^2} \frac{\partial D}{\partial \lambda} \eta d\eta & V_{11} &= \int_0^\eta - \frac{(\lambda + f_o)}{D^2} \frac{\partial D}{\partial \eta} \eta^2 d\eta
\end{aligned}$$

With these definitions, the integral

$$\int_0^\delta \rho v y \frac{\partial u}{\partial y} y dy$$

may be evaluated as follows:

$$\begin{aligned}
\frac{\int_0^\delta \rho v y \frac{\partial u}{\partial y} y dy}{\left(\frac{p U_j^2 \delta^3}{R_g T_{\infty} R_o} \right)} &= \int_0^\delta \frac{\rho v y}{\left(\frac{p U_j}{R_g T_{\infty}} \right) \left(\frac{\delta^2}{R_o} \right)} \frac{1}{U_j \delta} \frac{U_j}{\delta} \frac{\partial f_o}{\partial \eta} y dy \\
&= \int_0^1 \left[\frac{\rho v y}{\frac{p U_j}{R_g T_{\infty}} \frac{\delta^2}{R_o}} \right] \frac{\partial f_o}{\partial \eta} \eta d\eta
\end{aligned}$$

$$\begin{aligned}
&= \frac{U_j'}{U_j} \left[- \int_0^1 V_1 \frac{\partial f_o}{\partial \eta} \eta d\eta - \frac{U_j}{U_{jo}} \int_0^1 V_2 \frac{\partial f_o}{\partial \eta} \eta d\eta \right] + \lambda' \left[- \int_0^1 V_3 \frac{\partial f_o}{\partial \eta} \eta d\eta - \int_0^1 V_4 \frac{\partial f_o}{\partial \eta} \eta d\eta \right] \\
&+ \frac{\delta'}{\delta} \left[\int_0^1 (V_{10} + V_{11}) \frac{\partial f_o}{\partial \eta} \eta d\eta \right] + \frac{p'}{p} \left[- \int_0^1 V_1 \frac{\partial f_o}{\partial \eta} \eta d\eta \right] + T' \left[- \int_0^1 (V_5 + V_6) \frac{\partial f_o}{\partial \eta} \eta d\eta \right] \\
&= \frac{U_j'}{U_j} \left[R_1 + \frac{U_j}{U_{jo}} R_2 \right] + \lambda' R_{34} + \frac{\delta'}{\delta} [R_{10} + R_{11}] + \frac{p'}{p} R_1 + T' R_{56}
\end{aligned}$$

$$\begin{aligned}
\text{in which } R_1 &= - \int_0^1 V_1 \frac{\partial f_o}{\partial \eta} \eta d\eta & R_{10} &= \int_0^1 V_{10} \frac{\partial f_o}{\partial \eta} \eta d\eta \\
R_2 &= - \int_0^1 V_2 \frac{\partial f_o}{\partial \eta} \eta d\eta & R_{11} &= \int_0^1 V_{11} \frac{\partial f_o}{\partial \eta} \eta d\eta \\
R_{34} &= - \int_0^1 (V_3 + V_4) \frac{\partial f_o}{\partial \eta} \eta d\eta & R_{56} &= - \int_0^1 (V_5 + V_6) \frac{\partial f_o}{\partial \eta} \eta d\eta
\end{aligned}$$

The pressure gradient term may be rewritten as follows:

$$\int_0^\delta \frac{dp}{dx} y^2 dy = \frac{p U_j^2 \delta^3}{R_g T_{oo} R_o} \left[\frac{p'}{p} \frac{1}{3} - \frac{BP}{U_j^2} \frac{U_j}{U_{jo}^2} \right]$$

The shear stress term may be evaluated as follows:

$$\int_0^\delta \frac{\partial (\tau y)}{\partial y} y dy = \tau y^2 \Big|_0^\delta - \int_0^\delta \tau y dy$$

$$\tau = \rho \epsilon \frac{\partial u}{\partial y} = \rho \epsilon \frac{U_j}{\delta} \frac{\partial f_o}{\partial \eta} \quad \text{where } \epsilon \text{ is the eddy kinematic viscosity}$$

$$\begin{aligned} \frac{\int_0^\delta \frac{\partial (\tau y)}{\partial y} y dy}{\left(\frac{p U_j^2 \delta^3}{R_g T_{oo} R_o} \right)} &= - \int_0^1 \rho \epsilon \frac{1}{U_j \delta} \frac{\partial f_o}{\partial \eta} \eta d\eta \frac{R_g T_{oo} R_o}{p} \\ &= - \int_0^1 \frac{\epsilon}{U_j \delta} \frac{R_o}{\delta} \frac{1}{D} \frac{\partial f_o}{\partial \eta} \eta d\eta \\ &= - \left(\frac{\epsilon}{U_j \delta} \right)_{\text{avg}} \left(\frac{R_o}{\delta} \right) \int_0^1 \frac{\epsilon}{\epsilon_{\text{avg}}} \frac{1}{D} \frac{\partial f_o}{\partial \eta} \eta d\eta \\ &= \frac{EA_\tau}{(\delta/R_o)} \end{aligned}$$

$$\text{where } A_\tau = - \int_0^1 \frac{\epsilon}{\epsilon_{\text{avg}}} \frac{1}{D} \frac{\partial f_o}{\partial \eta} \eta d\eta \cong 0.377 \text{ as in incompressible jet mixing}$$

$$E = \left(\frac{\epsilon}{U_j \delta} \right)_{\text{avg}} \text{ is the inverse of the local turbulent Reynolds number.}$$

Assembling all the terms, the final moment-of-momentum integral equation is as follows:

$$\begin{aligned} \frac{U_j'}{U_j} \left(Q_1 + R_1 + R_2 \frac{U_j}{U_{jo}} \right) + \lambda' (Q_2 + R_{34}) + \frac{\delta'}{\delta} (Q_3 + R_{10} + R_{11}) + \frac{p'}{p} \left(R_1 + \frac{BP}{\frac{U_j^2}{3 \frac{U_j^2}{U_{jo}^2}}} \right) \\ + U' R_{56} = \frac{EA_\tau}{(\delta/R_o)} \end{aligned}$$

The values of the coefficients follow:

$$\begin{aligned}
 W(5, 1) &= Q_1 + R_1 + R_2 \frac{U_j}{U_{jo}} & W(5, 5) &= R_{56} \\
 W(5, 2) &= Q_2 + R_{34} & W(5, 6) &= 0 \\
 W(5, 3) &= Q_3 + R_{10} + R_{11} & W(5, 7) &= 0 \\
 W(5, 4) &= R_1 + \frac{BP}{3 \frac{U_j^2}{U_{jo}^2}} & V(5) &= \frac{EA_\tau}{(\delta/R_o)}
 \end{aligned}$$

A1-6 Equation for J = 6; Boundary Layer Momentum Equation

The boundary layer momentum equation, equation (40), is discussed in Section 3.4 of this report.

A1-7 Equation for J = 7; Boundary Layer Moment-of-Momentum Equation

The boundary layer moment-of-momentum equation was used to derive the shape factor equation (41). This equation is discussed in Section 3.4 of this report.

A1-8 Initial Conditions for the Part 1 Analysis

The initial conditions for the Part 1 analysis are established from the transition zone analysis described in Section 3.3. The initial values were set as follows:

$$\frac{U_j}{U_{jo}} = 1$$

$$\frac{T_{oj}}{T_{oo}} = \frac{T_{o1} - T_{oo}}{T_{oo}} \quad \text{From transition zone Analysis}$$

$$\lambda = \lambda \quad \text{From transition zone Analysis}$$

$$\frac{\theta}{R_o} = \frac{\theta}{R_o} \quad \text{Calculated from Equation (14)}$$

$$\frac{\delta}{R_o} = \frac{R}{R_o} \left(\frac{\delta}{R} \right) \quad \text{From transition zone analysis}$$

$$H = 1.4 \quad \text{Input value to program}$$

$$\frac{p}{P_{oo}} = \left[1 - S_o \frac{k}{k-1} \lambda^2 \right] \left[1 - \frac{\Delta P_{sD}}{P_{oo}} \right]$$

A2 - Part 2 - Downstream of Jet Attachment

The general form of the flow equations, as described in Section 3.4, is as follows:

$$\sum_{K=1}^6 W(J, K) * Y(K) = V(J)$$

The 6 variables employed in Part 2 are tabulated below. The superscript (') represents the derivative $\frac{\partial}{\partial \left(\frac{x}{R_o} \right)}$.

$$K = \quad 1 \quad \quad 2 \quad \quad 3 \quad \quad 4 \quad \quad 5 \quad \quad 6$$

$$Y(K) = \left(\frac{U_c}{U_{jo}} \right)' \left(\frac{U_o}{U_c} \right)' \gamma' \left(\frac{p}{P_{ooi}} \right)' \mathcal{T}' \left(\frac{T_{oo}}{T_{ooi}} \right)'$$

where P_{ooi} and T_{ooi} are the stagnation pressure and stagnation temperature for the wall streamline at the end of Part 1 just as the jet reaches the duct wall.

The variable $Y(2)$ remains zero throughout the Part 2 analysis; this variable is a redundant parameter which remains from an earlier version of the computer program.

The $W(J, K)$ coefficients and $V(J)$ terms are determined in this section of the appendix.

A2-1 Equation for $J = 1$; Continuity Equation

$$W_o + W_1 = \int_0^R \rho u \cdot 2\pi y dy$$

$$\frac{W_o + W_1}{\pi g_o} = \frac{p}{R_g T_{oo}} U_c R^2 \int_0^1 \frac{T_{oo}}{T} \frac{u}{U_c} 2\eta d\eta$$

Now $\frac{u}{U_c} = f_2(\eta) + \gamma g_2(\eta)$

$$\frac{T}{T_{oo}} = 1 + \sqrt{f_o(\eta)} - S_o \left(\frac{U_c}{U_{jo}} \right)^2 \left[f_2(\eta) + \gamma g_2(\eta) \right]^2$$

where $\frac{T_o - T_{oo}}{T_{oj}} = \sqrt{f_o(\eta)}$ (Free jet temperature profile) is assumed to hold in Part 2 as a simplification of the analysis.

The value of T_{oo} used in the definitions of BP and S_o , and throughout the Part 2 analysis, is the stagnation temperature for the wall streamline at the axial position selected. T_{oo} varies with x in Part 2.

Let
$$D = \frac{T}{T_{oo}}$$

$$BP = \frac{R_g T_{oo}}{U_{jo}^2}$$

The continuity equation may be rewritten as follows:

$$\frac{T_{ooi}}{P_{ooi}} \frac{R_g}{R_o^2} \frac{W_o + W}{\pi g_o U_{jo}} = \frac{\frac{P}{P_{ooi}}}{\left(\frac{T_{oo}}{T_{ooi}}\right)} \frac{U_c}{U_{jo}} \frac{R_o^2}{R_o^2} Z_{11}$$

where
$$Z_{11} = \int_0^1 \frac{(f_2 + \gamma g_2) 2\eta d\eta}{D}$$

In the computer analysis, the integration is approximated by a summation across the flow:

$$Z_{1J} = \frac{2}{n_s} \sum_{i=1}^{n_s} \frac{N_{iJ}}{D_{iJ}} \eta_i$$

In this equation, N_i and D_i are average values of the numerator and denominator across the i^{th} equal-radius annular segment of the flow.

The following additional definitions will be used:

$$Z_{2J} = \frac{\partial Z_{1J}}{\partial \left(\frac{U_c}{U_{jo}}\right)} = \frac{2}{n_s} \sum_{i=1}^{n_s} - \frac{N_{iJ}}{D_{iJ}^2} \frac{\partial D_{iJ}}{\partial \left(\frac{U_c}{U_{jo}}\right)} \eta_i$$

$$Z_{5J} + Z_{6J} = \frac{\partial Z_{1J}}{\partial \eta} = \frac{2}{n_s} \sum_{i=1}^{n_s} \frac{1}{D_{iJ}} \frac{\partial N_{iJ}}{\partial \eta} \eta_i + \frac{2}{n_s} \sum_{i=1}^{n_s} - \frac{N_{iJ}}{D_{iJ}^2} \frac{\partial D_{iJ}}{\partial \eta} \eta_i$$

$$Z_{7J} + Z_{9J} = \frac{\partial Z_{1J}}{\partial \gamma} = \frac{2}{n_s} \sum_{i=1}^{n_s} \frac{1}{D_{iJ}} \frac{\partial N_{iJ}}{\partial \gamma} \eta_i + \frac{2}{n_s} \sum_{i=1}^{n_s} - \frac{N_{iJ}}{D_{iJ}^2} \frac{\partial D_{iJ}}{\partial \gamma} \eta_i$$

$$Z_{8J} = \frac{\partial Z_{1J}}{\partial \left(\frac{T_{oo}}{T_{ool}} \right)} = \frac{2}{n_s} \sum_{i=1}^{n_s} - \frac{N_{iJ}}{D_{iJ}^2} \frac{\partial D_{iJ}}{\partial \left(\frac{T_{oo}}{T_{ool}} \right)} \eta_i$$

Employing these definitions in the continuity equation, the following equation is obtained after differentiating:

$$\begin{aligned} 0 = & \left(\frac{p}{P_{ool}} \right)' \frac{U_c}{\left(\frac{T_{oo}}{T_{ool}} \right)} \frac{R_o^2}{R_o^2} Z_{11} + \left(\frac{U_c}{U_{jo}} \right)' \frac{p}{\left(\frac{T_{oo}}{T_{ool}} \right)} \frac{R_o^2}{R_o^2} Z_{11} + 2 \frac{p}{\left(\frac{T_{oo}}{T_{ool}} \right)} \frac{U_c}{U_{jo}} \frac{R_o}{R_o} \left(\frac{R_o'}{R_o} \right) Z_{11} \\ & - \left(\frac{T_{oo}}{T_{ool}} \right)' \frac{p}{\left(\frac{T_{oo}}{T_{ool}} \right)^2} \frac{U_c}{U_{jo}} \frac{R_o^2}{R_o^2} Z_{11} + \frac{p}{\left(\frac{T_{oo}}{T_{ool}} \right)} \frac{U_c}{U_{jo}} \frac{R_o^2}{R_o^2} \left[Z_{21} \frac{U_c'}{U_{jo}} + (Z_{51} + Z_{61}) \eta' \right] \\ & + \frac{p}{\left(\frac{T_{oo}}{T_{ool}} \right)} \frac{U_c}{U_{jo}} \frac{R_o^2}{R_o^2} \left[(Z_{71} + Z_{91}) \gamma' + Z_{81} \left(\frac{T_{oo}}{T_{ool}} \right)' \right] \end{aligned}$$

Collecting terms and dividing each by $\left(\frac{p}{P_{ool}} \right) \frac{U_c}{U_{jo}} \frac{R_o^2}{R_o^2}$;

$$W(1,1) = \frac{Z_{11}}{\left(\frac{U_c}{U_{jo}}\right)} + Z_{21}$$

$$W(1,5) = Z_{51} + Z_{61}$$

$$W(1,2) = 0$$

$$W(1,6) = Z_{81} - \frac{Z_{11}}{\left(\frac{T_{oo}}{T_{ool}}\right)}$$

$$W(1,3) = Z_{71} + Z_{91}$$

$$V(1) = -2 \frac{\left(\frac{R}{R_o}\right)'}{\left(\frac{R}{R_o}\right)} Z_{11}$$

$$W(1,4) = \frac{Z_{11}}{\left(\frac{p}{p_{ool}}\right)}$$

Table A2 lists the values of N_i , D_i , and their derivatives which are required to evaluate the Z parameters in the previous equations.

A2.2 Equation for $J = 2$; Energy Equation

$$\text{constant} = \int_0^R \rho u T_o \cdot 2\pi y dy$$

assuming constant specific
heat throughout the flow

Using the substitutions for ρ , the velocity profile functions, and η as in Section A2.1, the energy equation may be rewritten as follows:

$$\text{constant} = \frac{p}{R_g T_{oo}} U_c R^2 \int_0^1 \frac{[f_2(\eta) + \gamma g_2(\eta)]}{D} T_o 2\eta d\eta$$

As in Section A2.1, the free-jet temperature profile is assumed to hold:

$$\frac{T_o}{T_{oo}} = 1 + \sqrt{f_o(\eta)}$$

With this, the energy equation becomes:

$$\text{constant} = \frac{p}{R_g} U_c R^2 \int_0^1 \frac{(f_2 + \gamma g_2) (1 + T f_o^{1/2})}{D} 2\eta d\eta$$

$$\text{constant} = \frac{p}{P_{ooi}} \frac{U_c}{U_{jo}} \frac{R^2}{R_o^2} Z_{12}$$

$$\text{where } Z_{12} = \int_0^1 \frac{(f_2 + \gamma g_2) (1 + T f_o^{1/2})}{D} 2\eta d\eta$$

After differentiating with respect to $\frac{x}{R_o}$, the energy equation takes the following form:

$$0 = \left(\frac{p}{P_{ooi}} \right)' \frac{U_c}{U_{jo}} \frac{R^2}{R_o^2} Z_{12} + \left(\frac{U_c}{U_{jo}} \right)' \frac{p}{P_{ooi}} \frac{R^2}{R_o^2} Z_{12} + \left(\frac{R}{R_o} \right)'^2 \frac{p}{P_{ooi}} \frac{U_c}{U_{jo}} \frac{R}{R_o} Z_{12} \\ + \frac{p}{P_{ooi}} \frac{U_c}{U_{jo}} \frac{R^2}{R_o^2} \left[Z_{22} \left(\frac{U_c}{U_{jo}} \right)' + (Z_{52} + Z_{62}) T' + (Z_{72} + Z_{92}) \gamma' + Z_{82} \left(\frac{T_{oo}}{T_{ooi}} \right)' \right]$$

Collecting terms and dividing each by $\frac{p}{P_{ooi}} \frac{U_c}{U_{jo}} \frac{R^2}{R_o^2}$,

$$W(2,1) = \frac{Z_{12}}{\left(\frac{U_c}{U_{jo}} \right)} + Z_{22}$$

$$W(2,5) = Z_{52} + Z_{62}$$

$$W(2,2) = 0$$

$$W(2,6) = Z_{82}$$

$$W(2,3) = Z_{72} + Z_{92}$$

$$V(2) = -2Z_{12} \frac{(R'/R_o)}{(R/R_o)}$$

$$W(2,4) = \frac{Z_{12}}{\left(\frac{p}{P_{ooi}} \right)}$$

Table A2 lists the values of N_i , D_i , and their derivatives which are required to evaluate the Z parameters in the equations above.

A2.3 Equation for $J = 3$; Momentum Equation

$$-\pi R^2 \frac{dp}{dx} - 2\pi R \tau_w = \frac{d}{dx} \int_0^R \rho u^2 2\pi y dy$$

Using the previously-developed substitution for ρ , the velocity profile functions, and η :

$$-R^2 \frac{dp}{dx} - 2R \tau_w = \frac{d}{dx} \left\{ \frac{p}{R_g T_{oo}} U_c^2 R^2 \int_0^1 \frac{2 [f_2(\eta) + \gamma g_2(\eta)]^2}{D} \eta d\eta \right\}$$

Let $\tau_w = C_{fd} \frac{1}{2} \frac{\rho U_c^2}{g_o}$ where $\frac{\rho}{g_o} \cong \frac{p}{R_g T_{oo}}$

The momentum equation may be rewritten as follows:

$$-R^2 \frac{dp}{dx} - RC_{fd} U_c^2 \frac{p}{R_g T_{oo}} = \frac{d}{dx} \left\{ \frac{p}{R_g T_{oo}} U_c^2 R^2 Z_{13} \right\}$$

where

$$Z_{13} = \int_0^1 \frac{(f_2 + \gamma g_2)^2 2\eta d\eta}{D}$$

Normalizing:

$$-\left(\frac{R}{R_o}\right)^2 \left(\frac{p}{P_{ooi}}\right)' - \frac{R}{R_o} C_{fd} \left(\frac{U_c}{U_{jo}}\right)^2 \frac{p}{P_{ooi}} \frac{1}{BP} = \frac{d}{d\left(\frac{x}{R_o}\right)} \left\{ \frac{p}{P_{ooi}} \frac{U_{jo}^2}{R_g T_{oo}} \frac{U_c^2}{U_{jo}^2} \frac{R^2}{R_o^2} Z_{13} \right\}$$

Differentiating:

$$\left[-\left(\frac{R}{R_o}\right)^2 \left(\frac{p}{P_{ooi}}\right)' - \frac{R}{R_o} C_{fd} \left(\frac{U_c}{U_{jo}}\right)^2 \frac{p}{P_{ooi}} \frac{1}{BP} \right] = \frac{Z_{13}}{BP} \left[\left(\frac{p}{P_{ooi}}\right)' \left(\frac{U_c}{U_{jo}}\right)^2 \frac{R^2}{R_o^2} + \left(\frac{U_c}{U_{jo}}\right)' \frac{2p}{P_{ooi}} \frac{U_c}{U_{jo}} \frac{R^2}{R_o^2} \right] + (\text{see next page})$$

$$\begin{aligned}
& + \frac{Z_{13}}{BP} \left(\frac{R}{R_o} \right)' \frac{p}{P_{ooi}} \frac{U_c^2}{U_{jo}^2} \frac{R}{R_o} \\
& - \frac{T_{oo}'}{T_{ooi}} \frac{p}{P_{ooi}} \left(\frac{T_{oo}}{T_{ooi}} \right) \frac{U_c^2}{U_{jo}^2} \frac{R^2}{R_o^2} \frac{Z_{13}}{BP} \\
& + \frac{p}{P_{ooi}} \frac{\frac{U_c^2}{U_{jo}^2}}{BP} \frac{R^2}{R_o^2} \left[Z_{23} \left(\frac{U_c}{U_{jo}} \right)' + (Z_{53} + Z_{63}) \mathcal{U}' + (Z_{73} + Z_{93}) \gamma' + Z_{83} \frac{T_{oo}'}{T_{ooi}} \right]
\end{aligned}$$

Collecting terms and dividing each by $\frac{p}{P_{ooi}} \frac{U_c^2}{U_{jo}^2} \frac{R^2}{R_o^2} \frac{1}{BP}$;

$$W(3, 1) = \frac{2Z_{13}}{\left(\frac{U_c}{U_{jo}} \right)} + Z_{23}$$

$$W(3, 5) = Z_{53} + Z_{63}$$

$$W(3, 2) = 0$$

$$W(3, 6) = \frac{-Z_{13}}{\left(\frac{T_{oo}}{T_{ooi}} \right)} + Z_{83}$$

$$W(3, 3) = Z_{73} + Z_{93}$$

$$W(3, 4) = \frac{BP}{\frac{p}{P_{ooi}} \frac{U_c^2}{U_{jo}^2}} + \left(\frac{Z_{13}}{\frac{p}{P_{ooi}}} \right)$$

$$V(3) = - \frac{C_{fd}}{\frac{R}{R_o}} - 2Z_{13} \frac{\left(\frac{R'}{R_o} \right)}{\left(\frac{R}{R_o} \right)}$$

Table A2 lists the values of N_i , D_i , and their derivatives which are required to evaluate the Z parameters in the equations above.

A2.4 Equation for J = 4; Moment-of-Momentum Integral Equation

The moment-of-momentum integral equation is taken from Section A1.5 of this appendix:

$$\int_0^R \rho u y \frac{\partial u}{\partial x} y dy + \int_0^R \rho v y \frac{\partial u}{\partial y} y dy = \int_0^R \frac{\partial (\tau y)}{\partial y} y dy - \int_0^R \frac{dp}{dx} y^2 dy$$

Noting that, in Part 2, $u = U_c (f_2 + \gamma g_2)$

$$\frac{\partial u}{\partial x} = \frac{1}{R_o} U_c' (f_2 + \gamma g_2) - \frac{U_c}{R_o} \left(\frac{\partial f_2}{\partial \eta} + \gamma \frac{\partial g_2}{\partial \eta} \right) \eta \frac{\left(\frac{R'}{R_o} \right)}{\left(\frac{R}{R_o} \right)} + \frac{U_c g_2}{R_o} \gamma'$$

$$\frac{\partial u}{\partial y} = \frac{U_c}{R} \left(\frac{\partial f_2}{\partial \eta} + \gamma \frac{\partial g_2}{\partial \eta} \right)$$

$$\begin{aligned} \text{then } \int_0^R \rho u y \frac{\partial u}{\partial x} y dy &= \int_0^1 \frac{p}{R_g T_{oo}} \frac{U_c (f_2 + \gamma g_2) \frac{\partial u}{\partial x} \eta^2 d\eta}{D} R^3 \\ &= \frac{p}{R_g T_{oo}} U_c^2 R^3 \int_0^1 \frac{\frac{1}{U_c} (f_2 + \gamma g_2) \frac{\partial u}{\partial x} \eta^2 d\eta}{D} \\ &= \frac{p U_c^2 R^3}{R_g T_{oo} R_o} \left[\frac{U_c'}{U_c} Q_1 + \frac{\left(\frac{R'}{R_o} \right)}{\left(\frac{R}{R_o} \right)} Q_3 + \gamma' Q_4 \right] \end{aligned}$$

In which

$$Q_1 = \int_0^1 \frac{(f_2 + \gamma g_2)^2 \eta^2 d\eta}{D}$$

$$Q_3 = - \int_0^1 \frac{\left(\frac{\partial f_2}{\partial \eta} + \gamma \frac{\partial g_2}{\partial \eta} \right)}{D} (f_2 + \gamma g_2) \eta^3 d\eta$$

$$Q_4 = \int_0^1 \frac{(f_2 + \gamma g_2)}{D} g_2 \eta^2 d\eta$$

$$D = 1 + \mathcal{T} \sqrt{f_o(\eta)} - S_o \left(\frac{U_c}{U_{jo}} \right)^2 (f_2 + \gamma g_2)^2$$

Following the analysis in Section A1.5, the second integral is evaluated as follows:

$$\rho v y = - \int_0^y \frac{\partial}{\partial x} \left[\frac{p}{R_g T_{oo}} \frac{U_c (f_2 + \gamma g_2)}{D} \right] y dy$$

$$\rho v y = - \int_0^\eta \frac{R^2}{R_o R_g T_{oo}} \left\{ \frac{p' U_c (f_2 + \gamma g_2)}{D} + \frac{p U_c' (f_2 + \gamma g_2)}{D} \right.$$

$$\left. + \frac{p U_c}{D} \left[- \left(\frac{\partial f_2}{\partial \eta} + \gamma \frac{\partial g_2}{\partial \eta} \right) \eta \frac{\left(\frac{R'}{R_o} \right)}{\left(\frac{R}{R_o} \right)} + g_2 \gamma' \right] \right\}$$

$$- \frac{p U_c (f_2 + \gamma g_2)}{D^2} \left[\mathcal{T}' \frac{\partial D}{\partial \mathcal{T}} + U_c' \frac{\partial D}{\partial U_c} + \gamma' \frac{\partial D}{\partial \gamma} - \eta \frac{\left(\frac{R'}{R_o} \right)}{\left(\frac{R}{R_o} \right)} \frac{\partial D}{\partial \eta} \right] \eta d\eta$$

$$\begin{aligned}
& \frac{-\rho v y}{\frac{p}{R_g T_{\infty}} U_c \frac{R^2}{R_o}} \left[\begin{aligned} & \frac{U_c'}{U_c} \int_0^\eta \left[\frac{(f_2 + \gamma g_2)}{D} - \frac{(f_2 + \gamma g_2)}{D^2} \frac{\partial D}{\partial \frac{U_c}{U_{jo}}} \frac{U_c}{U_{jo}} \right] \eta d\eta \\ & + \gamma' \int_0^\eta \left[\frac{g_2}{D} - \frac{(f_2 + \gamma g_2)}{D^2} \frac{\partial D}{\partial \gamma} \right] \eta d\eta \\ & + \frac{p'}{p} \int_0^\eta \frac{(f_2 + \gamma g_2)}{D} \eta d\eta \\ & + T' \int_0^\eta - \frac{(f_2 + \gamma g_2)}{D^2} \frac{\partial D}{\partial T} \eta d\eta \\ & + \left(\frac{R'}{R_o} \right) \int_0^\eta \left[- \left(\frac{\partial f_2}{\partial \eta} + \gamma \frac{\partial g_2}{\partial \eta} \right) \frac{1}{D} + \frac{(f_2 + \gamma g_2)}{D^2} \frac{\partial D}{\partial \eta} \right] \eta^2 d\eta \end{aligned} \right] = \left[\begin{aligned} & \frac{U_c'}{U_c} \left[V_1 + V_2 \frac{U_c}{U_{jo}} \right] \\ & + \gamma' [V_7 + V_9] \\ & + \frac{p'}{p} [V_1] \\ & + T' [V_5 + V_6] \\ & + \left(\frac{R'}{R_o} \right) \left[-V_{10} - V_{11} \right] \end{aligned} \right]
\end{aligned}$$

in which

$$V_1 = \int_0^\eta \frac{(f_2 + \gamma g_2)}{D} \eta d\eta$$

$$V_7 = \int_0^\eta \frac{g_2}{D} \eta d\eta$$

$$V_2 = \int_0^\eta - \frac{(f_2 + \gamma g_2)}{D^2} \frac{\partial D}{\partial \frac{U_c}{U_{jo}}} \eta d\eta$$

$$V_9 = \int_0^\eta \frac{-(f_2 + \gamma g_2)}{D^2} \frac{\partial D}{\partial \gamma} \eta d\eta$$

$$V_5 = 0$$

$$V_{10} = \int_0^\eta \frac{\left(\frac{\partial f_2}{\partial \eta} + \gamma \frac{\partial g_2}{\partial \eta} \right)}{D} \eta^2 d\eta$$

$$V_6 = \int_0^\eta - \frac{(f_2 + \gamma g_2)}{D^2} \frac{\partial D}{\partial \mathcal{U}} \eta d\eta \quad V_{11} = \int_0^\eta \frac{-(f_2 + \gamma g_2)}{D^2} \frac{\partial D}{\partial \eta} \eta^2 d\eta$$

With these definitions, the integral

$$\int_0^R \rho v y \frac{\partial u}{\partial y} y dy$$

may be evaluated as follows:

$$\begin{aligned} \frac{\int_0^R \rho v y \frac{\partial u}{\partial y} y dy}{\frac{p}{R_g T_{oo}} \frac{U_c R^3}{R_o}} &= \int_0^1 \left[\frac{\rho v y}{\frac{p}{R_g T_{oo}} U_c \frac{R^2}{R_o}} \right] \left(\frac{\partial f_2}{\partial \eta} + \gamma \frac{\partial g_2}{\partial \eta} \right) \eta d\eta \\ &= \frac{U_c'}{U_c} \left[- \int_0^1 V_1 \left(\frac{\partial f_2}{\partial \eta} + \gamma \frac{\partial g_2}{\partial \eta} \right) \eta d\eta - \frac{U_c}{U_{jo}} \int_0^1 V_2 \left(\frac{\partial f_2}{\partial \eta} + \gamma \frac{\partial g_2}{\partial \eta} \right) \eta d\eta \right] \\ &+ \gamma' \left[- \int_0^1 (V_7 + V_9) \left(\frac{\partial f_2}{\partial \eta} + \gamma \frac{\partial g_2}{\partial \eta} \right) \eta d\eta \right] + \frac{p'}{p} \left[- \int_0^1 V_1 \left(\frac{\partial f_2}{\partial \eta} + \gamma \frac{\partial g_2}{\partial \eta} \right) \eta d\eta \right] \\ &+ \mathcal{U}' \left[- \int_0^1 (V_5 + V_6) \left(\frac{\partial f_2}{\partial \eta} + \gamma \frac{\partial g_2}{\partial \eta} \right) \eta d\eta \right] + \left(\frac{R'}{R_o} \right) \left[\int_0^1 (V_{10} + V_{11}) \left(\frac{\partial f_2}{\partial \eta} + \gamma \frac{\partial g_2}{\partial \eta} \right) \eta d\eta \right] \\ &= \frac{U_c'}{U_c} \left[R_1 + \frac{U_c}{U_{jo}} R_2 \right] + \gamma' [R_{79}] + \frac{p'}{p} R_1 + \mathcal{U}' R_{56} + \left(\frac{R'}{R_o} \right) (R_{10} + R_{11}) \end{aligned}$$

in which $R_1 = - \int_0^1 V_1 \left(\frac{\partial f_2}{\partial \eta} + \gamma \frac{\partial g_2}{\partial \eta} \right) \eta d\eta$ $R_{79} = - \int_0^1 (V_7 + V_9) \left(\frac{\partial f_2}{\partial \eta} + \gamma \frac{\partial g_2}{\partial \eta} \right) \eta d\eta$

$R_2 = - \int_0^1 V_2 \left(\frac{\partial f_2}{\partial \eta} + \gamma \frac{\partial g_2}{\partial \eta} \right) \eta d\eta$ $R_{10} = \int_0^1 V_{10} \left(\frac{\partial f_2}{\partial \eta} + \gamma \frac{\partial g_2}{\partial \eta} \right) \eta d\eta$

$R_{56} = - \int_0^1 (V_5 + V_6) \left(\frac{\partial f_2}{\partial \eta} + \gamma \frac{\partial g_2}{\partial \eta} \right) \eta d\eta$ $R_{11} = \int_0^1 V_{11} \left(\frac{\partial f_2}{\partial \eta} + \gamma \frac{\partial g_2}{\partial \eta} \right) \eta d\eta$

The pressure gradient term may be written as follows:

$$\int_0^R \frac{dp}{dx} y^2 dy = \frac{p}{R_g T_{oo}} \frac{U_c^2 R^3}{R_o} \left[\frac{p'}{p} \frac{1}{3} - \frac{BP}{\frac{U_c^2}{U_{jo}^2}} \right]$$

The shear stress term may be evaluated as follows:

$$\int_0^R \frac{\partial(\tau y)}{\partial y} y dy = \tau y^2 \Big|_0^R - \int_0^R \tau y dy$$

$$\tau = \rho \epsilon \frac{\partial u}{\partial y} = \rho \epsilon \frac{U_c}{R} \left(\frac{\partial f_2}{\partial \eta} + \gamma \frac{\partial g_2}{\partial \eta} \right) \text{ where } \epsilon \text{ is the eddy kinematic viscosity}$$

$$\frac{\int_0^R \frac{\partial(\tau y)}{\partial y} y dy}{\frac{p}{R_g T_{oo}} \frac{U_c^2 R^3}{R_o}} = -(1/2) C_{fd} \frac{R_o}{R} - \int_0^1 \rho \epsilon \frac{1}{U_c R^2} \left(\frac{\partial f_2}{\partial \eta} + \gamma \frac{\partial g_2}{\partial \eta} \right) \frac{R_g T_{oo} R_o}{p} \eta d\eta$$

$$= -(1/2)C_{fd} \frac{R_o}{R} - \frac{R_o}{R} \int_0^1 \frac{\epsilon}{U_c R} \frac{1}{D} \left(\frac{\partial f_2}{\partial \eta} + \gamma \frac{\partial g_2}{\partial \eta} \right) \eta d\eta$$

$$= \frac{R_o}{R} A_\tau - \frac{R_o}{R} \frac{C_{fd}}{2}$$

$$\text{where } A_\tau = - \int_0^1 E_2 \frac{\left(\frac{\partial f_2}{\partial \eta} + \gamma \frac{\partial g_2}{\partial \eta} \right)}{D} \eta d\eta$$

$$E_2 = \frac{\epsilon}{U_c R} \text{ in Part 2}$$

Assembling all the terms, the final moment-of-momentum integral equation is as follows:

$$\begin{aligned} & \frac{U_c'}{U_c} \left[Q_1 + R_1 + \frac{U_c}{U_{jo}} R_2 \right] + \gamma' \left[Q_4 + R_{79} \right] + \frac{p'}{p} \left[R_1 + \frac{1}{3} \frac{\frac{BP}{2}}{\left(\frac{U_c}{U_{jo}} \right)^2} \right] + \mathcal{T}'_{R56} \\ & = - \frac{\left(\frac{R'}{R_o} \right)}{\left(\frac{R}{R_o} \right)} \left[Q_3 + R_{10} + R_{11} \right] + \frac{R_o}{R} A_\tau - \frac{C_{fd}}{2} \frac{R_o}{R} \end{aligned}$$

The values of the coefficients follow:

$$W(4, 1) = Q_1 + R_1 + \frac{U_c}{U_{jo}} R_2 \quad W(4, 5) = R_{56}$$

$$W(4, 2) = 0 \quad W(4, 6) = 0$$

$$\begin{aligned}
W(4,3) &= Q_4 + R_{79} & V(4) &= -\left(\frac{R'}{R_o}\right) \left[Q_3 + R_{10} + R_{11}\right] \\
&& &+ \frac{R_o}{R} A_\tau - \frac{C_{fd}}{2} \frac{R_o}{R} \\
W(4,4) &= R_1 + \frac{1}{3} \frac{BP}{\left(\frac{U_c}{U_{jo}}\right)^2}
\end{aligned}$$

A2.5 Equation for J = 5; Centerline Velocity - Temperature Relationship

The experimental measurements made during this investigation have shown, as in figure 10, that for any value of $\frac{x}{R_o}$ in part 2,

$$\frac{T_j}{T_{jo}} \cong \frac{U_c}{U_{jo}} \times \text{const} \quad \text{Note } U_c = U_J \text{ in Part 2 Because } U_o = 0 \text{ is assumed}$$

$$\frac{1}{\frac{T_j}{T_{jo}}} \frac{\partial \left(\frac{T_j}{T_{jo}} \right)}{\partial \left(\frac{x}{R_o} \right)} = \frac{1}{\frac{U_c}{U_{jo}}} \frac{\partial \left(\frac{U_c}{U_{jo}} \right)}{\partial \left(\frac{x}{R_o} \right)}$$

$$\text{now} \quad \frac{T_j}{T_{jo}} = \mathcal{U} \frac{T_{ooi}}{T_{jo}} \frac{T_{oo}}{T_{ooi}}$$

$$\text{so} \quad \left(\frac{T_j}{T_{jo}} \right)' = \frac{T_{ooi}}{T_{jo}} \left[\mathcal{U}' \frac{T_{oo}}{T_{ooi}} + \mathcal{U} \left(\frac{T_{oo}}{T_{ooi}} \right)' \right]$$

$$\frac{\left(\frac{T_j}{T_{jo}}\right)'}{\left(\frac{T_j}{T_{jo}}\right)} = \frac{U' \frac{T_{oo}}{T_{ooi}} + U \left(\frac{T_{oo}}{T_{ooi}}\right)'}{\frac{T_{oo}}{T_{ooi}}} = \frac{\left(\frac{U_c}{U_{jo}}\right)'}{\left(\frac{U_c}{U_{jo}}\right)}$$

finally,

$$\frac{U'}{U} + \frac{\left(\frac{T_{oo}}{T_{ooi}}\right)'}{\left(\frac{T_{oo}}{T_{ooi}}\right)} = \frac{\left(\frac{U_c}{U_{jo}}\right)'}{\left(\frac{U_c}{U_{jo}}\right)}$$

The values of the coefficients follow:

$$W(5, 1) = \frac{1}{\left(\frac{U_c}{U_{jo}}\right)}$$

$$W(5, 5) = - \frac{1}{U}$$

$$W(5, 2) = 0$$

$$W(5, 6) = - \frac{1}{\left(\frac{T_{oo}}{T_{ooi}}\right)}$$

$$W(5, 3) = 0$$

$$V(5) = 0$$

$$W(5, 4) = 0$$

A2.6 Equation for J = 6; Wall Velocity = 0

The value of U_o is assumed to be zero throughout Part 2. Therefore,

$$\frac{U_o'}{U_c} = 0$$

$$\text{and } W(6, 1) = W(6, 3) = W(6, 4) = W(6, 5) = W(6, 6) = V(6) = 0$$

$$W(6, 2) = 1$$

Table A1
Values Required to Determine Z Parameters in Part 1

	J = 2 Momentum	J = 3 Continuity	J = 4 Energy
N_{ij}	$(\lambda + f_{oi})^2$	$\lambda + f_{oi}$	$(\lambda + f_{oi})(1 + \mathcal{T} f_{oi}^{1/2})$
$\frac{\partial N_{ij}}{\partial \lambda}$	$2 (\lambda + f_{oi})$	1	$1 + \mathcal{T} f_{oi}^{1/2}$
$\frac{\partial N_{ij}}{\partial \mathcal{T}}$	0	0	$(\lambda + f_{oi}) f_{oi}^{1/2}$
D_{ij}	$1 + \mathcal{T} f_{oi}^{1/2} - S_o \frac{U_j^2}{U_{jo}^2} (\lambda + f_{oi})^2$		
$\frac{\partial D_{ij}}{\partial (\frac{U_j}{U_{jo}})}$	$- 2 S_o \frac{U_j}{U_{jo}} (\lambda + f_{oi})^2$		
$\frac{\partial D_{ij}}{\partial \lambda}$	$- 2 S_o \frac{U_j^2}{U_{jo}^2} (\lambda + f_{oi})$		
$\frac{\partial D_{ij}}{\partial \mathcal{T}}$	$f_{oi}^{1/2}$		

Table A2
Values Required to Determine Z Parameters in Part 2

	J = 1 Continuity	J = 2 Energy	J = 3 Momentum
N_{ij}	$(f_{2i} + \gamma g_{2i})$	$(f_{2i} + \gamma g_{2i}) (1 + \mathcal{T} f_{oi}^{1/2})$	$(f_{2i} + \gamma g_{2i})^2$
$\frac{\partial N_{ij}}{\partial \mathcal{T}}$	0	$(f_{2i} + \gamma g_{2i}) f_{oi}^{1/2}$	0
$\frac{\partial N_{ij}}{\partial \gamma}$	g_{2i}	$g_{2i} (1 + \mathcal{T} f_{oi}^{1/2})$	$2g_{2i} (f_{2i} + \gamma g_{2i})$
D_{ij}	$1 + \mathcal{T} \sqrt{f_{oi}(\eta)} - S_o \left(\frac{U_c}{U_{jo}} \right)^2 [f_2(\eta) + \gamma g_2(\eta)]^2$		
$\frac{\partial D_{ij}}{\partial \frac{U_c}{U_{jo}}}$	$-2 \frac{U_c}{U_{jo}} S_o [f_{2i} + \gamma g_{2i}]^2$		
$\frac{\partial D_{ij}}{\partial \mathcal{T}}$	$f_{oi}^{1/2}$		
$\frac{\partial D_{ij}}{\partial \gamma}$	$-2 S_o \left(\frac{U_c}{U_{jo}} \right)^2 (f_{2i} + \gamma g_{2i}) g_{2i}$		
$\frac{\partial D_{ij}}{\partial \left(\frac{T_{oo}}{T_{ool}} \right)}$	$-\left(\frac{U_c}{U_{jo}} \right)^2 (f_{2i} + \gamma g_{2i})^2 \frac{\partial S_o}{\partial \left(\frac{T_{oo}}{T_{ool}} \right)}$		

Appendix B

THE COMPUTER PROGRAM

B.1 General Description

The computer program has 10 sections. The general functions of each section are described below.

MAIN: The program begins and ends in MAIN. Input data concerning the jet pump geometry, inlet gas flow properties, free jet velocity profile, and stations along the mixing tube where output values are desired, are all read in by MAIN and by two subroutines called by MAIN--DIFFEQ and SUB. MAIN converts the units of the input parameters into other units which are more convenient for subsequent analysis.

After conversion of units, MAIN computes the primary and secondary flow conditions at the top-hat section as described in Section 3.3 of this report. Then MAIN sets up the initial trial values for the velocity profile after transition and calls VBO4A to perform the iterations required to obtain an accurate solution for the profile.

After the transition zone analysis has been completed, MAIN sets up the initial conditions for the flow analysis upstream of the point of jet attachment to the wall. It also defines the stations along the mixing tube for which data will be printed out. MAIN then calls RUNGE to carry out the solution for the remainder of the flow analysis.

SUB: The first section of SUB, called when $J = 3$, reads in data on the mixing tube geometry--inner diameter vs. length. The diameters are converted to radii and all radii and length values are made non-dimensional by dividing by R_0 . The second section of SUB, called when $J = 1$ or 2 , finds the duct radius and slope at any axial position x specified as an input value to the subroutine.

The procedure used is linear interpolation between the nearest upstream and downstream radii which were read as input data by the first section of SUB.

CALXFG: The purpose of CALXFG is to perform the computations required to set up the three transition zone equations (27), (33), and (35) for solution by VBO4A. The three equations and derivatives of each of the three equations with respect to the three variables U_r , λ , and δ/R_{eff} are computed in CALXFG.

VBO4A, VDO2A, and SPNIST: These subroutines are library routines employed to solve the three simultaneous non-linear algebraic equations (27), (33), and (35). A two-page discussion of these subroutines is included at the end of section B.3.

DIFFEQ: The DIFFEQ subroutine is divided into two parts. Part I establishes the 7 simultaneous equations (39) which must be solved to determine the flow conditions upstream of jet attachment. The equations used are outlined in section 3.4 and detailed in appendix A.1. When the simultaneous equations are set up, DIFFEQ calls subroutine SIMQ to solve the equations for the values of the 7 derivatives in equation (38). Then subroutine RUNGE is called to integrate the derivatives using Runge-Kutta-Merson techniques. This integration yields the values of U_j , U_o , δ , p , T_{oj} , Θ , and H at stations closely spaced along the duct.

Part 2 of DIFFEQ establishes the 6 simultaneous equations (48) which must be solved to determine the flow conditions in the mixing tube downstream of jet attachment to the wall. The equations used are outlined in section 3.5 and detailed in appendix A.2. Subroutine SIMQ is called to solve for the 6 derivatives in equation (47). Then subroutine RUNGE integrates the derivatives to find the values of U_o , γ , p , T_{oj} , and T_{oo} at stations closely spaced along the duct.

SIMQ: This is a library subroutine which is called by DIFFEQ to solve simultaneous linear equations to find the values of the $Y(K)$ derivatives in equations (38) and (47).

RUNGE: The RUNGE subroutine performs a Runge-Kutta-Merson integration procedure to integrate the derivatives of the Y(K) quantities which are developed by DIFFEQ and SIMQ as described above. RUNGE also calls the subroutine PRINT to print the desired output values of jet pump flow parameters at each mixing tube station (XOUT) which has been specified by input data and equations in MAIN.

PRINT: This subroutine contains instructions for printing the computer jet pump flow parameters at selected stations along the mixing tube downstream of the transition zone.

B.2 Input Data Format

The input data to the program must be prepared according to the following sequence:

<u>Card No.</u>	<u>Parameters</u>	<u>Format</u>
1	NS	3I2
2	GG(I), I = 1, NS	10F5.4
3	SDLOSS, ASD	2F10.3
4	THETA, SHAPE, VISC, RZERO	4F10.6
5	1-CARD MESSAGE identifying solution desired	80H
6	DELTA _X , XTUBE, TURBNO, NSUB, NGAM, XCORE, ANOZ	3F10.4, 2I5, 2F10.5
7	POO, TOO, PO1, T01, AMASS1, AMASSO, AG, RG	8F7.3
8 to 8 + I	X(I), A(I)	2F15.4
8 + I + 1	0.0	2F15.4
} omit if NSUB = 2		

Cards 1 through 7 are required for each solution desired. The cards from 8 on are required to define a new mixing tube geometry for analysis. If the same mixing tube geometry is to be used for additional solutions with altered flow conditions, the cards from 8 on do not have to be included for these additional solutions. The input parameter NSUB tells the computer whether the cards from 8 on are included with a data set, i. e., whether the same mixing tube geometry is to be used for additional solutions.

The input parameters are described below.

NS	number (= 10) of equal-radial-increment strips used to approximate the jet mass flow, momentum, and energy integrals across the jet
GG(I)	average values of $\frac{U}{U_c}(\eta)$ for $I = NS$ equal-radial-increment strips for the turbulent pipe flow velocity profile
SDLOSS	suction duct loss coefficient; K_L in equation (55)
ASD	suction duct area, ft^2 ; A_{SD} in equation (55)
THETA	boundary layer momentum thickness at $x = 0$, ft
SHAPE	boundary layer shape factor at $x = 0$
VISC	gas kinematic viscosity for secondary flow at inlet, ft^2/sec
RZERO	mixing tube radius at nozzle exit section; $x = 0$, ft
DELTA X	steps of x/R_o at which data printouts are desired in the mixing tube
XTUBE	mixing tube length, ft
TURBNO	turbulent Reynolds number value = 147
NSUB	control instruction: if 1, a new mixing tube geometry is read in if 2, the tube geometry from the previous solution will be used.
NGAM	control instruction: if 0, incompressible flow solution (not operable) if 1, compressible flow solution
XCORE	length of the transition zone divided by R_o
ANOZ	primary nozzle exit flow area, ft^2
POO	stagnation pressure upstream of the suction duct losses, psia
TOO	stagnation temperature of the secondary flow, $^{\circ}R$
PO1	stagnation pressure of the primary flow, psia
TO1	stagnation temperature of the primary flow, $^{\circ}R$

AMASS1	mass flow rate of the primary flow, lbm/sec
AMASSO	mass flow rate of the secondary flow, lbm/sec
AG	specific heat ratio of the gas
RG	gas constant, ft-lbf/lbm-°R
X(I)	x stations along the mixing tube at which A(I) values are defined, ft
A(I)	diameter of the mixing tube at the corresponding x_{station} , ft
B.3	<u>Output Data</u>

A complete sample of output data from the computer program is given in section B.5 of this appendix. The first section of the output repeats the input data and thus requires no comment. The remainder of the data is summarized below.

F (I)'s: values of $f_o(\eta)$ at $\eta = 0.05, 0.15, 0.25, \dots, 0.95$

CONDITIONS AT BEGINNING OF THE TRANSITION SECTION

lists values of $U_{oo}, \rho_{oo}, U_{joo}, T_{oo}, p_{oo}$ (psfa and in.H₂O), $\lambda_{oo} = \frac{U_{oo}}{U_{joo}}$, and primary jet momentum = $W_1 U_1$ where U_1 is the velocity achieved by isentropic expansion of the primary flow to the static pressure at the end of the accomodation process, p_{oo} .

The next portion of the printout monitors the solution by VB04A of equations (27), (33), and (35) for the transition zone. Each iteration employing CALXFG is recorded. The VARIABLES are the values of U_r , λ , and δ/R_{eff} determined during the particular iteration reported. The FUNCTIONS are the values of the functions:

$$\frac{C_{mass_new} - C_{mass_old}}{C_{mass_old}}, \quad \frac{C_{mom_new} - C_{mom_old}}{C_{mom_old}}, \quad \frac{P_{const_new} - P_{const_old}}{P_{const_old}}$$

where C_{mass} is defined by equation (27)

C_{mom} is defined by equation (32)

$$P_{const} \text{ is } \left(\frac{P_{ol}}{P_{oo}} \right)^{\frac{k-1}{k}}$$

()_{new} is the value for the current iteration.

()_{old} is the value for the previous iteration.

If these functions are computed to within ERR times the "old" value of C_{mass} , C_{mom} , or P_{const} , VB04A is judged to have converged satisfactorily. In the present program, ERR is set at 10^{-6} , an excessively tight tolerance. As a result, the message "VB04A ACCURACY CANNOT BE ACHIEVED" is often printed out. Following this message, the values of the VARIABLES and FUNCTIONS for the current iteration are printed. These values are used as the first values for subsequent calculations.

Four lines of print follow the end of the VB04A material. The first line restates the values of $XX(1) = U_r$, $XX(2) = \lambda$, and $XX(3) = \delta/R_{eff}$ in numerical form. The second line compares the values of EN, a dimensionless jet pump parameter developed in reference 2, before and after transition (EN vs. EN2).

$$EN = \frac{W_1 + W_o}{\sqrt{2\pi R_o^2 \rho_{oo} \left[g_o(p - P_{oo})\pi R_{eff}^2 + W_1 U_1 + W_o U_o \right]}}$$

The two values should be identical; differences which exist provide a measure of the accuracy of the transition analysis. Following the EN values, the values of S_O and B_P (see appendix A, section A1.1) are printed. Then the final values of U_{jo} and U_{co} are given.

The printing continues with a tabulation of values along the mixing tube given by Part 1 of the analysis. The parameters listed are as follows:

X/RZERO;	values of $\frac{x}{R_o}$ beginning with $\frac{x_{core}}{R_o}$
AREA;	local value of $\frac{\pi R_{tube}^2}{\pi R_o^2}$
PH20;	wall static pressure, in H_2O relative to P_{oo}
U0;	value of U_o , secondary flow velocity
UCENT;	value of U_c , velocity of flow at the centerline
UR;	value of U_c/U_{co}
LAMBDA;	value of $\lambda = \frac{U_o}{U_j}$
DELTA/R;	value of δ/R_o
TOCENT;	value of stagnation temperature at the duct centerline
TOWALL;	value of stagnation temperature in the secondary flow outside the mixing region
THETA/RO;	value of θ/R_o
SHAPE;	value of H

When the Part 1 analysis indicates that the jet reaches the wall, the message "DELTA/R = 1 -- DIFFERENTIAL EQUATIONS CHANGE" is printed. The local value of U_j , called CL, is also printed. Next, two lines are printed as follows:

F2(I)'s: values of $f_2(\eta)$ at $\eta = 0.05, 0.15, 0.25, \text{-----}, 0.95$
 G2(I)'s: values of $g_2(\eta)$ at $\eta = 0.05, 0.15, 0.25, \text{-----}, 0.95$

The printing concludes with the tabulated results obtained from the Part 2 analysis. The parameters listed are as follows:

X/RZERO, AREA, PH20, UCENT, UR, TOCENT, TOWALL; same as in Part 1
 TOWALL/TOO; stagnation temperature of wall streamline divided by secondary
 flow inlet stagnation temperature, T_{oo}

AUGMENT: the value of the local momentum flux, $\int_0^R \frac{\rho u^2}{g_o} 2\pi y dy$, divided
 by the primary jet momentum, $W_1 U_1$, which is printed out earlier.

GAMMA; local value of γ

B.3 Listing

```

C*****
C COJET, ANALYSIS OF FLOW BEHAVIOR IN AXISYMMETRIC COMPRESSIBLE FLOW
C EJECTORS WITH VARIABLE AREA MIXING TUBES
C*****
COMMON TURBNO,CF,EN,NPART,C,JRUNGE,NGAM
1,POO,PO1,TOO,TO1,AMACH,AG,RG
2,AMASS1,AMASSO,T
3,SOO,CMAS,CMOM,CENR
4,SO,BP,CM,VISC1
COMMON ZA,ZB,UJO,DORIN
6,MASRAT,RZERO,AFAC,CFD,HD,F,A1,AAZERO,TF,FP,GP
7,SDLOSS,ASD
8,AUG1,U1,UCENT
DIMENSION Y(10),TOL(10),YMIN(10),XOUT(201),MARK(5)
1,DY(50),F(10)
DIMENSION FF(3),XX(3),ERR(3),AA(3,10),WORK(10)
1,A1(10),FX(10),TF(10)
5,FP(10),GP(10)
REAL MASRAT
C JET MIXING WITH PRIMARY AND SECONDARY STREAMS OF THE SAME PERFECT GAS
C AND CORRECT NOZZLE EXPANSION
C READ DATA
100 CONTINUE
CALL DIFFEQ(1,X,Y,DY)
READ(5,18,END=200)THETA,SHAPE,VISC,RZERO
C THETA = INLET B.L. MOMENTUM THICKNESS, FT
C SHAPE = INLET B.L. SHAPE FACTOR
C VISC = KINEMATIC VISCOSITY, FT**2/SEC
C RZERO = INLET DUCT RADIUS, FT
18 FORMAT(4F10.6)
READ(5,19)
C ONE CARD TO IDENTIFY THE SOLUTION
19 FORMAT(80H
1
C DUCT GEOMETRY AT INLET
A = 3.1416*RZERO*RZERO
C APPROXIMATE NOZZLE AREA FT**2
READ(5,15)DELTAX,XTURE,TURBNO,NSUB,NGAM,XCORE,ANZ
C NGAM=0 SUPPRESS GAMMA =1 DO NOT
C NSUB = 1 READ NEW MIXING TUBE PROFILE DATA = 2 DO NOT
15 FORMAT(3F10.4,2I5,2F10.5)
READ(5,16)POO,TOO,PO1,TO1,AMASS1,AMASSO,AG,RG
C PO - PSIA
C TO - DEGR
C AMASS - LBM/SEC
C RG - FT-LBF/LBM-DEGR
16 FORMAT(8F7.3)
WRITE(6,19)
WRITE(6,17)DELTAX,SHAPE,RZERO,XTURE,NSUB,THETA,TURBNO,NGAM,VISC,
1,AG,RG,POO,TOO,PO1,TO1,AMASSO,AMASS1,ANZ,XCORE
17 FORMAT(///,5X,7HDELTAX=,F10.4,3X,6HSHAPE=,F10.6,4X,6HRZERO=,F10.6,
12HFT,/,5X,6HXTURE=,F10.4,4X,5HNSUB=,I5,9X,6HTHETA=,F10.6,2HFT,/,
25X,7HTURBNO=,F10.4,4X,5HNGAM=,I5,10X,5HVI SC=,F10.6,9HFT**2/SEC,/,
39X,3HAG=,F10.4,26X,3HAG=,F10.4,15HFT-LBF/LBM-DEGR,/,
48X,4HPOO=,F10.4,4HPSIA,/,8X,4HTOO=,F10.4,4HDEGR,/,
58X,4HPO1=,F10.4,4HPSIA,/,8X,4HTO1=,F10.4,4HDEGR,/,
65X,7HAMASSO=,F10.4,7HLBM/SEC,/,5X,7HAMASS1=,F10.4,7HLBM/SEC,/,

```

```

----- 77X,5HANOZ=,F10.5,5HFT**2,/,6X,6HXCORE=,F10.4,/)
C   THETA = INLET B.L. MOMENTUM THICKNESS, FT
C   SHAPE = INLET B.L. SHAPE FACTOR
C   VISC = KINEMATIC VISCOSITY, FT**2/SEC
C   RZERO = INLET DUCT RADIUS, FT
C   ANOZ = APPROXIMATE NOZZLE AREA FT**2
C   XCORE = LENGTH OF POTENTIAL CORE/RZERO
C   DUCT GEOMETRY AT INLET
----- NS = 10
      JPOLY = 5
C   CALCULATION OF F(I) FROM POLYNOMIAL
      AAZERO= 1.(JC4
      A1(1)= -0.0175
      A1(2)= -8.3821
      A1(3)= 16.5806
      A1(4)= -12.7877
      A1(5)= 3.6058
      CTR = -.05
      DO 807 I=1,NS
        CTR = CTR + 0.1
        F(I) = A1(JPOLY)
        FP(I) = FLOAT(JPOLY)*F(I)
        DO 808 J=2,JPOLY
          JJ = JPOLY - J + 1
          F(I) = F(I)*CTR + A1(JJ)
          FP(I) = FP(I)*CTR + FLOAT(JJ)*A1(JJ)
608      CONTINUE
        F(I) = F(I)*CTR + AAZERO
        TF(I) = SQRT(F(I))
807      CONTINUE
      WRITE (6,403) (F(I), I =1,NS)
403      FORMAT(5X,6HF(I)'S,5X,10F10.4,/)
      A = 3.1416*RZERO*RZERO
      P01 = P01 *144.
      P00 = P00*144.
      RG =RG*32.2
      AMASS1=AMASS1/32.2
      AMASS0=AMASS0/32.2
      XYZ=0.0
      GO TO (10,11),NSUB
10      CALL SUB(XYZ,R,DR,3,RZERO)
11      JRUNGE = 4
      NPART=1
C
C
C   TO DETERMINE TOP HAT PARAMETERS
C
C   TO DETERMINE EFFECTIVE DUCT AREA AT END OF CORE
      CALL SUB(XCORE,R,DR,2,RZERO)
      THETA = THETA + XCORE*.0010*RZERO
      RCORE = R*RZERO - THETA*SHAPE
      ACORE = 3.1416*RCORE*RCORE
      AEFF = ACORE -ANOZ
      AM = ACORE
      AFAC = 1.
      AGG = AG/(AG-1.)
      RH00=P00/(RG*T00)
C   CORRECTION FOR INLET DUCT PRESSURE LOSS
C   P0C LOSS AT INLET OR NOT
      P02=P00-SDLOSS*AMASS0**2./(2.*RHC0*ASD**2.)

```

```

----- RHO0 = P02/(RG*T00)
C FIRST APPROXIMATION FOR OUTER VELOCITY
----- U0 = AMASS0/(RHO0*AEFF)
----- T0 = T00 - (AG-1.)*.5*U0*U0/(AG*RG)
----- P = P02*(T0/T00)**AGG
----- RHO=P/(RG*T0)
C SECOND APPROXIMATION FOR OUTER VELOCITY
----- U0 = AMASS0/(RHO*AEFF)
----- T0 = T00 - (AG-1.)*.5*U0*U0/(AG*RG)
----- P = P02*(T0/T00)**AGG
----- RHO=P/(RG*T0)
C ASSUME PRIMARY STREAM EXPANDS TO OUTER STREAM PRESSURE
----- T1 = T01*(P/PC1)**(1./AGG)
----- RH1=P/(RG*T1)
----- U1 = SQRT(2.*AGG*RG*(T01-T1))
C
C
C
C
C
C
C
----- UJ00=U1-U0
----- T = (T01-T00)/T00
----- S00=0.5*(AG-1.)*UJ00*UJ00/(AG*RG*T00)
----- CMAS = AMASS1 + AMASS0
----- CMOM = (P-P00)*AM+AMASS1*U1 + AMASS0*U0
----- CM = CMOM/A*2.
----- CENR = -AMASS1*T01 + -AMASS0*T00
----- EN=CMAS/SQRT(2.*CMOM*A*RHO0)
----- C=UJ00*SQRT(A*RHO0*.5/CMOM)
----- W2 = ACORE*RHO0*UJ00
----- CMAS = CMAS/W2
----- CMOM = CMOM/(W2*UJ00)
----- CENR = CENR/(W2*T00)
C FIRST GUESS OF PARAMETERS AFTER CONSTANT AREA TRANSITION
C UR = UJ/UJ00
C Y2 = LAMBDA
C DCR = DELTA/R
C UR = 1.
C Y2 = U0/UJ00
C PH20 = -(P00-P)*.193
C TMOM = AMASS1*U1
C RHOC = RHO*32.2
C WRITE(6,67) U0,RHOC,UJ00,T0,P, TMOM,Y2,PH20
67 FORMAT(5X,40HCONDITIONS AT BEGINNING OF THE TRANSITION SECTION,
1//,9X,3HU0=,F6.0,6HFT/SEC,6X,4HRHC=,F6.4,9HLBM/FT**3,6X,
25HUJ00=,F6.0,6HFT/SEC,/,9X,3HT0=,F6.0,4HDEGR,10X,2HP=,F6.0,
39HLBM/FT**2,6X,13HPRIMARY MOM.=,F6.2,3HLBF,/,5X,7HLAMBDA=,F6.4,12X
4,5HPH20=,F6.2,6HIN.H20)
C XX(1) = UR
C XX(2) = Y2
C XX(3) = SQRT(SQRT(ANZ/3.14161)/RZERO)
C
C DO 121 J = 1,3
121 ERR(J) = 1.E-6*XX(J)
C IP = 1
C MAX = 120
C CALL VRO4A(3,3,FF,XX,ERR,AA,300000.,IP,MAX,3,WORK)
C CHECK CALCULATION OF EN AFTER TRANSITION

```

ALIT 440

ALIT 5

```

----- CMAS2 = (FF(1) + CMAS1)*W2
----- CMOM2 = (FF(2) + CMOM1)*W2*UJ00
----- EN2 = CMAS2/SQRT(2.*CMOM2*A*RH00)
----- WRITE(6,69)XX(1),XX(2),XX(3),EN,FN2
68----- FORMAT(7,7,7X,6HXX(1)=,F15.10,3X,6HXX(2)=,F15.10,3X,6HXX(3)=,F15.
1 .10,7,7X,6HXX(1)=,F10.4,10X,4HEN2=,F10.4)
C
C
----- C = C*XX(1)
----- S0 = S00*XX(1)*XX(1)
----- BP = (AG-1.)/(-2.*AG*S0)
----- UJO = XX(1)*UJ00
----- UCENT = UJO*(1.+XX(2))
----- WRITE(6,69)S0,BP,UJO,UCENT
69----- FORMAT(/,10X,3HS0=,F10.4,11X,3HBP=,F10.4,7,7X,4HUJO=,F10.1,6HFT/
1SEC,2X,6HUCENT=,F10.1,6HFT/SEC)
----- VISC1 = VISC/(UJ00*XX(1)*RZERO)
----- Y(1) = 1.
----- Y(2) = XX(2)
----- Y(3) = XX(3)*R
----- Y(4) = (1. - Y(2)*Y(2)*S0*AG/(AG-1.))*P02/P00
----- Y(5) = (T01 - T00)/T00
----- Y(6) = 1.0
----- Y(7) = THETA/RZERO
----- Y(8) = SHAPE
C
C
C
C
----- D=4.08*Y(3)*(1.+Y(2))
----- D = XCORE
----- XOUT(1)=D
----- XTRO = XTUBE/RZERO
----- M1 = 2.* XTRO
----- DO 5 I=2,M1
----- XOUT(I)=XOUT(I-1)+DELTAX
----- IF(XOUT(I).GT.XTRO) GO TO 300
5----- CONTINUE
300----- CONTINUE
----- M1 = I-1
----- DC-8 K = 1,8
----- YMIN(K) = .01
----- TOL(K) = .00001
----- TOL(K) = .0001
8----- CONTINUE
----- YMIN(5) = 1.
----- YMIN(6) = 1.
----- YMIN(7) = 1.
----- YMIN(8) = 10.
----- MARK(1)=1
----- MARK(2)=M1
----- MARK(4)=0
----- H=.1
----- CALL RUNGE (8,D,Y,TOL,YMIN,H,XOUT,MARK)
----- GO TO 100
200----- STOP
----- END
----- SUBROUTINE CIFFEO (N,X,Y,DY)
----- COMMON TURBNO,CF,EN,NPART,C,JRUNGE,NGAM
----- 1,P00,P01,T00,T01,AMACH,AG,RG
ALIT 10
ALIT 20
ALIT 30

```

```

2      ,AMASS1, AMASSO, T
3      ,SOO, CMAS, CMOM, CENR
4      ,SO, BP, CM, VISC1
COMMON ZA, ZB, UJO, DORIN
6      ,MASRAT,RZERO,AFAC, CFD, HD, F, A1, AAZERO, TF, FP, GP
7      ,SDLOSS,ASD
8      ,AUG1,U1,UCENT
DIMENSION Y(10),DY(50), W(8,8), V(8,1), K(40), XCUT(100)
1      , A1(10), TF(10)
2      ,A(70),B(10),F(10),G(20),DLF(20),DLG(20)
3      ,AA(10), GG(10)
4      ,DLF1(20)
5      ,FP(10),GP(10)
EQUIVALENCE (SO,SO)
REAL MASRAT
IF (N-1)1,1,10
CONTINUE
LM = 0
MM=0
MMM=0
READ(5,399)NS
399  FORMAT(3I2)
JPOLY = 5
READ (5,401) (GG(I),I=1,NS)
401  FORMAT(10F5.4)
READ(5,950)SDLOSS,ASD
950  FORMAT(2F10.3)
WRITE(6,405)
405  FORMAT(1H1)
WRITE(6,400) NS
400  FORMAT(5X,5HNS = ,I2)
404  FORMAT(5X,7PGG(1)'S,5X,10F10.4,/)
WRITE(6,404) (GG(I),I=1,NS)
WRITE(6,951)SDLOSS,ASD
951  FORMAT(5X,24HDUCT LOSS COEFFICIENT = ,F10.3,/,17X,12HDUCT AREA = ,
1F10.3,5HFT**2,/)
C
C
DIVNS = 2./FLOAT(NS)
DIVDEL = FLOAT(NS)
RETURN
C
C
Y1=UJ/UJZFC
C
Y2=LAMDA = UO/UJ
C
Y3= DELTA/RZERO
C
Y4 = P/P00INITIAL
C
Y5=(TOCENTER--TOO)/TOO
C
Y6=TOO/TQCINITIAL
C
Y7 = B. L. MOMENTUM THICKNESS/RZERO
C
Y8 = B. L. SHAPE FACTOR
C
10  CONTINUE
402  FORMAT (4F10.4)
IF (LM) 913,913,914
913  CONTINUE
DY(1) = 0.
DY(2) = 0.
914  LM = 1
E=1./TURBNQ
Y1=Y(1)

```

```

Y2=Y(2)
Y3=Y(3)
Y4=Y(4)
Y5=Y(5)
Y6=Y(6)
Y7=Y(7)
Y8=Y(8)
Y11=Y(11)*Y(1)
Y22=Y(2)*Y(2)
Y33=Y(3)*Y(3)
DIVY1=1./Y1
DIVY11 = DIVY1*DIVY1
DIVY4=1./Y4
DIVY6 = 1./Y(6)
S2=Y2/(1.-S0*Y11*Y22)
DS2Y1=2.*S0*S2*S2*Y1*Y2
DS2Y2 = 1./((1.-S0*Y11*Y22) + 2.*S0*Y11*S2*S2)
CALL SUB(X,R,DR,2,RZERO)
C
C
R=R-Y7*Y8
C NOW BRANCH TO PART 1 OR PART 2
GO TO (11,20),NPART
11 CONTINUE
C
C PART 1
IF (Y2) 409,410,411
409 WRITE(6,1000)
1000 FORMAT(10X,46HRECIRCULATION PRESENT. CALCULATION NOT CORRECT)
410 DERU = 0
DY(7) = 0.
DY(8) = 0.
GO TO 412
411 CONTINUE
Y7 = Y7 + .0001
RTH = Y2*Y1*Y7/VISC1
CF=0.246/((RTH)**.268*10.**(.678*Y8))
CFD = CF
412 CONTINUE
DIVY3=1./Y3
E = E
1 *(1. + 1.5*(1. - 2.718**(-1.1*Y2)))
HD = E
C
C J = 1 P00 = CONSTANT
C J = 2 MOMENTUM INTEGRAL
C J = 3 CONTINUITY INTEGRAL
C J = 4 ENERGY INTEGRAL
C J = 5 MOMENTUM HALF INTEGRAL
C J = 7 B.L. MOMENTUM EQUATION EQN
C J = 8 B.L. MOMENT-OF-MOMENTUM EQUATION
13 CONTINUE
DCNR=Y33/(R*R)
C CALCULATION OF EN PART 1
ZA = 0.
ZB = 0.
CTR = -.05
DC 369 I = 1,NS
CTR = CTR + .1
Y2FI = Y2 + F(I)

```

ALIT 65J
ALIT 65J

ALIT 70J
ALIT 71J
ALIT 63J
ALIT 72J

ALIT 73J
ALIT 74J
ALIT 75J
ALIT 76J
ALIT 77J
ALIT 78J
ALIT 79J
ALIT 80J


```

FS = TF(I)
ANA = Y2FI
ANB = Y2FI*Y2FI
D = 1. + Y(5)*FS -S0*Y11*Y2FI*Y2FI
DIVD = 1./D
ZA = ZA + DIVNS*ANA*DIVD
1 *CTR
ZB = ZB + DIVNS*ANB*DIVD
1 *CTR
369 CONTINUE
S2 = Y2/(1.-S0*Y11*Y2*Y2)
AMAS = ZA*DNR + (1.-DNR)*S2
AMOM = ZB*DNR + (1.-DNR)*Y2*S2
EN = AMAS/SQRT(AMOM + BP*(1.-1./Y(4))*DIVY11)
EN = EN*.707
RLOCAL = R*RZERO
RLOCAL = RLOCAL*RLOCAL
MASRAT = AMAS*Y4*P00*Y1*UJ0*RLOCAL *3.1416/(RG*T00*AMASS1) - 1.
C
C
W(1,1)=Y22*Y1
W(1,2)=Y11*Y2
W(1,3) = 0.
W(1,4)=BP*(1.-S0*Y11*Y22)*DIVY4
W(1,5) = 0.
W(1,7) = 0.
W(1,8) = 0.
V(1,1) = 0.
J = 1
71 J=J+1
Z1=0.
Z2=0.
Z3=0.
Z4=0.
Z5=0.
Z6=0.
CTR = -.05
DO 66 I=1,NS
CTR = CTR + .1
FS = TF(I)
FI=F(I)
Y2FI=Y2+F(I)
JJ = J-1
GO TO (270,70,67) ,JJ
270 CONTINUE
AN=Y2FI*Y2FI
D2N=Y2FI*2.
D5N=0
GO TO 68
70 AN=Y2FI
D2N=1.
D5N=0.
GO TO 68
67 AN=Y2FI*(1.+Y5*FS)
D2N=1.+Y5*FS
D5N=Y2FI*FS
68 D=1.+Y5*FS-S0*Y11*Y2FI*Y2FI
DIVD=1./D
DIVDD=DIVD*DIVD
D20=-2.*S0*Y11*Y2FI

```

ALIT 830

ALIT 850

ALIT 860

ALIT 910

ALIT 920

ALIT 930

ALIT 940

ALIT 950

ALIT 960

ALIT 970

ALIT 980

ALIT1010

ALIT1020

ALIT1030

ALIT1070

ALIT1110

```

D1D=-2.*S0*Y1*Y2FI*Y2FI
D5D=FS
Z1=Z1+DIVNS*AN*DIVD
1 *CTR
Z2=Z2-DIVNS*AN*D1D*DIVDD
1 *CTR
Z3=Z3+DIVNS*D2N*DIVD
1 *CTR
Z4=Z4-DIVNS*AN*D2D*DIVDD
1 *CTR
Z5=Z5+DIVNS*D5N*DIVD
1 *CTR
Z6=Z6-DIVNS*D5D*DIVDD*AN
1 *CTR
66 CONTINUE ALIT1250
IF (J-2) 210,211,210 ALIT1250
211 W(J,1)=DONR*(2.*Z1*DIVY1+Z2)+(1.-DONR)*(2.*Y2*S2*DIVY1+Y2*DS2Y1)
W(J,2)=DONR*(Z3+Z4)+(1.-DONR)*(S2+Y2*DS2Y2)
W(J,3)=2.*DONR*(Z1-Y2*S2)*DIVY3
W(J,4)=(DONR*(Z1-Y2*S2)+Y2*S2)*DIVY4
1 + BP*DIVY4*DIVY1
W(J,5)=DONR*(Z5+Z6)
W(J,7)=-2.*S2*Y8/R*Y2
W(J,8)=-2.*S2*Y7/R*Y2
V(J,1)=-2.*DR/R*Y2*S2 ALIT1370
GO TO 212
210 W(J,1)=DONR*(Z1*DIVY1+Z2)+(1.-DONR)*(S2*DIVY1+DS2Y1)
W(J,2)=DONR*(Z3+Z4)+(1.-DONR)*DS2Y2
W(J,3)=2.*DONR*(Z1-S2)*DIVY3
W(J,4)=(DONR*(Z1-S2)+S2)*DIVY4
W(J,5)=DONR*(Z5+Z6)
W(J,7)=-2.*S2*Y8/R
W(J,8)=-2.*S2*Y7/R
V(J,1)=-2.*DR/R*S2
212 CONTINUE ALIT1490
IF (J-4) 71,69,69 ALIT1500
69 CONTINUE ALIT1510
J = 5 ALIT1530
226 I = 0 ALIT 10
Z1 = 0 ALIT 20
Z2 = 0 ALIT 30
Z3 = 0 ALIT 40
Z4 = 0 ALIT 50
Z5 = 0 ALIT 60
Z6 = 0 ALIT 70
Z7 = 0. ALIT 80
Z8 = 0. ALIT 90
Z9 = 0. ALIT 100
Z10 = 0. ALIT 110
Z11 = 0. ALIT 120
Q1 = 0. ALIT 130
Q2 = 0. ALIT 140
Q3 = 0. ALIT 150
Q4 = 0. ALIT 160
R1 = 0. ALIT 170
R2 = 0. ALIT 180
R34 = 0. ALIT 190
R56 = 0. ALIT 200
R79 = 0. ALIT 210
R10 = 0.

```

	R11 = 0.	
	V1 = 0.	ALIT 220
	V2 = 0.	ALIT 230
	V3 = 0.	ALIT 240
	V4 = 0.	ALIT 250
	V5 = 0.	ALIT 260
	V6 = 0.	ALIT 270
	V7 = 0.	ALIT 280
	V9 = 0.	ALIT 290
	V10 = 0.	ALIT 300
	V11 = 0.	
	CTR = -.25*DIVNS	ALIT 310
224	I = I+1	ALIT 320
	CTR = CTR + 0.5*DIVNS	ALIT 330
	FS = TF(I)	ALIT 340
	Y2FI = Y2 + F(I)	ALIT 350
	FDER = FP(I)	
221	AN = Y2FI	ALIT 360
	D2N=1.	ALIT 370
	D5N=0.	ALIT 400
223	D=1.+Y5*FS-S0*Y11*Y2FI*Y2FI	ALIT 420
	DIVD=1./D	ALIT 430
	DIVDD=DIVD*DIVD	ALIT 440
	D2D=-2.*S0*Y11*Y2FI	ALIT 450
	D1D=-2.*S0*Y1*Y2FI*Y2FI	ALIT 460
	D5D=FS	ALIT 470
	CCC = DIVNS*CTR*.5	ALIT 490
	DZ1 = CCC*AN*DIVD	ALIT 500
	DZ2 = -CCC*AN*D1D*DIVDD	ALIT 510
	DZ3 = CCC*D2N*DIVD	ALIT 520
	DZ4 = -CCC*AN*D2D*DIVDD	ALIT 530
	DZ5 = CCC*D5N*DIVD	ALIT 540
	DZ6 = -CCC*AN*D5D*DIVDD	ALIT 550
	DZ10 = FDER*CTR*CCC*DIVD	ALIT 580
	DZ11 = CCC*CTR*Y2FI*DIVDD*2.*S0*Y11*Y2FI*FDER	
	V1 = Z1 + 0.5*DZ1	ALIT 590
	V2 = Z2 + 0.5*DZ2	ALIT 600
	V3 = Z3 + 0.5*DZ3	ALIT 610
	V4 = Z4 + 0.5*DZ4	ALIT 620
	V5 = Z5 + 0.5*DZ5	ALIT 630
	V6 = Z6 + 0.5*DZ6	ALIT 640
	V10 = Z10 + 0.5*DZ10	ALIT 670
	V11 = Z11 + .5*DZ11	
	Z1 = Z1 + DZ1	ALIT 680
	Z2 = Z2 + DZ2	ALIT 690
	Z3 = Z3 + DZ3	ALIT 700
	Z4 = Z4 + DZ4	ALIT 710
	Z5 = Z5 + DZ5	ALIT 720
	Z6 = Z6 + DZ6	ALIT 730
	Z10 = Z10 + DZ10	ALIT 760
	Z11 = Z11 + DZ11	
492	CCC = DIVNS*CTR*CTR	ALIT 770
1	*.5	ALIT 800
	ATAU = .377	ALIT 810
	BTAU = .0333	ALIT 820
	Q1 = Q1 + CCC*Y2FI*DIVD	ALIT 830
1	*Y2FI	ALIT 840
	Q2 = Q2 + CCC*Y2FI*DIVD	ALIT 850
	Q3 = Q3 - CCC*CTR*Y2FI*FDER*DIVD	ALIT 860
	CCC = -CCC/CTR	ALIT 870

```

R1 = R1 + CCC*V1*FDER
R2 = R2 + CCC*V2*FDER
R34 = R34 + CCC*(V3 + V4)*FDER
R56 = R56 + CCC*(V5 + V6)*FDER
R10 = R10 - CCC*V10*FDER
R11 = R11 - CCC*V11*FDER
IF (I-NS) 224,225,225
225 CONTINUE
W(J,1) = (Q1 + R1)*DIVY1 + R2
W(J,2) = Q2 + R34
W(J,3) = (Q3 + R10 + R11)*DIVY3
W(J,4) = R1*DIVY4 + BP*DIVY4*DIVY11*.3333
W(J,5) = R56
W(J,7) = 0.
W(J,8) = 0.
V(J,1) = E*DIVY3*ATAU
MMM = MMM + 1
245 CONTINUE
246 CONTINUE
247 CONTINUE
947 CCNTINUE
C      B.L. MOMENTUM EQUATION
W(7,1) = (2. + Y8)*Y7*DIVY1*Y2
W(7,2) = (2. + Y8)*Y7
W(7,3) = 0.
W(7,4) = 0.
W(7,5) = 0.
W(7,6) = 0.
W(7,7) = Y2
W(7,8) = 0.
V(7,1) = .5*CF*Y2
C      B.L. MOMENT-OF-MOMENTUM EQUATION
W(8,2) = .5*Y8*(Y8 + 1.)*(Y8*Y8-1.)
W(8,1) = W(8,2)*DIVY1*Y2
W(8,3) = 0.
W(8,4) = 0.
W(8,5) = 0.
W(8,6) = 0.
W(8,7) = 0.
W(8,8) = Y2
V(8,1) = (Y8*Y8 - 1.)*Y2/Y7*(.5*Y8*CF-.06*(Y8-1.)/((Y8+3.-)
1 *RTH*.1))
IF (Y(2)) 200,201,201
200 W(1,1) = 0.
W(1,2) = 0.
W(7,1) = 0.
W(7,2) = 0.
V(7,1) = 0.
W(8,1) = 0.
W(8,2) = 0.
V(8,1) = 0.
201 CONTINUE
IF (Y8-2.) 481,481,481
481 W(7,1) = 0.
W(7,2) = 0.
W(7,7) = 1.
V(7,1) = 0.
W(8,1) = 0.
W(8,2) = 0.
W(8,8) = 1.

```

ALIT 950

ALIT 950

ALIT 970

ALIT 990

ALIT1000

ALIT1010

ALIT1020

ALIT 870

ALIT 880

ALIT 890

ALIT 900

```

V(8,1) = 0.
W(1,1) = 0.
W(1,2) = 0.
482 CONTINUE
C COLLAPSE FROM 8X8 TO 7X7 MATRIX
DO 687 I=1,8
W(6,I) = W(7,I)
W(7,I) = W(8,I)
687 CONTINUE
V(6,1) = V(7,1)
V(7,1) = V(8,1)
C
C
DO 688 J=1,7
W(J,6) = W(J,7)
W(J,7) = W(J,8)
688 CONTINUE
C
C
C SOLVING SIMULTANEOUS EQUATIONS BY SIMQ SUBROUTINE ALIT2150
C ALIT2160
C ALIT2170
NN = 7
DO 101 J=1,NN ALIT2190
B(J)=V(J,1) ALIT2200
DO 101 I=1,NN ALIT2210
IJ = I + NN*(J-1) ALIT2220
A(IJ)=W(I,J) ALIT2230
101 CONTINUE ALIT2240
CALL SIMQ (A,B,NN,KS) ALIT2250
DO 18 I=1,NN ALIT2260
18 DY(I)=B(I) ALIT2270
DY(8) = DY(7)
DY(7) = DY(6)
DY(6)=0. ALIT2280
249 CONTINUE
JRUNGE=JRUNGE +1 ALIT2140
C CHECK FOR EQUATION CHANGE ALIT2340
IF (JRUNGE-5) 14,15,15 ALIT2350
15 JRUNGE=0 ALIT2360
IF (Y(3)-R) 14,16,16 ALIT2370
14 RETURN ALIT2380
16 XOUT(100)=X ALIT2390
CALL PRINT (N,XOUT,Y,DY,100) ALIT2400
Y(3)=0. ALIT2410
Y3 = Y(3)
NPART=2 ALIT2420
BPPT1 = BP ALIT2430
SOPT1 = SO ALIT2440
DLSTAR = Y8*Y7
DELTA = DLSTAR*(Y8+1.)/(Y8-1.)
POW = 0.5*(Y8-1.)
R = R + DLSTAR
C EVALUATE NEW VELOCITY PROFILES
CTR = -.05
DO 876 I=1,NS
CTR = CTR + 0.1
IF (1.-CTR-DLSTAR/R) 875,875,874
875 F(I) = 0.
TF(I) = 0.

```

```

GO TO 840
874 CTR1 = CTR/(1.-DLSTAR/R)
F(I) = A1(JPOLY)
DO 873 J=2,JPOLY
JJ = JPOLY - J + 1
F(I) = F(I)*CTR1 + A1(JJ)
873 CONTINUE
F(I) = F(I)*CTR1 + AAZERO
TF(I) = SQRT(F(I))
840 BL = (R/DELTA*(1.-CTR))**POW
IF (BL-I.) 860,860,861
861 BL = 1.
860 CONTINUE
F(I) = (F(I) + Y2*BL)/(1. + Y2)
G(I) = GG(I) - F(I)
876 CONTINUE
WRITE(6,403) (F(I),I=1,NS)
403 FORMAT(5X,7HF2(I)'S,5X,10F10.4,/)
WRITE(6,406) (G(I),I=1,NS)
406 FORMAT(5X,7HG2(I)'S,5X,10F10.4,/)
WRITE(6,407)
407 FORMAT(
//4X,7HX/RZERO,5X,4HAREA,5X,4HPH2C,5X,35HTOWALL
27T00 UCENT(FT/SEC) UR 7HAUGMENT,6X,5HGAMMA,3X, 25HTOCE
3NT(DEGR) TOWALL(DEGR))
L = NS - 1
DO 877 I=2,L
FP(I) = .5 *DIVDEL*(F(I+1)-F(I-1))
GP(I) = .5 *DIVDEL*(G(I+1)-G(I-1))
877 CONTINUE
FP(1) = DIVDEL*(F(2) - F(1))
GP(1) = DIVDEL*(G(2) - G(1))
FP(NS) = DIVDEL*(F(NS) - F(NS-1))
GP(NS) = DIVDEL*(G(NS) - G(NS-1))
Y1 = Y1*(1. + Y2)
Y11 = Y1*Y1
Y(1) = Y(1)*(1. + Y2)
DIVY11 = 1./Y11
E2I = E/(1. + Y2)
E2I = 2.*E2I
CFDI = CF/((1. + Y2)*(1. + Y2))
Y2 = 0.
Y(2) = 0.
Y7 = 0.
Y(7) = 0.
Y8 = 0.
Y(8) = 0.
C ALIT245J
C ALIT246J
C PART 2 ALIT247J
C TURBULENT PRANDTL NUMRER = PR ALIT248J
C PR = 1. ALIT250J
C Y3=GAMMA
C CONTINUE ALIT252J
20 Y23=Y(2)*Y(3) ALIT253J
S0 = S0PT1/Y(6) ALIT254J
DSOY6 = -S0/Y(6) ALIT255J
BP = BPPT1*Y(6) ALIT256J
C
C PHASE OUT THE B.L. DISPLACEMENT THICKNESS INHERITED FROM PART 1
C DY(7) = 0.

```

```

      DY(8) = 0.
C      CALCULATION OF EN      PART 2
      ZA = 0.
      ZB = 0.
      CTR = -.05
      DO 370 I = 1, NS
      CTR = CTR + .1
      YFGG = Y2 + F(I) + Y3*G(I)
      FS = TF(I)
      ANA = YFGG
      ANB = YFGG*YFGG
      D = 1. + Y5*FS - S0*Y11*YFGG*YFGG
      DIVD = 1./D
      ZA = ZA + DIVNS*ANA*DIVD
      1  *CTR
      ZB = ZB + DIVNS*ANB*DIVD
      1  *CTR
370  CONTINUE
      AMAS = ZA
      AMOM = ZB
      EN = AMAS/SQRT(AMOM + BP*(1.-1./Y(4))*DIVY11)
      EN = EN*.707
      RLOCAL = R*RZERO
      RLOCAL = RLOCAL*RLOCAL
      MASRAT = AMAS*Y4*P00*Y1*UJO*RLOCAL *3.1416/(RG*T00*Y6*AMASS1)-1.
      UM = AMAS*Y1
      RM = UM*2.*R/VISC1
      CFDF = AMAS*AMAS*.048*RM**(-.20)
      CFDF = 2.*CFDF
      CFQ = CFDF
C
C      J=1      CONTINUITY      ALIT257J
C      J=2      ENERGY
C      J=3      MOMENTUM
C      J=4      MOMENT OF MOMENTUM EQUATION
C      J=5      T' / T = UJ'/UJ
C      J=6      D(LAMBDA)/DX = 0.
      J=0
86  J=J+1
87  Z1=0
      Z2=0
      Z3=0
      Z4=0
      Z5=0
      Z6=0
      Z7=0
      Z8=0
      Z9 = 0.
      CTR = -.05
      I=0
82  I=I+1
      CTR = CTR + .1
      FS = TF(I)
      YFGG=Y2+F(I)+Y3*G(I)
      GO TO (81,83,41),J
81  AN=YFGG
      D2N=1.
      D5N=0
      D3N=G(I)
      GO TO 85

```

```

83 AN=YFGG*(1.+Y5*FS)
   D2N=1.+Y5*FS
   D5N=YFGG*FS
   D3N=G(I)*(1.+Y5*FS)
   GO TO 85
41 AN=YFGG*YFGG
   D2N=2.*YFGG
   D3N=2.*YFGG*G(I)
   D5N=0
   IF (F(I)) 720,720,721
720 AN=-AN
   D2N=-D2N
   D3N=-D3N
721 CONTINUE
85 O=1.+Y5*FS-SO*Y11*YFGG*YFGG
   DIVD=1./D
   DIVDD=DIVD*DIVD
   D1D=-SO*Y11*2.*YFGG*YFGG
   D2D=-SO*Y11*2.*YFGG
   D3D=-SO*Y11*2.*YFGG*G(I)
   D5D=FS
   D6D=-DSOY6*Y11*YFGG*YFGG
   Z1=Z1+DIVNS*AN*DIVD
1   *CTR
   Z2=Z2-DIVNS*AN*D1D*DIVDD
1   *CTR
   Z3=Z3+DIVNS*D2N*DIVD
1   *CTR
   Z4=Z4-DIVNS*D2D*DIVDD*AN
1   *CTR
   Z5=Z5+DIVNS*D5N*DIVD
1   *CTR
   Z6=Z6-DIVNS*AN*D5D*DIVDD
1   *CTR
   Z7=Z7+DIVNS*D3N*DIVD
1   *CTR
   Z8=Z8-DIVNS*AN*D6D*DIVDD
1   *CTR
   Z9=Z9-DIVNS*DIVDD*AN*D3D
1   *CTR
   IF(I-NS)82,601,601
601 W(J,1)=Z1*DIVY1+Z2
   W(J,2)=Z3+Z4
   W(J,3)=Z7+Z9
   W(J,4)=Z1*DIVY4
   W(J,5)=Z5+Z6
   W(J,6)=Z8
   IF (J-2) 602,603,602
602 W(J,6)=W(J,6)-Z1*DIVY6
603 CONTINUE
   V(J,1)=-2.*DR/R*Z1
   IF (J-3) 86,709,709
709 CONTINUE
   W(3,1)=W(3,1)+Z1*DIVY1
   AUG1=Z1
   W(3,4)=W(3,4)+8P*DIVY11*DIVY4
   V(3,1)=V(3,1)-CFD/R
   J=4
   I=0
   Z1=0

```

ALIT 43

Z2 = 0	ALIT 50
Z3 = 0	ALIT 60
Z4 = 0	ALIT 70
Z5 = 0	ALIT 80
Z6 = 0	ALIT 90
Z7 = 0.	ALIT 100
Z8 = 0.	ALIT 110
Z9 = 0.	ALIT 120
Z10 = 0.	ALIT 130
Z11 = 0.	
Q1 = 0.	ALIT 140
Q2 = 0.	ALIT 150
Q3 = 0.	ALIT 160
Q4 = 0.	ALIT 170
R1 = 0.	ALIT 180
R2 = 0.	ALIT 190
R34 = 0.	ALIT 200
R56 = 0.	ALIT 210
R79 = 0.	ALIT 220
R10 = 0.	ALIT 230
R11 = 0.	
RTAU = 0.	
V1 = 0.	ALIT 240
V2 = 0.	ALIT 250
V3 = 0.	ALIT 260
V4 = 0.	ALIT 270
V5 = 0.	ALIT 280
V6 = 0.	ALIT 290
V7 = 0.	ALIT 300
V9 = 0.	ALIT 310
V10 = 0.	ALIT 320
V11 = 0.	
E2FMAX = -.5*CFD*.45/(FP(5) + GP(5))	
HD = (1.-Y33)*E2I + Y33*E2FMAX	
CTR = -.25*DIVNS	ALIT 330
924 I = I + 1	
CTR = CTR + 0.5*DIVNS	ALIT 350
FS = TF(I)	ALIT 360
Y2FI = Y2 + F(I)	ALIT 370
1 + Y3*G(I)	
FDER = FP(I) + Y3*GP(I)	
GGDER = FP(I) + GP(I)	
E2F = -.5*CFD*CTR/GGDER	
E = (1.-Y33)*E2I + Y33*E2F	
AN = Y2FI	
D2N=1.	ALIT 410
D5N=0.	ALIT 420
D6N = G(I)	ALIT 430
D=1.+Y5*FS-S0*Y11*Y2FI*Y2FI	
DIVD=1./D	ALIT 450
DIVDD=DIVD*DIVD	ALIT 460
D2D=-2.*S0*Y11*Y2FI	ALIT 470
D1D=-2.*S0*Y1*Y2FI*Y2FI	ALIT 480
D5D=FS	ALIT 490
D6D = -S0*Y11*2.*Y2FI*G(I)	ALIT 500
CCC = DIVNS*CTR*.5	ALIT 510
D21 = CCC*AN*DIVD	ALIT 520
D72 = -CCC*AN*D1D*DIVDD	ALIT 530
D73 = CCC*D2N*DIVD	ALIT 540
D74 = -CCC*AN*D2D*DIVDD	ALIT 550

```

-----DZ5 = CCC*DSN*DIVD -----ALIT 563
DZ6 = -CCC*AN*DSO*DIVDD -----ALIT 573
DZ7 = CCC*D6N*DIVD -----ALIT 580
DZ8 = -CCC*DIVDD*AN*D6D -----
DZ9 = -CCC*D6C*AN*DIVDD -----ALIT 570
DZ10 = FDER*CTR*CCC*DIVD -----ALIT 630
DZ11 = CCC*CTR*Y2FI*DIVDD*2.*SO*Y11*Y2FI*FDER
RTAU = RTAU-E*FDER*CCC*DIVD
-----V1 = Z1 + 0.5*DZ1 -----ALIT 613
V2 = Z2 + 0.5*DZ2 -----ALIT 623
V3 = Z3 + 0.5*DZ3 -----ALIT 633
V4 = Z4 + 0.5*DZ4 -----ALIT 643
V5 = Z5 + 0.5*DZ5 -----ALIT 653
V6 = Z6 + 0.5*DZ6 -----ALIT 663
V7 = Z7 + 0.5*DZ7 -----ALIT 673
V9 = Z9 + 0.5*DZ9 -----ALIT 683
V10 = Z10 + 0.5*DZ10 -----ALIT 693
V11 = Z11 + .5*DZ11
-----Z1 = Z1 + DZ1 -----ALIT 733
Z2 = Z2 + DZ2 -----ALIT 713
Z3 = Z3 + DZ3 -----ALIT 723
Z4 = Z4 + DZ4 -----ALIT 733
Z5 = Z5 + DZ5 -----ALIT 743
Z6 = Z6 + DZ6 -----ALIT 753
Z7 = Z7 + DZ7 -----ALIT 763
Z8 = Z8 + DZ8 -----
Z9 = Z9 + DZ9 -----ALIT 773
Z10 = Z10 + DZ10 -----ALIT 783
Z11 = Z11 + DZ11
CCC = DIVNS*CTR*CTR -----
-----1 * .5 -----ALIT 920
Q1 = Q1 + CCC*Y2FI*DIVD -----ALIT 910
-----1 *Y2FI -----ALIT 920
Q2 = Q2 + CCC*Y2FI*DIVD -----ALIT 933
Q3 = Q3 - CCC*CTR*Y2FI*FDER*DIVD -----ALIT 940
Q4 = Q4 + CCC*Y2FI*G(I)*DIVD -----ALIT 950
CCC = -CCC/CTR -----ALIT 963
R1 = R1 + CCC*V1*FDER -----ALIT 970
R2 = R2 + CCC*V2*FDER -----ALIT 983
R34 = R34 + CCC*(V3 + V4)*FDER -----ALIT 990
R56 = R56 + CCC*(V5 + V6)*FDER -----ALIT1003
R79 = R79 + CCC*(V7 + V9)*FDER -----ALIT1013
R10 = R10 - CCC*V10*FDER -----ALIT1023
R11 = R11-CCC*V11*FDER
IF (I-NS) 924,925,925
925 CONTINUE -----ALIT1050
W(J,1) = (Q1 + R1)*DIVY1 + R2
W(J,2) = Q2 + R34
W(J,3) = R79 + Q4
W(J,4) = R1*DIVY4 + BP*DIVY4*DIVY11*.3333
W(J,5) = R56
W(J,6) = 0.
V(J,1) = RTAU/R
1 -(Q3 + R10 + R11)*DR/R
2 -CFD*.5
W(5,1) = DIVY1
W(5,2) = 0.
W(5,3) = 0.
W(5,4) = 0.
W(5,5) = -1./Y5

```

```

      W(5,6) = -1./Y6
      V(5,1) = 0.
31  W(6,1) = 0.
      W(6,2) = 1.
      W(6,3) = 0.
      W(6,4) = 0.
      W(6,5) = 0.
      W(6,6) = 0.
      V(6,1) = 0.
30  CONTINUE
C
      MM=MM+1
168  CONTINUE
169  CONTINUE
C
C      SOLVING SIMULTANEOUS EQUATIONS BY SIMQ SUBROUTINE
C
      NN = 6
      DO 102 J=1,NN
      B(J)=V(J,1)
      DO 102 I=1,NN
      IJ = I + NN*(J-1)
      A(IJ)=W(I,J)
102  CONTINUE
      CALLSIMQ (A,B,NN,KS)
      DO 103 I=1,NN
-103  DY(I)=B(I)
165  CONTINUE
-166  CONTINUE
      RETURN
      END
      SUBROUTINE PRINT (N,XOUT,YOUT,DY,J)
      DIMENSION YOUT(10),XOUT(200),DY(50),Y(10),YSAVE(10)
      1 ,F(10), A1(10), TF(10)
      5 ,FP(10),GP(10)
      COMMON TURBNO,CF,EN,NPART,C,JRUNGE,NGAM
      1,P00,P01,T00,T01,AMACH,AG,RG
      2 ,AMASS1, AMASS0, T
      3 ,S00, CMAS, CMQM, CENR
      4 ,S0, BP, CM, VISC1
      COMMON ZA, ZB, UJ0, DDRIN
      6 ,MASRAT,RZERO,AFAC, CFD, HD, F, A1, AAZERO, TF, FP, GP
      7 ,SDLOSS,ASC
      8 ,AUG1,U1,UCENT
      REAL MASRAT
      X=XOUT(J)
      CALL SUB(X,R,DR,2,RZERO)
C      CHECK FOR INITIAL PRINT
-2  IF (J-1) 5,5,100
      5  WRITE (6,50)
C
C      PRINT FOR ALL PARTS
100 UJ=YOUT(1)*UJ0
      PH20 = YOUT(4)*P00*.193
      1  P00*.193
      U0=YOUT(1)*YOUT(2)*UJ0
      SUM= YOUT(1)*UJ0 +U0
      UR=SUM/UCENT
      TOWALL=YOUT(6)*T00
      TOCENT=TOWALL*YOUT(5)+TOWALL

```

ALIT4160

ALIT2050

ALIT2320

ALIT2330

```

      AREA = R**2.
      GO TO (29,30),NPART
29  WRITE(6,55)X,AREA,PH20,U0,SUM,UR,YOUT(2),YOUT(3),TOCENT,TOWALL,
      YOUT(7),YOUT(8)
      GO TO 31
30  AUG2= 3.1416*((YOUT(4)*P00)/BP)*(YOUT(1)**2.)*AUG1
      1*((R*RZERO)**2.)
      AUG=(AUG2/(AMASS1*U1))
      WRITE(6,56)X,AREA,PH20,YOUT(6),SUM,UR,AUG,YOUT(3),TOCENT,TOWALL
31  CONTINUE
      IF (J-100) 40,41,40
41  WRITE (6,60) UJ
40  RETURN
50  FORMAT(///,4X,7HX/RZERO,5X,4HAREA, 5X,4HPH20,5X,24HU0(FT/SEC) UCE
      INT(FT/SEC),4X,2HUR,5X,6HLAMBDA,6X,7HDELTA/R,2X,34HTOCENT(DEGR) TOW
      2ALL(DEGR) THETA/R0,4X,5HSHAPE)
55  FORMAT(3X,F7.3,4X,F6.3,4X,F6.2,5X,F7.1,5X,F7.1,4X,F7.4,4X,F7.3,5X
      1,F7.4,5X,F7.1,5X,F7.1,5X,F7.4,4X,F5.2)
56  FORMAT(3X,F7.3,4X,F6.3,4X,F6.2,5X,F7.4,5X,F7.1,4X,F7.4,4X,F7.3,5X
      1,F7.4,5X,F7.1,5X,F7.1)
60  FORMAT (//52H DELTA/R = 1 -- DIFFERENTIAL EQUATIONS CHANGE,
      115X,5HCL = ,F10.5//)
      END
      SUBROUTINE CALXFG (J,X,FF,GG)
      COMMON TURBNO,CF,EN,NPART,C,JRUNGE,NGAM
      1,P00,P01,T00,T01,AMACH,AG,RG
      2 ,AMASS1,AMASS0,T
      3 ,S00,CMAS,CMOM,CENR
      4 ,S0,BP,CM,VISC1
      COMMON ZA,ZR,UJ0,DORIN
      6,MASRAT,RZERO,AFAC,CFO,HD,F,AL,AAZERO,TF,FP,GP
      7,SDLOSS,ASD
      8 ,AUG1,U1,UCENT
      REAL MASRAT
      DIMENSION X(3),FF(3),GG(3),F(10)
      1 ,AN(10),D(10),D2N(10),D1D(10),D2D(10)
      1 ,AL(10),TF(10)
      5 ,FP(10),GP(10)
      UR = X(1)
      Y2 = X(2)
      DOR = X(3)
      Z1 = 0.
      Z2 = 0
      Z3 = 0
      Z4 = 0
      Z5 = 0
      Z6 = 0
      CTR = -.05
      S10 = 1./(1.-S00*UR*UR*Y2*Y2)
      S20 = Y2*S10
      DS20Y2 = S10 + S20*S20*2.*S00*UR*UR
      DS20UR = S20*S20*Y2*S00*UR*2.
      DO 89 I=1,10
      CTR = CTR + .1
      FS = TF(I)
      GO TO (60,61,62) ,J
      60 AN(I) = Y2 + F(I)
      D2N(I) = 1.
      GO TO 63
      61 AN(I) = (Y2 + F(I))*(Y2 + F(I))

```

```

ALIT 10
ALIT 20
ALIT 30
ALIT 40
ALIT 50
ALIT 60
ALIT 70
ALIT 80
ALIT 90
ALIT 100
ALIT 110
ALIT 120
ALIT 130
ALIT 140
ALIT 150
ALIT 160
ALIT 270
ALIT 280
ALIT 290
ALIT 300
ALIT 310
ALIT 340
ALIT 350
ALIT 360
ALIT 370

```

```

----- D2N(I) = 2.*(Y2 + F(I)) ----- ALIT 390
GO TO 63 ----- ALIT 390
62 AN(I) = (Y2 + F(I))*(1. + T*FS) ----- ALIT 400
D2N(I) = 1. + T*FS ----- ALIT 410
63 D(I) = 1. + T*FS - S00*UR*UR*(Y2 + F(I))*(Y2 + F(I)) ----- ALIT 420
D1D(I) = -2.*S00*UR*(Y2 + F(I))*(Y2 + F(I)) ----- ALIT 430
D2D(I) = -2.*S00*UR*UR*(Y2 + F(I)) ----- ALIT 440
Z1 = Z1 + 0.2*AN(I)/D(I) ----- ALIT
1 *CTR
Z2 = Z2 - 0.2*AN(I)*D1D(I)/(D(I)*D(I)) ----- ALIT
1 *CTR
Z3 = Z3 + 0.2*D2N(I)/D(I)
1 *CTR
Z4 = Z4 - 0.2*AN(I)*D2D(I)/(D(I)*D(I))
1 *CTR
89 CONTINUE ----- ALIT 490
C THREE EQUATIONS AND THEIR DERIVATIVES WITH RESPECT TO UR, Y2, DOR ----- ALIT 500
RH00 = P00/(RG*TO01
C P00 LOSS AT INLET OR NOT
P02 = P00
P02 = P00 - 9.16*(AMASS0*32.2/2.372)**2.*.072/(32.2*RH00)
AGG = AG/(AG-1.) ----- ALIT 510
S3 = 1. - S00*UR*UR*Y2*Y2 ----- ALIT 520
Y4 = S3**AGG*P02/P00
DY4UR = -Y4*AGG/S3*2.*S00*UR*Y2*Y2
DY4Y2 = -Y4*AGG/S3*2.*S00*UR*UR*Y2
GO TO (23,24,241),J ----- ALIT 550
23 FF(J) = (DOR*DOR*UR*(Z1-S20) + UR*S20)*Y4 ----- ALIT 570
GG(1) = (DOR*DOR*(Z1-S20) + S20)*Y4 ----- ALIT 580
1 + (DOR*DOR*UR*(Z2-DS20UR) + UR*DS20UR)*Y4 ----- ALIT 590
2 + (DOR*DOR*UR*(Z1-S20) + UR*S20)*DY4UR ----- ALIT 600
GG(2) = (DOR*DOR*UR*(Z3+Z4-DS20Y2) + UR*DS20Y2)*Y4 ----- ALIT 610
2 + (DOR*DOR*UR*(Z1-S20) + UR*S20)*DY4Y2 ----- ALIT 620
GG(3) = 2.*DOR*UR*(Z1-S20)*Y4 ----- ALIT 630
DIVDN = 1./CMAS
GO TO 88 ----- ALIT 640
24 FF(J) = (DOR*DOR*UR*UR*(Z1-S20*Y2)
1 + UR*UR*Y2*S20)*Y4 + (Y4-1.)*.5/(AGG*S00)*AFAC
GG(1) = (DOR*DOR*2.*UR*(Z1-S20*Y2)
1 + DOR*DOR*UR*UR*(Z2-DS20UR*Y2)
2 + 2.*UR*S20*Y2 + UR*UR*DS20UR*Y2) *Y4
3 + DY4UR*.5/(AGG*S00)*AFAC
4 + (DOR*DOR*UR*UR*(Z1-S20*Y2) + UR*UR*Y2*S20)*DY4UR
GG(2) = (DOR*DOR*UR*UR*(Z3+Z4-DS20Y2*Y2 - S20) ----- ALIT
1 + UR*UR*(Y2*DS20Y2 + S20))*Y4
3 + DY4Y2*.5/(AGG*S00)*AFAC
4 + (DOR*DOR*UR*UR*(Z1-S20*Y2) + UR*UR*Y2*S20)*DY4Y2
GG(3) = 2.*DOR*UR*UR*(Z1-S20*Y2)*Y4
DIVDN = 1./CMOM
GO TO 88
241 DV1 = 1. - S00*UR*UR*Y2*Y2 ----- ALIT 760
WV = S00*TOG/TO1 ----- ALIT 770
DV2 = 1. - WV*UR*UR*(1. + Y2)*(1. + Y2) ----- ALIT 780
DV2 = 1./DV2 ----- ALIT 790
FF(J) = DV1*DV2 ----- ALIT 800
GG(1) = -DV2*S00*2.*UR*Y2*Y2 ----- ALIT 810
1 + DV1*DV2*DV2*WV*2.*UR*(1.+Y2)*(1.+Y2) ----- ALIT 820
GG(2) = -DV2*S00*UR*UR*2.*Y2 ----- ALIT 830
1 + DV1*DV2*DV2*WV*UR*UR*2.*(1.+Y2) ----- ALIT 840
GG(3) = 0. ----- ALIT 850

```

```

-----PCONST= (P01/P02)**((AG-1.)/AG)
DIVDN = 1./PCONST
88 CONTINUE ALIT 863
GO TO (25,26,27), J ALIT 873
25 FF(1) = FF(1) - CMAS ALIT 883
GO TO 28 ALIT 893
26 FF(2) = FF(2) - CMCM ALIT 903
GO TO 29 ALIT 913
27 CONTINUE ALIT 923
FF(3) = FF(3) - PCONST ALIT 943
28 CONTINUE ALIT 953
C TO NORMALIZE THE FUNCTIONS FF( ) AND ITS DERIVATIVES GG( )
FF(J) = FF(J)*DIVDN
DO 111 I=1,3
GG(I) = GG(I)*DIVDN
111 CONTINUE
C CALCULATION OF INITIAL VALUE OF DELTA/ R (APPROXIMATE)
DORIN = SQRT ((CMOM + 0.5*Y2*Y2 - Y2*S20)/(Z1-S20*Y2))
RETURN
END
SUBROUTINE SUB(X,X,R,DR,J,RZERO)
DIMENSION A(50), X(50), D(50), DD(50) ALIT1060
GO TO (2,2,1),J ALIT1070
1 I=0 ALIT1080
C READ X AND DIAM ALIT1090
C XX=X/RZERO ,R=R/RZERO ALIT1100
WRITE(6,5)
5 FORMAT(15X,12HPROFILE DATA,/,10X,5HX(FT),9X,7HDIA(FT),/)
11 I=I+1 ALIT1110
READ (5,10) X(I),A(I) ALIT1120
10 FORMAT (2F15.4)
IF (A(I)) 11,12,11 ALIT1140
12 IEND=I-1 ALIT1150
SCALE = 1./RZERO
DO 50 I=1, IEND ALIT1170
WRITE(6,10)X(I),A(I)
A(I)=A(I)*.5*SCALE ALIT1190
50 X(I)=X(I)*SCALE ALIT1190
WRITE(6,15)
15 FORMAT(///)
I=1 ALIT1200
C ALIT1210
C FIND R AND DR ALIT1220
C ALIT1230
2 IF (XX-X(I)) 20,23,22 ALIT1240
20 I=I-1 ALIT1250
IF (XX-X(I)) 20,23,23 ALIT1260
23 IB=I ALIT1270
IA=I+1 ALIT1280
GO TO 24 ALIT1290
22 I=I+1 ALIT1300
IF (XX-X(I)) 25,23,22 ALIT1310
25 IA=I ALIT1320
IB=I-1 ALIT1330
24 DR=(A(IA)-A(IB))/(X(IA)-X(IB)) ALIT1340
R=A(IB)+(XX-X(IB))*DR ALIT1350
RETURN ALIT1360
END ALIT1370
SUBROUTINE RUNGE (N, X, Y, TOL, YMIN, H, XOUT, MARK) ALIT 300
C FIRST ORDER DIFF. EQ. ROUTINE--ADJUSTS STEP SIZE ALIT 310

```

DIMENSION Y(10),YMIN(10),TOL(10),SUR(10),XOUT(100),MARK(5)	ALIT 320
DIMENSION DY(50), YA(50), FA(50), FB(50), FC(50), YKEEP(50)	ALIT 330
KBTWN = 1	ALIT 340
KBIG = 1	ALIT 350
KLOW = 1	ALIT 360
NCOUNT = 15	ALIT 370
J = MARK(1)	ALIT 380
MAX = MARK(2)	ALIT 390
230 DO 250 I = 1, N	ALIT 400
250 SUB(I) = TOL(I)/32.0	ALIT 410
10 IF (MAX = J) 20, 30, 30	ALIT 420
20 RETURN	ALIT 430
30 A = XOUT(J) - X	ALIT 440
B = ABS (2.E-6*X)	ALIT 450
IF (A + B) 40, 35, 35	ALIT 460
35 IF (A - B) 50, 50, 60	ALIT 470
40 J = J + 1	ALIT 480
GO TO 10	ALIT 490
50 CONTINUE	ALIT 500
CALL PRINT (N, XOUT, Y, DY, J)	ALIT 510
J = J + 1	ALIT 520
GO TO 10	ALIT 530
60 IF (A - 1.5*H) 70, 70, 80	ALIT 540
70 H = A	ALIT 550
GO TO 1000	ALIT 560
80 IF (A - 3.*H) 90, 1000, 1000	ALIT 570
90 H = .5*A	ALIT 580
C	ALIT 590
C DO RUNGE-KUTTE-MERSON INTEGRATION	ALIT 600
C	ALIT 610
1000 XA = X + H/3.	ALIT 620
XB = X + .5*H	ALIT 630
CALL DIFFEQ (N, X, Y, DY)	ALIT 640
X = X + H	ALIT 650
DO 1030 I = 1, N	ALIT 660
YKEEP(I) = Y(I)	ALIT 670
FA(I) = H*DY(I)	ALIT 680
1030 YA(I) = Y(I) + FA(I)/3.	ALIT 690
CALL DIFFEQ (N, XA, YA, DY)	ALIT 700
DO 1040 I = 1, N	ALIT 710
1040 YA(I) = Y(I) + FA(I)/6. + H*DY(I)/6.	ALIT 720
CALL DIFFEQ (N, XA, YA, DY)	ALIT 730
DO 1050 I = 1, N	ALIT 740
FB(I) = H*DY(I)	ALIT 750
1050 YA(I) = Y(I) + .125*FA(I) + .375*FB(I)	ALIT 760
CALL DIFFEQ (N, XB, YA, DY)	ALIT 770
DO 1060 I = 1, N	ALIT 780
FC(I) = H*DY(I)	ALIT 790
1060 YA(I) = Y(I) + .5*FA(I) - 1.5*FB(I) + 2.*FC(I)	ALIT 800
CALL DIFFEQ (N, X, YA, DY)	ALIT 810
DO 1130 I = 1, N	ALIT 820
Y(I) = Y(I) + FA(I)/6. + .666666667*FC(I) + H*DY(I)/6.	ALIT 830
1061 U = Y(I)	ALIT 840
IF (ABS (U) - YMIN(I)) 1130, 1130, 1090	ALIT 850
1090 KLOW = 2	ALIT 860
E = .2*ABS (U - YA(I))	ALIT 870
IF (E - ABS (TOL(I)*U)) 1110, 1110, 1100	ALIT 880
1100 KBIG = 2	ALIT 890
GO TO 1130	ALIT 900
1110 IF (E - ABS (SUB(I)*U)) 1130, 1120, 1120	ALIT 910

1120	KBTWN = 2	ALIT 920
1130	CONTINUE	ALIT 930
	GO TO (100, 1135), KLOW	ALIT 940
1135	GO TO (1180, 1140), KBIG	ALIT 950
1140	NCOUNT = NCOUNT - 1	ALIT 960
	IF (NCOUNT) 1150, 1150, 1170	ALIT 970
1150	PRINT 1160, X, H	ALIT 980
	PRINT 1165, (I, Y(I), DY(I), I = 1, N)	ALIT 990
	RETURN	ALIT1000
1160	FORMAT (58H4STEP SIZE HALVED 15 TIMES CONSECUTIVELY SINCE LAST PR	ALIT1010
	1NT /29H PROGRAM TERMINATED AT X = , E16.8, 8H, H = , E16.8,	ALIT1020
	2//3H I, 13X, 4HY(I), 16X, 5HDY(I),//)	ALIT1030
1165	FORMAT (13,7X,E16.8,4X,E16.8)	ALIT1040
1170	KBIG = 1	ALIT1050
	IF (H - B) 1176, 1172, 1172	ALIT1060
1172	X = X - H	ALIT1070
	H = .5*H	ALIT1080
	DO 1174 I = 1, N	ALIT1090
1174	Y(I) = YKEEP(I)	ALIT1100
	KBTWN = 1	ALIT1110
	KLOW = 1	ALIT1120
	GO TO 1000	ALIT1130
1176	M = 15 - NCOUNT	ALIT1140
	PRINT 1178, M, X, H	ALIT1150
	PRINT 1165, (I, Y(I), DY(I), I = 1, N)	ALIT1160
	RETURN	ALIT1170
1178	FORMAT (41H4STEP SIZE BECAME TOO SMALL FOR COMPUTER./20H IT HAS	ALIT1180
	1EN HALVED , 12, 21H TIMES CONSECUTIVELY./29H PROGRAM TERMINATED	ALIT1190
	2 X = , E16.8, 8H, H = , E16.8//3H I, 13X, 4HY(I), 16X,	ALIT1200
	35HDY(I),//)	ALIT1210
1180	NCOUNT = 15	ALIT1220
	GO TO (1190, 1200), KBTWN	ALIT1230
1190	H = 2.*H	ALIT1240
1200	KBTWN = 1	ALIT1250
	KLOW = 1	ALIT1260
C		ALIT1270
C	CHECK FOR INTERMEDIATE PRINT OUT	ALIT1280
C		ALIT1290
100	XOUT(50)=X	ALIT1300
	JK=0	ALIT1310
C	CALL PRINT (N,XOUT,Y,DY,JK)	ALIT1320
	IF (JK) 10,10,20	ALIT1330
130	FORMAT (5H X = , E16.8, 4X, 4HH = , E16.8, 11X, 1HI, 13X, 4HY(I),	ALIT1340
	116X, 5HDY(I)/)	ALIT1350
140	FORMAT (55X, 13, 7X, 2(E16.8, 4X))	ALIT1360
	END	ALIT1370
	SUBROUTINE SIMQ(A,B,N,KS)	ALIT1380
	DIMENSION A(1),B(1)	ALIT1390
C		ALIT1400
C	ALIT1410
C		ALIT1420
C	SUBROUTINE SIMQ	ALIT1430
C	PURPOSE	ALIT1440
C	OBTAIN SOLUTION OF A SET OF SIMULTANEOUS LINEAR EQUATIONS,	ALIT1450
C	AX=B	ALIT1460
C		ALIT1470
C	USAGE	ALIT1480
C	CALL SIMQ(A,B,N,KS)	ALIT1490
C		

C	DESCRIPTION OF PARAMETERS	ALIT1500
C	A - MATRIX OF COEFFICIENTS STORED COLUMNWISE. THESE ARE	ALIT1510
C	DESTROYED IN THE COMPUTATION. THE SIZE OF MATRIX A IS	ALIT1520
C	N BY N.	ALIT1530
C	B - VECTOR OF ORIGINAL CONSTANTS (LENGTH N). THESE ARE	ALIT1540
C	REPLACED BY FINAL SOLUTION VALUES, VECTOR X.	ALIT1550
C	N - NUMBER OF EQUATIONS AND VARIABLES. N MUST BE .GT. ONE.	ALIT1560
C	KS - OUTPUT DIGIT	ALIT1570
C	6 FOR A NORMAL SOLUTION	ALIT1580
C	1 FOR A SINGULAR SET OF EQUATIONS	ALIT1590
C	REMARKS	ALIT1600
C	MATRIX A MUST BE GENERAL.	ALIT1610
C	IF MATRIX IS SINGULAR, SOLUTION VALUES ARE MEANINGLESS.	ALIT1620
C	AN ALTERNATIVE SOLUTION MAY BE OBTAINED BY USING MATRIX	ALIT1630
C	INVERSION (MINV) AND MATRIX PRODUCT (GMPRD).	ALIT1640
C	SUBROUTINES AND FUNCTION SUBPROGRAMS REQUIRED	ALIT1650
C	NONE	ALIT1660
C	METHOD	ALIT1670
C	METHOD OF SOLUTION IS BY ELIMINATION USING LARGEST PIVOTAL	ALIT1680
C	DIVISOR. EACH STAGE OF ELIMINATION CONSISTS OF INTERCHANGING	ALIT1690
C	ROWS WHEN NECESSARY TO AVOID DIVISION BY ZERO OR SMALL	ALIT1700
C	ELEMENTS.	ALIT1710
C	THE FORWARD SOLUTION TO OBTAIN VARIABLE N IS DONE IN	ALIT1720
C	N STAGES. THE BACK SOLUTION FOR THE OTHER VARIABLES IS	ALIT1730
C	CALCULATED BY SUCCESSIVE SUBSTITUTIONS. FINAL SOLUTION	ALIT1740
C	VALUES ARE DEVELOPED IN VECTOR B, WITH VARIABLE 1 IN B(1),	ALIT1750
C	VARIABLE 2 IN B(2),....., VARIABLE N IN B(N).	ALIT1760
C	IF NO PIVOT CAN BE FOUND EXCEEDING A TOLERANCE OF 0.0,	ALIT1770
C	THE MATRIX IS CONSIDERED SINGULAR AND KS IS SET TO 1. THIS	ALIT1780
C	TOLERANCE CAN BE MODIFIED BY REPLACING THE FIRST STATEMENT.	ALIT1790
C	ALIT1800
C	ALIT1810
C	ALIT1820
C	ALIT1830
C	ALIT1840
C	ALIT1850
C	ALIT1860
C	ALIT1870
C	ALIT1880
C	ALIT1890
C	ALIT1900
C	ALIT1910
C	ALIT1920
C	ALIT1930
C	ALIT1940
C	ALIT1950
C	ALIT1960
C	ALIT1970
C	ALIT1980
C	ALIT1990
C	ALIT2000
C	ALIT2010
C	ALIT2020
C	ALIT2030
C	ALIT2040
C	ALIT2050
C	ALIT2060
C	ALIT2070
C	ALIT2080
C	ALIT2090
C	ALIT2100
C	ALIT2110

35 KS=1	ALIT2129
RETURN	ALIT2139
C	ALIT2149
C INTERCHANGE ROWS IF NECESSARY	ALIT2159
C	ALIT2169
40 I1=J+N*(J-2)	ALIT2179
IT=IMAX-J	ALIT2189
DO 50 K=J,N	ALIT2199
I1=I1+N	ALIT2209
I2=I1+IT	ALIT2219
SAVE=A(I1)	ALIT2229
A(I1)=A(I2)	ALIT2239
A(I2)=SAVE	ALIT2249
C	ALIT2259
C DIVIDE EQUATION BY LEADING COEFFICIENT	ALIT2269
C	ALIT2279
50 A(I1)=A(I1)/BICA	ALIT2289
SAVE=B(IMAX)	ALIT2299
B(IMAX)=B(J)	ALIT2309
B(J)=SAVE/BICA	ALIT2319
C	ALIT2329
C ELIMINATE NEXT VARIABLE	ALIT2339
C	ALIT2349
IF(J-N) 55,70,55	ALIT2359
55 IQS=N*(J-1)	ALIT2369
DO 65 IX=JY,N	ALIT2379
IXJ=IQS+IX	ALIT2389
IT=J-IX	ALIT2399
DO 60 JX=JY,N	ALIT2409
IXJX=N*(JX-1)+IX	ALIT2419
JJX=IXJX+IT	ALIT2429
60 A(IXJX)=A(IXJX)-(A(IXJ)*A(JJX))	ALIT2439
65 B(IX)=B(IX)-(B(J)*A(IXJ))	ALIT2449
C	ALIT2459
C BACK SOLUTION	ALIT2469
C	ALIT2479
70 NY=N-1	ALIT2489
IT=N*N	ALIT2499
DO 80 J=1,NY	ALIT2509
IA=IT-J	ALIT2519
IB=N-J	ALIT2529
IC=N	ALIT2539
DO 80 K=1,J	ALIT2549
B(IB)=B(IB)-A(IA)*B(IC)	ALIT2559
IA=IA-N	ALIT2569
80 IC=IC-1	ALIT2579
RETURN	ALIT2589
END	
SUBROUTINE VB04A (M,N,F,X,E,A,ESCALE,IPRINT,MAXKFG,IA,W)	ALIT2599
DIMENSION A(3,10), W(10), F(3), E(3), X(3)	ALIT2109
IC=0	ALIT2119
IKFG=0	ALIT2129
IP=IPRINT	ALIT2139
IPSET=-IPRINT*(IPRINT-1)	ALIT2149
NN=N+N	ALIT2159
NP=N+1	ALIT2169
NNP=N+NP	ALIT2179
ICON=1	ALIT2189
IFS=1	ALIT2199
IS=2	ALIT2209

1 KK=N	ALIT2210
DO 3 I=1,N	ALIT2220
KK=KK+1	ALIT2230
DO 2 J=1,I	ALIT2240
2 A(I,J)=0.	ALIT2250
3 W(KK)=0.	ALIT2260
FF=0.	ALIT2270
IKFG=IKFG+1	ALIT2280
DO 4 K=1,M	ALIT2290
CALL CALXFG (K,X,F,W)	ALIT2300
KK=N	ALIT2310
DO 5 I=1,N	ALIT2320
KK=KK+1	ALIT2330
DO 6 J=1,I	ALIT2340
6 A(I,J)=A(I,J)+W(I)*W(J)	ALIT2350
5 W(KK)=W(KK)-W(I)*F(K)	ALIT2360
4 FF=FF+F(K)*F(K)	ALIT2370
GO TO (7,8),IS	ALIT2380
8 DO 45 I=2,N	ALIT2390
IK = I - 1	ALIT2400
DO 45 J=I,N	ALIT2410
45 A(IK,J) = A(J,IK)	ALIT2420
CALL SPNIST(A,N,N,IK)	ALIT2430
KK=NP	ALIT2440
DO 9 I=1,N	ALIT2450
W(I)=W(KK)	ALIT2460
9 KK=KK+1	ALIT2470
EM=0.	ALIT2480
DO 10 I=1,N	ALIT2490
W(KK)=0.	ALIT2500
DO 11 J=1,N	ALIT2510
11 W(KK)=W(KK)+A(I,J)*W(J)	ALIT2520
EM = MAX1(EM,ABS(W(KK)/E(I)))	ALIT2530
10 KK=KK+1	ALIT2540
IF (EM-ESCALE)-12,12,13	ALIT2550
13 EM=ESCALE/EM	ALIT2560
KK=NNP	ALIT2570
DO 14 I=1,N	ALIT2580
W(KK)=W(KK)*EM	ALIT2590
14 KK=KK+1	ALIT2600
GO TO 15	ALIT2610
12 IF (EM-1.) 16,16,15	ALIT2620
16 GO TO (27,18),ICON	ALIT2630
27 ICON=2	ALIT2640
GO TO 17	ALIT2650
18 IF (IPRINT) 19,19,20	ALIT2660
19 RETURN	ALIT2670
20 WRITE(6,21)	ALIT2680
21 FORMAT (//5X,18HV804A FINAL VALUES)	ALIT2690
IFS=2	ALIT2700
GO TO 22	ALIT2710
15 ICON=1	ALIT2720
17 IF (IKFG-MAXKFG) 28,29,29	ALIT2730
29 WRITE(6,30) IKFG	ALIT2740
30 FORMAT (//5X,5HV804A,I5,17HM CALLS OF CALXFG)	ALIT2750
GO TO 18	ALIT2760
28 IP=IP+IPRINT	ALIT2770
IF (IP) 23,23,22	ALIT2780
22 WRITE(6,26) IC, IKFG	ALIT2790
26 FORMAT (//5X,9HITERATION,I4,I10,17HM CALLS OF CALXFG)	ALIT2800

WRITE(6,24)(X(I),I=1,N)	ALIT2810
24 FORMAT (/5X,9HVARIALES/, (5E24.14))	ALIT2820
WRITE(6,25)(F(I),I=1,M)	ALIT2830
25 FORMAT (/5X,9HFUNCTIONS/, (5E24.14))	ALIT2840
GO TO (38,19),IFS	ALIT2850
38 IP=IPSET	ALIT2860
23 IC=IC+1	ALIT2870
ITEST=3	ALIT2880
FFX=FF	ALIT2890
XP=0.	ALIT2900
XC=0.	ALIT2910
IS=1	ALIT2920
7 GG=0.	ALIT2930
KK=NNP	ALIT2940
DQ 31 I=NP,NN	ALIT2950
GG=GG-W(I)*W(KK)	ALIT2960
31 KK=KK+1	ALIT2970
GG=GG+GG	ALIT2980
CALL VD02A (ITEST,XC,FF,GG,6,0.,0.3,1.)	ALIT2990
GO TO (32,33,33,33,33),ITEST	ALIT3000
32 XP=XC-XP	ALIT3010
KK=NNP	ALIT3020
DQ 34 I=1,N	ALIT3030
X(I)=X(I)+XP*W(KK)	ALIT3040
34 KK=KK+1	ALIT3050
XP=XC	ALIT3060
GO TO 1	ALIT3070
33 IF (FF-FFX) 39,40,40	ALIT3080
39 IF(ABS(EM*XC) - 1.) 36,36,37	ALIT3090
37 ICON=1	ALIT3100
36 IF (XP-XC) 35,8,35	ALIT3110
35 IS=2	ALIT3120
GO TO 32	ALIT3130
40 WRITE(6,41)	ALIT3140
41 FORMAT (/5X,33HVB04A ACCURACY CANNOT BE ACHIEVED)	ALIT3150
GO TO 18	ALIT3160
END	ALIT3170
SUBROUTINE VD02A (ITEST,X,F,G,MAXFUN,ABSACC,RELACC,XSTEP)	ALIT3180
ABSF(XYZ)=ABS(XYZ)	ALIT3190
SIGNF(ABC,XYZ)=SIGN(ABC,XYZ)	ALIT3200
SQRTF(XYZ)=SQRT(XYZ)	ALIT3210
GO TO (1,2,2),ITEST	ALIT3220
2 IS=ITEST	ALIT3230
ITEST=1	ALIT3240
IINC=1	ALIT3250
XINC=XSTEP	ALIT3260
MC=1	ALIT3270
GO TO (4,4,10),IS	ALIT3280
3 MC=MC+1	ALIT3290
IF (MC-MAXFUN) 4,4,5	ALIT3300
5 ITEST=4	ALIT3310
11 F=FA	ALIT3320
X=XA	ALIT3330
G=GA	ALIT3340
4 RETURN	ALIT3350
10 IS=2	ALIT3360
MC=0	ALIT3370
1 IF (G) 6,7,6	ALIT3380
7 ITEST=5	ALIT3390
GO TO 4	ALIT3400
6 GO TO (8,9),IS	ALIT3410
9 XA=X	ALIT3420

FA=F	ALIT3430
GA=G	ALIT3440
IS=1	ALIT3450
12 X=XA-SIGNF(XINC,GA)	ALIT3460
XINC=XINC+XINC	ALIT3470
GO TO 3	ALIT3480
8 IF (F-FA) 13,13,14	ALIT3490
13 DUM=FA	ALIT3500
FA=F	ALIT3510
F=DUM	ALIT3520
DUM=GA	ALIT3530
GA=G	ALIT3540
G=DUM	ALIT3550
DUM=XA	ALIT3560
XA=X	ALIT3570
X=DUM	ALIT3580
14 IF (GA*(X-XA)) 15,16,18	ALIT3590
15 IINC=2	ALIT3600
XINC=X	ALIT3610
16 Z=3.*(FA-F)/(X-XA)+G+GA	ALIT3620
W=Z*Z-G*GA	ALIT3630
IF (W) 20,20,17	ALIT3640
17 W=SIGNF(SQRTF(W),X-XA)	ALIT3650
XP=X-(X-XA)*(G+W-Z)/(G-GA+W+W)	ALIT3660
IF ((XP-XA)*GA) 18,19,20	ALIT3670
18 GO TO (21,22),IINC	ALIT3680
21 IF (ABSF(XP-XA)-ABSF(XINC)) 23,23,12	ALIT3690
22 IF (ABSF(XP-XA)-ABSF(XINC-XP)) 23,23,24	ALIT3700
24 X=0.5*(XINC+XA)	ALIT3710
IF ((X-XA)*(XINC-X)) 25,25,3	ALIT3720
25 ITEST=3	ALIT3730
GC TO 11	ALIT3740
23 X=XP	ALIT3750
IF (ABSF(XP-XA)-ABSF(ABSACC)) 19,19,26	ALIT3760
26 IF (ABSF(XP-XA)-ABSF(XP*RELACC)) 19,19,3	ALIT3770
19 ITEST=2	ALIT3780
GO TO 11	ALIT3790
20 GC TO (12,24),IINC	ALIT3800
END	ALIT3810
SUBROUTINE SPNIST(U,I,J,K)	ALIT3820
DIMENSION U(3,3),V(3,3)	ALIT3830
IF(I-3) 2,1,2	ALIT3840
2 I=J+K	ALIT3850
WRITE(6,4)	ALIT3860
4 FORMAT(14H0 MODIFY VR04A)	ALIT3870
STOP	ALIT3880
1 V(1,1)=U(2,2)*U(3,3)-U(3,2)**2	ALIT3890
V(2,2)=U(1,1)*U(3,3)-U(3,1)**2	ALIT3900
V(3,3)=U(1,1)*U(2,2)-U(2,1)**2	ALIT3910
V(2,1)=U(3,1)*U(3,2)-U(2,1)*U(3,3)	ALIT3920
V(1,2)=V(2,1)	ALIT3930
V(3,1)=U(2,1)*U(3,2)-U(2,2)*U(3,1)	ALIT3940
V(1,3)=V(3,1)	ALIT3950
V(3,2)=U(3,1)*U(2,1)-U(1,1)*U(3,2)	ALIT3960
V(2,3)=V(3,2)	ALIT3970
DET=U(1,1)*V(1,1)+U(2,1)*V(2,1)+U(3,1)*V(3,1)	ALIT3980
DC 5 L=1,3	ALIT3990
DO 5 M=1,3	ALIT4000
5 U(L,M)=V(L,M)/DET	ALIT4010
RETURN	ALIT4020
END	ALIT4030

B.4 Typical Sets of Input and Output Data

Input Data:

```
10
.9950.9850.9750.9650.9550.9450.9350.9250.9150.9050
  .33   .21
    .000223 1.400000 .000160 .223000
      M= 21.0
    .500    5.2981  147.0    1    1    2.50    .00046
  14.7  552.0  348.0 1267.0 .113  2.375  1.40  53.2
0.0      .445
1.6315   .3035
2.3815   .3037
3.7686   .4462
4.2148   .4463
5.2981   .5796
0.000000 0.000000
10
.9950.9850.9750.9650.9550.9450.9350.9250.9150.9050
  .33   .21
    .000223 1.400000 .000160 .223000
      M= 17.0 -.02
    .500    5.2981  147.0    2    1    2.00    .00046
  14.7  552.0  348.0 1267.0 .113  1.885  1.40  53.2
```

Output Data

NS = 10
G(I)S 0.9950 0.9850 0.9750 0.9650 0.9550 0.9450 0.9350 0.9250 0.9150 0.9050

DUCT LOSS COEFFICIENT = 0.330
DUCT AREA = 0.210FT**2

N= 21.0--02

DEL TAY= 0.5000 SHAPE= 1.400000 RZERO= 0.223000FT
RTUBE= 5.2981 NSUB= 2 THE TA= 0.000223FT
TURBNO= 147.0000 NGRN= 1 WISC= 0.00160FT**3/SEC
AS= 1.4000 RG= 53.200GFT-LBF/LBM-DEGR

POO= 14.7000PSIA
TOO= 552.0000DEGR
POL= 348.0000PSIA
TOT= 1267.9900DEGR
AMISSO= 2.3230LBM/SEC
AMASS1= 0.11309M/SEC
AMOT= 0.00044FT**2
XCORE= 2.5000

F(I)S 0.9806 0.8589 0.6848 0.5054 0.3482 0.2251 0.1367 0.0768 0.0367 0.0092

CONDITIONS AT BEGINNING OF THE TRANSITION SECTION

UO= 273. FT/SEC RHO= 0.0698LBM/FT**3 UJOO= 2747. FT/SEC
TO= 546. DEGR PH= 2026.0000PSIA PRIMARY NGRN= 10.6LBF
LAMBOA= 0.0994 PHZO= 17.49IN.H2O

ITERATION 0 1M CALLS OF CALXFG

VARIABLES
0.100000000000E 01 0.99405705078903E-01 0.23294270038605E 00

FUNCTIONS
0.14328718185425E-01 -0.54895021071364E-02 -0.12727778084809E-04

ITERATION 1 2M CALLS OF CALXFG

VARIABLES

0.10017890930176E 01 0.97278773784637E-01 0.23825997114182E 00
 FUNCTIONS
 -0.1650773690905E-04 0.34540961656537E-03 -0.16198788305605E-04

ITERATION 2 3M CALLS OF CALXFG

VARIABLES
 0.10017881307637E 01 0.97286164760500E-01 0.23817074298850E 00

FUNCTIONS
 0.59956214843420E-06 0.79679296050017E-06 -0.23141410545584E-05

V804A ACCURACY CANNOT BE ACHIEVED

V804A FINAL VALUES

ITERATION 3 8M CALLS OF CALXFG

VARIABLES
 0.10017862315946E 01 0.97286045551300E-01 0.23817068338394E 00

FUNCTIONS
 -0.17668861610855E-05 -0.59759468058472E-05 -0.80994950621971E-05

XX(1)= 1.0017862320 XX(2)= 0.0972860456 XX(3)= 0.2381706334

EN= 0.6539 EN2= 0.6541

SO= 1.1437 SP= 0.1744

UJO= -2751.4FT/SEC UCENT= 3019.1FT/SEC

PARAMETER	AREA	PHRO	UOFT/SEC	UCENT/SEC	UR	LAMBDA	DELTA/R	TRACER/TRACE	FORMAL/FORMAL	SHAPE
2.507	0.791	-17.09	267.7	3019.1	1.0000	0.007	0.2118	1267.0	552.0	0.0035
3.000	0.753	-18.03	275.9	2235.4	0.7403	0.141	0.2857	1041.6	552.0	0.0041
3.500	0.716	-19.14	285.4	1754.5	0.5811	0.194	0.3580	911.1	552.0	0.0046
4.000	0.679	-20.57	296.8	1449.3	0.4800	0.257	0.4268	830.1	552.0	0.0049
4.500	0.644	-22.25	310.5	1245.4	0.4125	0.332	0.4910	776.2	552.0	0.0051
5.000	0.610	-24.47	322.3	1104.0	0.3657	0.421	0.5400	730.2	552.0	0.0052
5.500	0.576	-27.31	347.9	1004.2	0.3326	0.530	0.6029	710.4	552.0	0.0051
6.000	0.544	-30.98	372.7	934.1	0.3094	0.644	0.6494	688.2	552.0	0.0050

6.500	0.512	-15.77	402.8	887.0	0.2938	0.882	0.6891	672.6	552.0	0.0047	1.26
7.000	0.499	-61.87	439.2	859.0	0.2845	1.046	0.7222	659.3	552.0	0.0045	1.25
7.500	0.492	-61.87	439.2	859.0	0.2845	1.046	0.7222	659.3	552.0	0.0045	1.25

DELTA/R = 1 -- DIFFERENTIAL EQUATIONS CHANGE CL = 419.82104

FZ(11)'S	0.9904	0.9301	0.8441	0.7558	0.6789	0.6190	0.5762	0.5474	0.5281	0.4905
----------	--------	--------	--------	--------	--------	--------	--------	--------	--------	--------

GZ(11)'S	0.0046	-0.0549	0.1308	0.2092	0.2761	0.3340	0.3508	0.3776	0.3869	0.4145
----------	--------	---------	--------	--------	--------	--------	--------	--------	--------	--------

Y/RZ/RO	AREA	PMZO	TOTAL/TDO	UCENT(F/T/SEC)	UR	AUGMENT	GAMMA	TOCENT (DFGR)	TOWALL (DFGR)
7.500	0.463	-46.17	1.0054	917.8	0.2709	3.944	3.1875	657.7	555.0
8.000	0.463	-45.98	1.0102	772.0	0.2557	3.924	3.1069	655.0	557.4
8.500	0.463	-46.00	1.0141	734.6	0.2433	3.911	0.4166	652.8	559.8
9.000	0.463	-46.37	1.0172	703.6	0.2331	3.904	0.5169	650.9	561.5
9.500	0.463	-46.72	1.0199	677.9	0.2245	3.901	0.6094	649.3	563.0
10.000	0.464	-47.25	1.0221	655.9	0.2173	3.901	0.6973	647.9	564.2
10.500	0.464	-47.78	1.0239	637.2	0.2110	3.904	0.7694	646.7	565.2
11.000	0.466	-48.13	1.0276	593.9	0.1967	3.695	0.8013	643.5	567.2
11.500	0.523	-48.60	1.0314	543.1	0.1700	3.372	0.8083	638.5	569.5
12.000	0.561	-48.56	1.0353	500.0	0.1656	3.115	0.8130	636.2	571.5

12.500	0.600	-23.66	1.0394	462.0	0.1533	2.836	0.8151	632.3	573.2
13.000	0.680	-19.63	1.0411	430.8	0.1476	2.896	0.8185	630.7	575.7
13.500	0.682	-16.28	1.0435	402.3	0.1333	2.535	0.8117	628.5	576.0
14.000	0.724	-13.48	1.0498	377.4	0.1290	2.343	0.8092	626.9	577.2
14.500	0.760	-11.08	1.0475	355.3	0.1177	2.200	0.7965	624.7	578.2
15.000	0.815	-9.05	1.0491	335.6	0.1112	2.070	0.7898	623.1	579.1
15.500	0.862	-7.30	1.0506	318.0	0.1053	1.952	0.7771	621.7	579.9
16.000	0.911	-6.80	1.0420	302.1	0.1001	1.844	0.7756	620.4	580.7
16.500	0.960	-6.50	1.0532	287.8	0.0953	1.765	0.7704	619.2	581.3
17.000	1.001	-3.54	1.0541	276.7	0.0910	1.694	0.7699	618.3	581.9
17.500	1.001	-3.66	1.0544	274.2	0.0908	1.670	0.7516	618.1	582.0
18.000	1.001	-3.72	1.0546	272.1	0.0901	1.659	0.7374	618.0	582.1
18.500	1.001	-3.79	1.0549	270.1	0.0895	1.650	0.7314	617.8	582.2
19.000	1.014	-3.60	1.0552	265.9	0.0881	1.649	0.7201	617.5	582.5
19.500	1.077	-2.42	1.0563	252.8	0.0837	1.551	0.7699	616.4	583.1
20.000	1.141	1.41	1.0572	241.0	0.0798	1.441	0.7390	615.4	583.6
20.500	1.208	-0.55	1.0581	230.4	0.0763	1.379	0.7048	614.5	584.1
21.000	1.273	0.20	1.0589	220.7	0.0731	1.304	0.6707	613.7	584.5
21.500	1.347	0.85	1.0597	211.9	0.0702	1.235	0.6361	613.0	584.9
22.000	1.419	1.42	1.0603	203.8	0.0675	1.172	0.6013	612.3	585.3
22.500	1.494	1.91	1.0609	196.3	0.0650	1.113	0.5664	611.7	585.6
23.000	1.570	2.35	1.0615	188.4	0.0627	1.050	0.5323	611.1	585.8
23.500	1.648	2.73	1.0620	182.9	0.0606	1.010	0.4996	610.5	586.3

REFERENCES

1. Hickman, K. E. , Gilbert, G. B. , and Carey, J. H. : "Analytical and Experimental Investigation of High Entrainment Jet Pumps," NASA CR-1602, July, 1970.
2. Hill, P. G. : "Incompressible Jet Mixing in Converging-Diverging Axisymmetric Ducts," Transactions of the ASME, J. B. E. , March, 1967.
3. Abramovitch, G. N. : The Theory of Turbulent Jets (translation), M. I. T. Press, Cambridge, Mass. , 1963.
4. Moses, H. L. : "The Behavior of Turbulent Boundary Layers in Adverse Pressure Gradients," M. I. T. Gas Turbine Laboratory Rpt. #73, January, 1964.
5. Hill, P. G. : "Turbulent Jets in Ducted Streams," Journal of Fluid Mechanics, Vol. 22, part 1, 1965, pp. 161-186.
6. Schlichting, H. : Boundary Layer Theory, 4th Ed. , Pergamon Press, N. Y.
7. Helmbold, H. B. , Luessen, G. , and Heinrich, A. M. : "An Experimental Comparison of Constant Pressure and Constant Diameter Jet Pumps," University of Wichita, School of Engineering, Engineering Report No. 147, 1954.

TABLE 1
MEASURED PARAMETERS AND INSTRUMENTATION

	Flow Parameter	Instrumentation Used to Measure Parameter	How Recorded	Required for Determining	Data Reduction Procedure
Primary Flow	P_{o1}	Bourdon Tube Gage	Manually	Jet Pump Input Conditions	None Needed
	T_{o1}	Thermocouple and Bridge	Manually	Jet Pump Input Conditions	None Needed
	W_1	Orifice Flow Meter and Panel Gage	Manually	Jet Pump Input Conditions	Standard calibration curves provided by flowmeter manu- facturer
Secondary	T_{oo}	Dial Gage in Suction Duct	Manually	Secondary Flow Temperature	None Needed
	$P_{atm} = P_{oo}$	Mercury Barom- eter	Manually	Atmospheric Pressure	None Needed
	P_b	Manometers	Manually and Photographically	Secondary Flow Rate	See Below
	W_o	Calibrated Bell- mouth	Manually	Secondary Flow Rate in lb/min	Equation (48)
Mixing Tube	p vs. length	Manometer Board	Photographically	Mixing Tube and Diffuser Static Pressures	None Needed
	P T_o	Kiel-Temperature Probe Traverse	Manually	Velocity and Tem- perature Profiles	See Text

TABLE 2
PRESSURE TAP LOCATIONS AND FINAL MIXING TUBE DIMENSIONS

Static Pressure Tap No.	Stagnation Pressure Traverse No.	Pressure Tap Location figure 4 x-inches	Dimensionless Location x/R_o ($R_o = 2.670''$)
1	1	0.46	0.172
2		2.21	0.828
3		4.71	1.76
4		6.71	2.51
5	2	9.71	3.63
6		12.21	4.57
7		14.71	5.51
8	3	17.21	6.45
9		20.46	7.66
10		22.21	8.32
11	4, 5	24.71	9.25
12		27.21	10.19
13		29.71	11.13
14		32.21	12.06
15	6	34.71	13.0
16		37.21	13.94
17		39.71	14.87
18		42.21	15.81
19		44.46	16.65
20		47.21	17.68
21		49.71	18.62
22		51.69	19.36
23		57.69	21.60
24		63.69	23.85
25		69.69	26.09

Measured Mixing
Tube Dimensions

x (in)	Dia. (in)	x/R_o
0	5.341	0
19.578	3.643	7.34
28.578	3.645	10.7
45.224	5.355	16.9
50.578	5.356	18.95
63.578	6.956	23.8

TABLE 3
STATIC PRESSURE VALUES MEASURED ALONG THE MIXING TUBE

Entrainment Ratio		17.0	19.4	21.0	23.6
Primary Flow Rate, lbm/min		6.76	6.76	6.76	6.76
Secondary Flow Rate, lbm/min		115.1	131.4	142.0	160.3
Static Pres- sure Tap No.	x/R_o station	all values in inches of water gage with respect to P_{∞}			
1	0.172	- 7.66	-10.3	-11.8	-15.6
2	0.828	- 8.25	-10.6	-12.4	-16.2
3	1.76	- 8.85	-11.8	-14.15	-18.9
4	2.51	- 9.15	-13.0	-15.6	-20.6
5	3.63	-10.9	-15.0	-18.6	-25.1
6	4.57	-12.1	-17.7	-21.8	-30.1
7	5.51	-14.45	-21.5	-26.8	-37.8
8	6.45	-17.7	-27.4	-34.6	-49.5
9	7.66	-23.0	-36.6	-46.4	-67.5
10	8.32	-22.7	-36.3	-46.4	-68.0
11	9.25	-22.1	-36.3	-46.4	-68.8
12	10.19	-21.8	-36.0	-46.6	-69.3
13	11.13	-17.4	-30.1	-39.6	-62.2
14	12.06	-10.05	-20.3	-28.0	-44.2
15	13.0		-13.55	-20.1	-33.9
16	13.94		- 8.85	-14.45	-26.8
17	14.87	1.4	- 5.4	-10.3	-21.2
18	15.81	3.5	- 2.7	- 7.2	-17.4
19	16.65	5.0	- 0.9	- 5.0	-14.6
20	17.68	5.7	0.3	- 3.6	-12.7
21	18.62	6.0	0.7	- 3.0	-11.4
22	19.36	6.6	1.6	- 2.0	-10.2
23	21.60	9.0	4.6	1.5	- 5.9
24	23.85	10.3	6.4	3.4	- 3.4
25	26.09	11.1	7.5	4.7	- 1.7

TABLE 4

VELOCITY AND TEMPERATURE PROFILES AT TRAVERSE STATION 1

Traverse Probe Position	From Traverse Probe Data			Analytical Predictions for $X_{\text{core}} = 2.5R_o$			Analytical Predictions for $X_{\text{core}} = 2.0R_o$		
y/R	p/P	Mach number	T/T _o	To oR	U ft/sec	Mach No.	To oR	U ft/sec	Mach Number
0.949	0.967	0.218	0.991	552	268	.235	552	261	.226
0.837	0.966	0.223	0.990						
0.707	0.965	0.226	0.990						
0.548	0.964	0.229	0.990						
0.447	0.964	0.230	0.990						
0.316	0.949	0.273	0.985				577		.226
0.224	0.830	0.522	0.948	631	296	.245	713	477	.373
0.100	0.544	0.975	0.840	1002	1350	.950	923	1400	1.03
0	0.311	1.45	0.705	1267	3020	2.66	1040	2230	1.80
0.100	0.524	1.01	0.831	1002	1350	.955	923	1400	1.03
0.224	0.897	0.398	0.969	631	296	.245	713	477	.370
0.316	0.962	0.237	0.989	552	268	.235	577	261	.226
0.447	0.962	0.236	0.989				552		.226
0.548	0.963	0.232	0.989						
0.707	0.964	0.229	0.990						
0.837	0.964	0.229	0.990						
0.949	0.966	0.222	0.990						

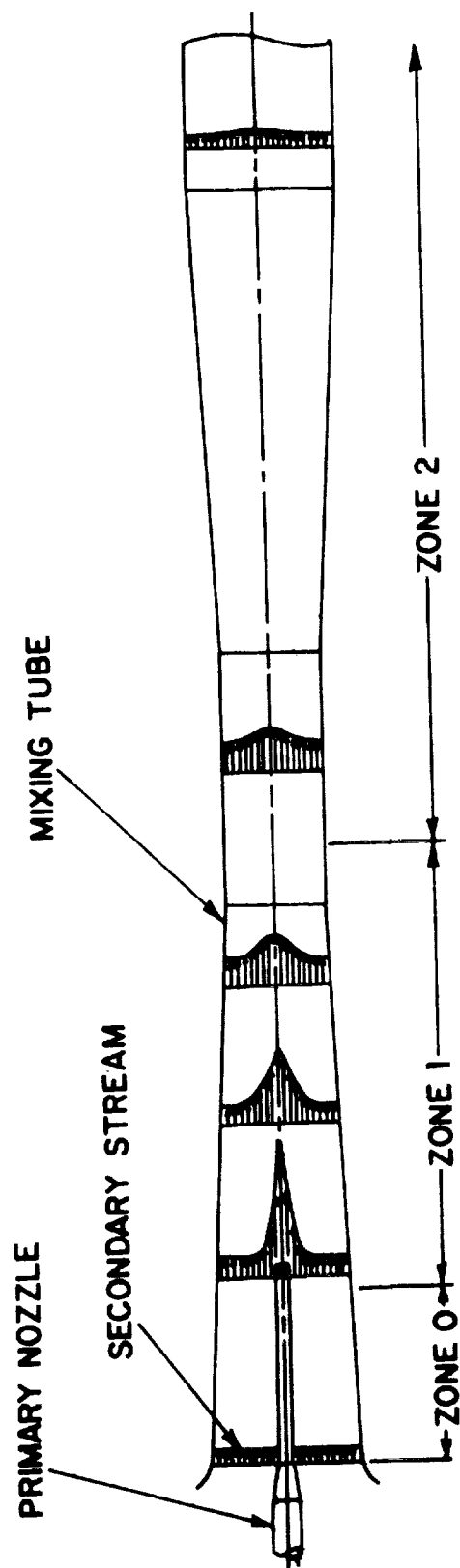


Figure 1 Jet Mixing in a Converging-Diverging Duct

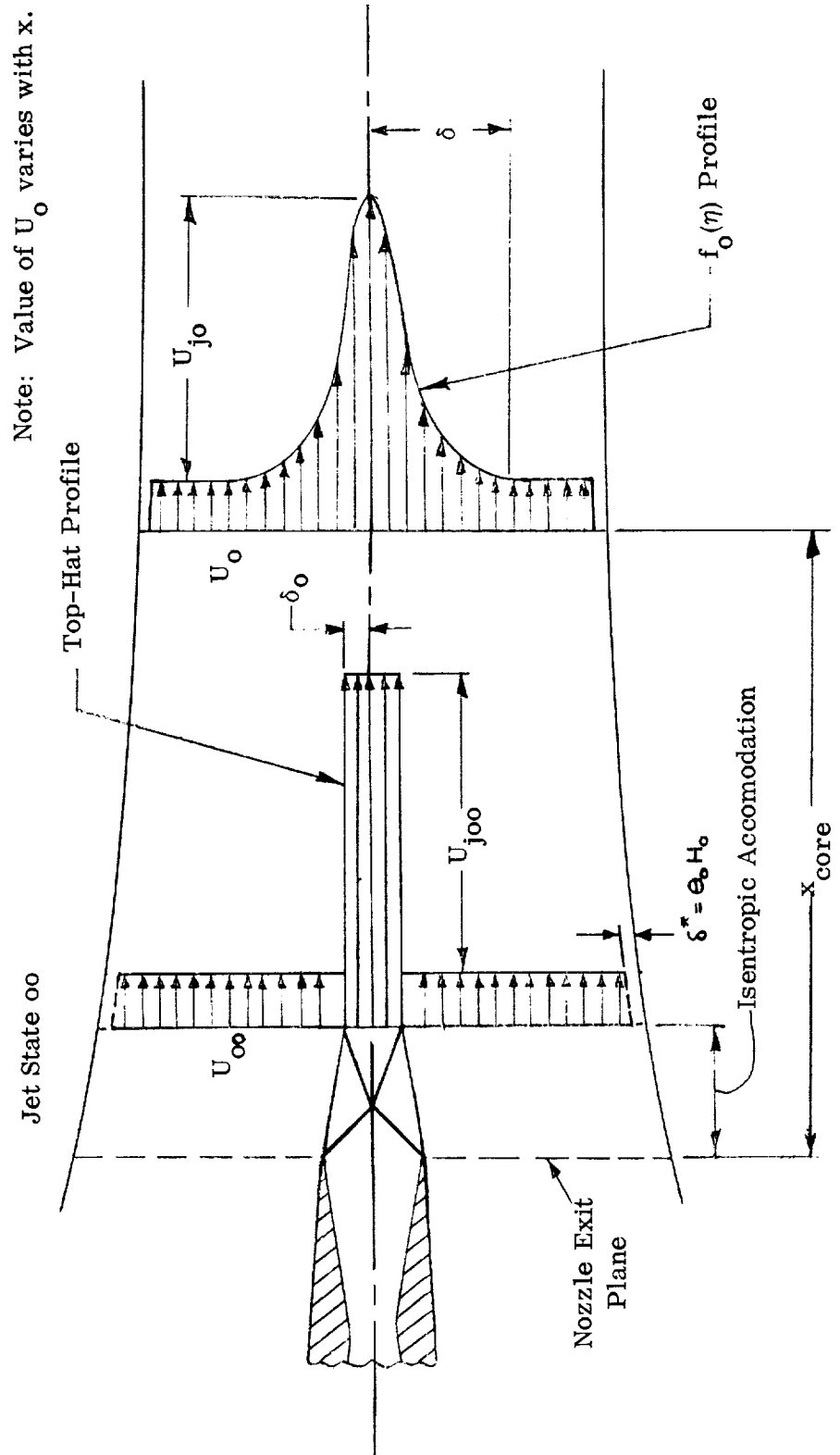


Figure 2. Velocity Profiles in the Transition Zone

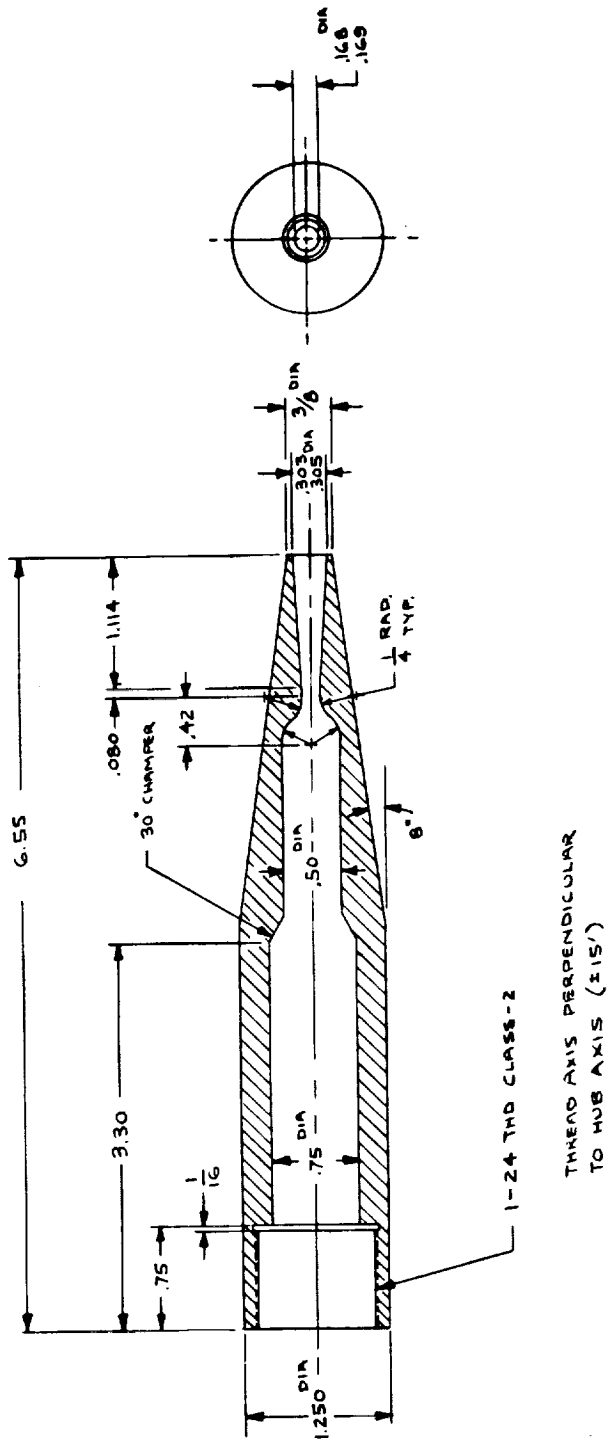


Figure 3 Primary Nozzle Geometry

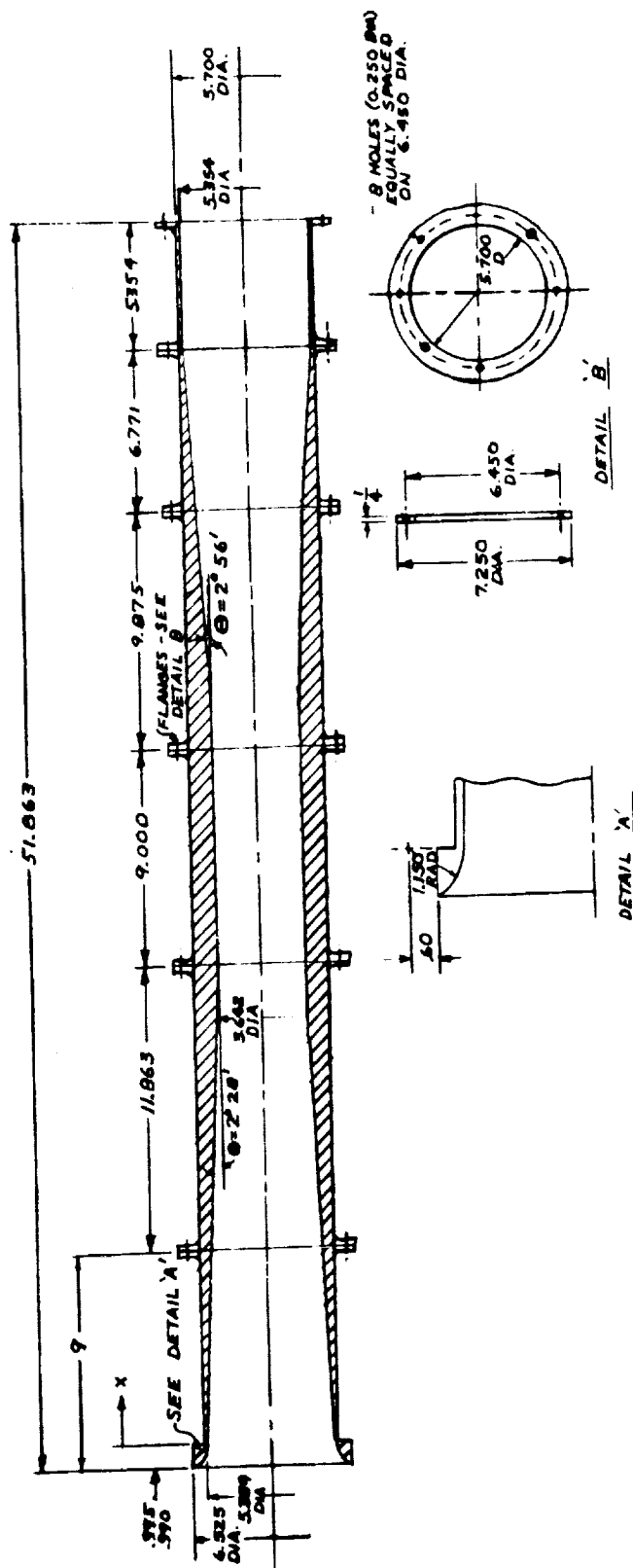


Figure 4 Mixing Tube Geometry

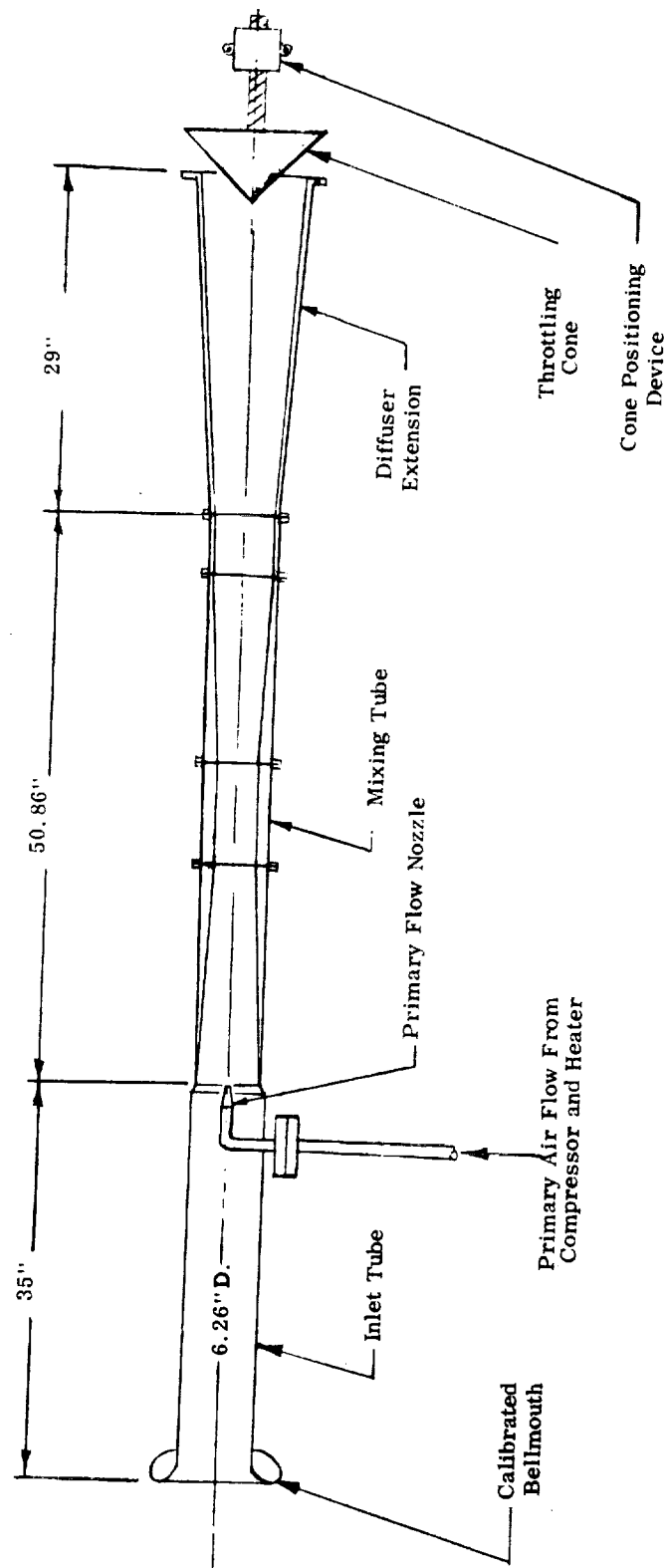


Figure 5 Jet Pump Test Rig

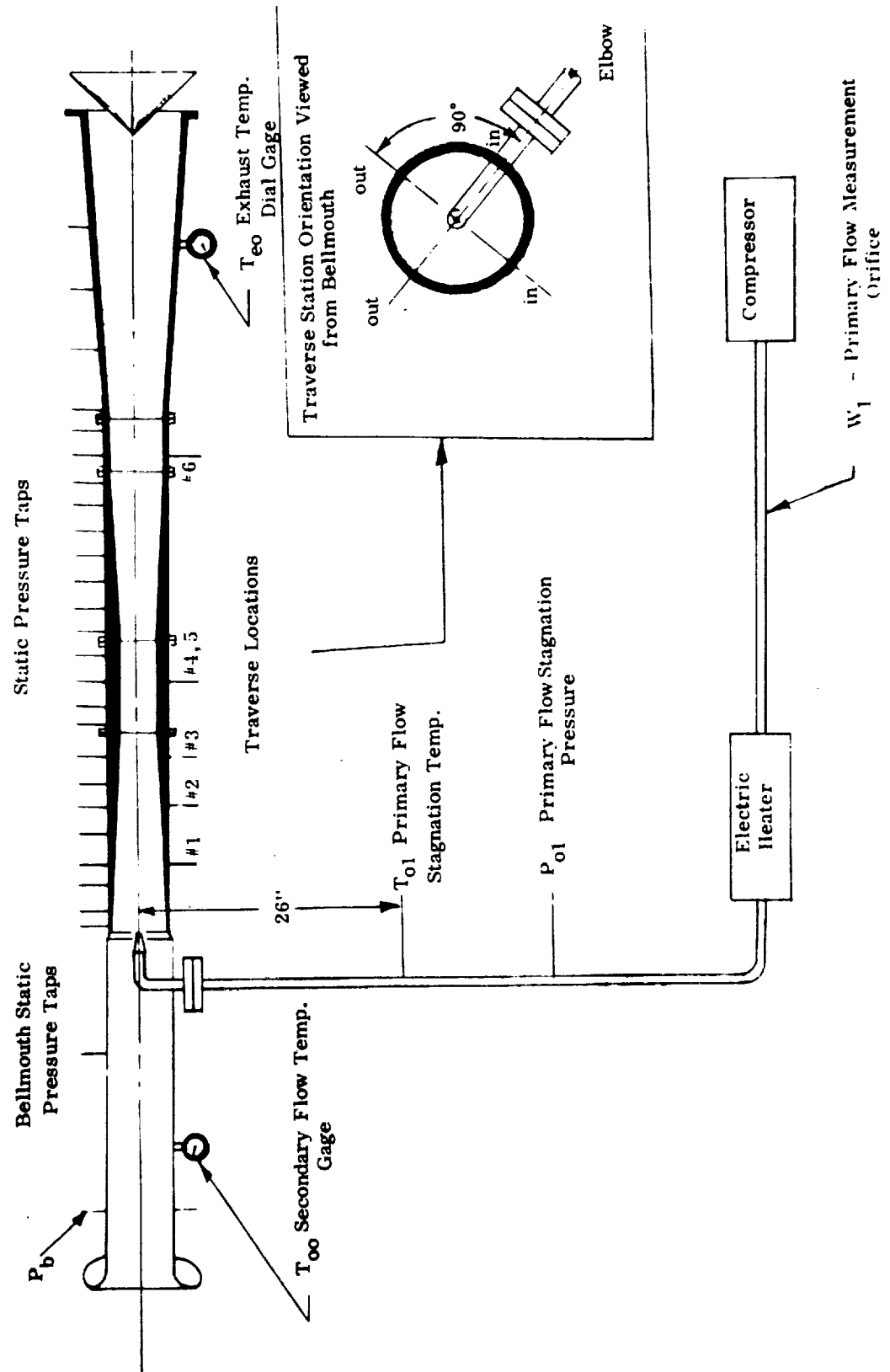


Figure 6 Jet Pump Test Instrumentation

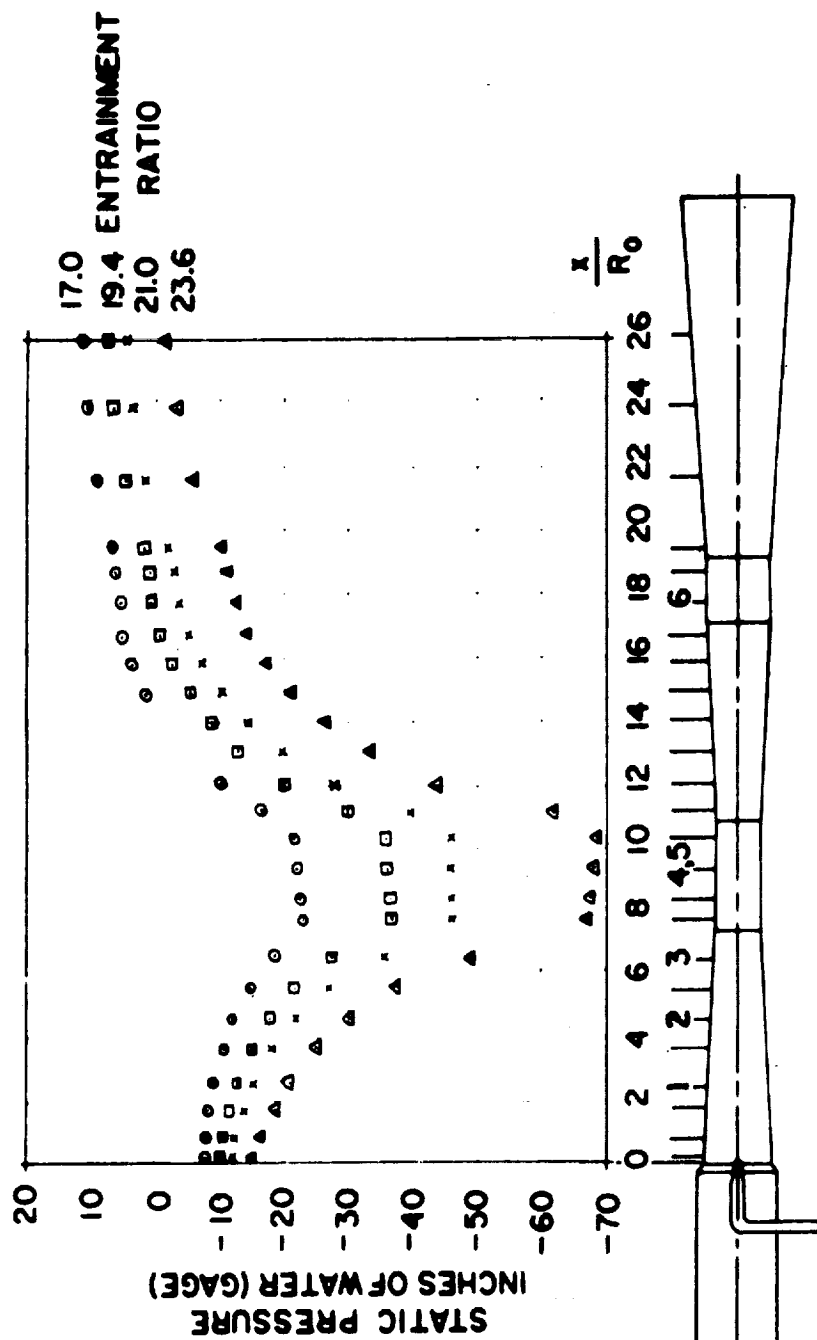


Figure 7 Mixing Tube Static Pressure Variations

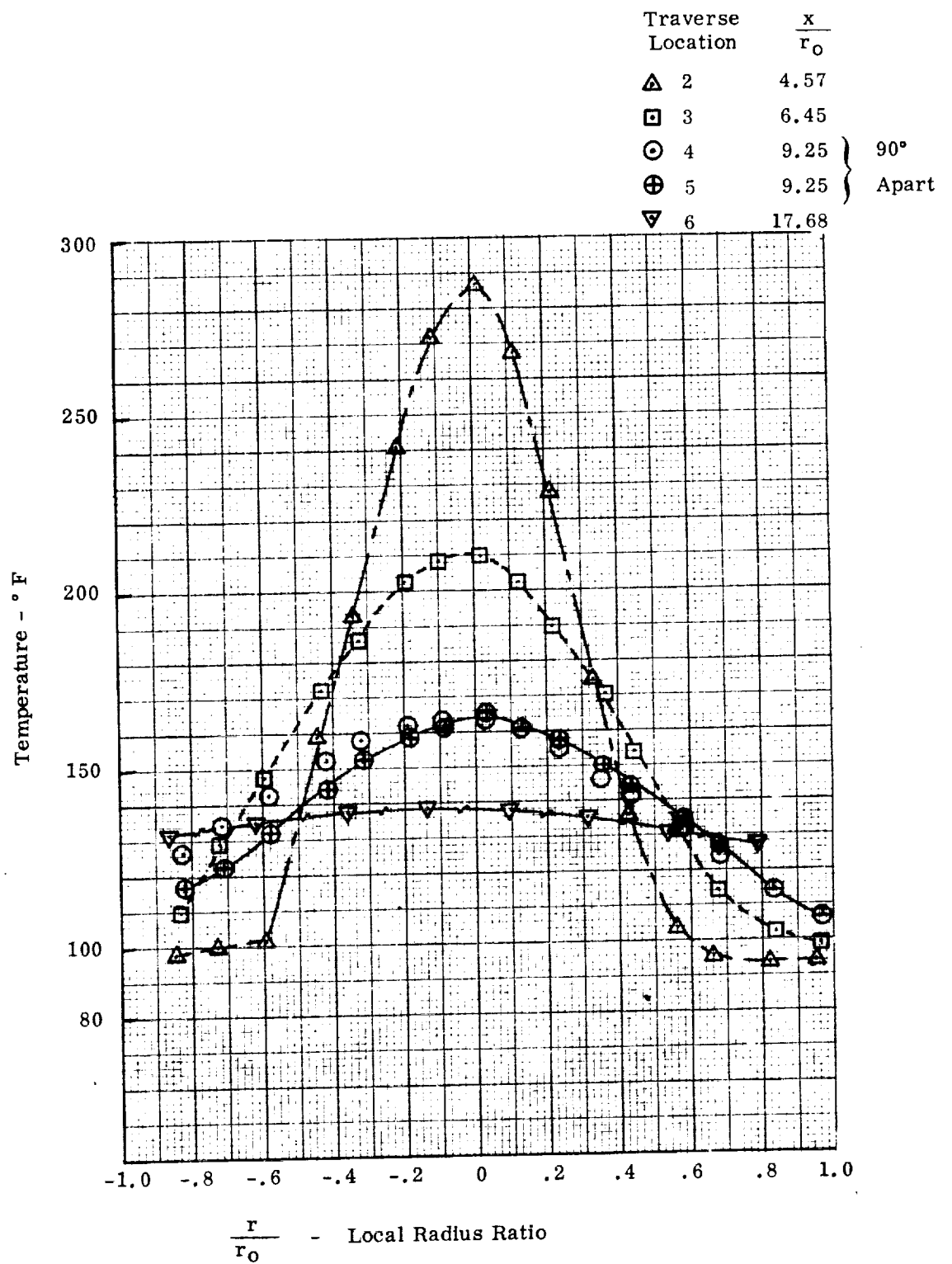


Figure 8 Measured Velocity Profiles in Mixing Tube

Traverse Location	$\frac{x}{r_0}$
\triangle 2	4.57
\square 3	6.45
\odot 4	9.25
\oplus 5	9.25
∇ 6	17.68

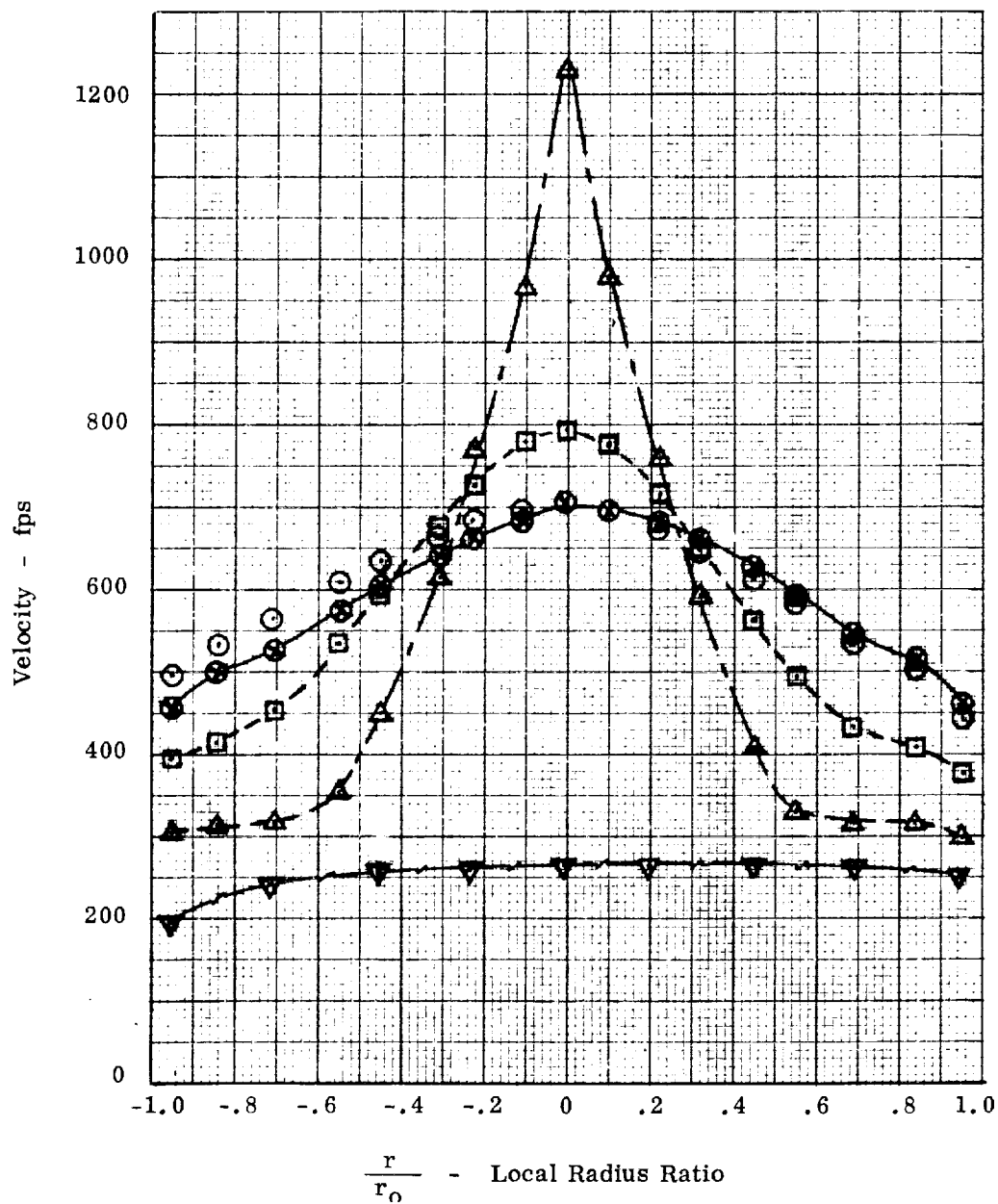


Figure 9 Measured Temperature Profiles in Mixing Tube

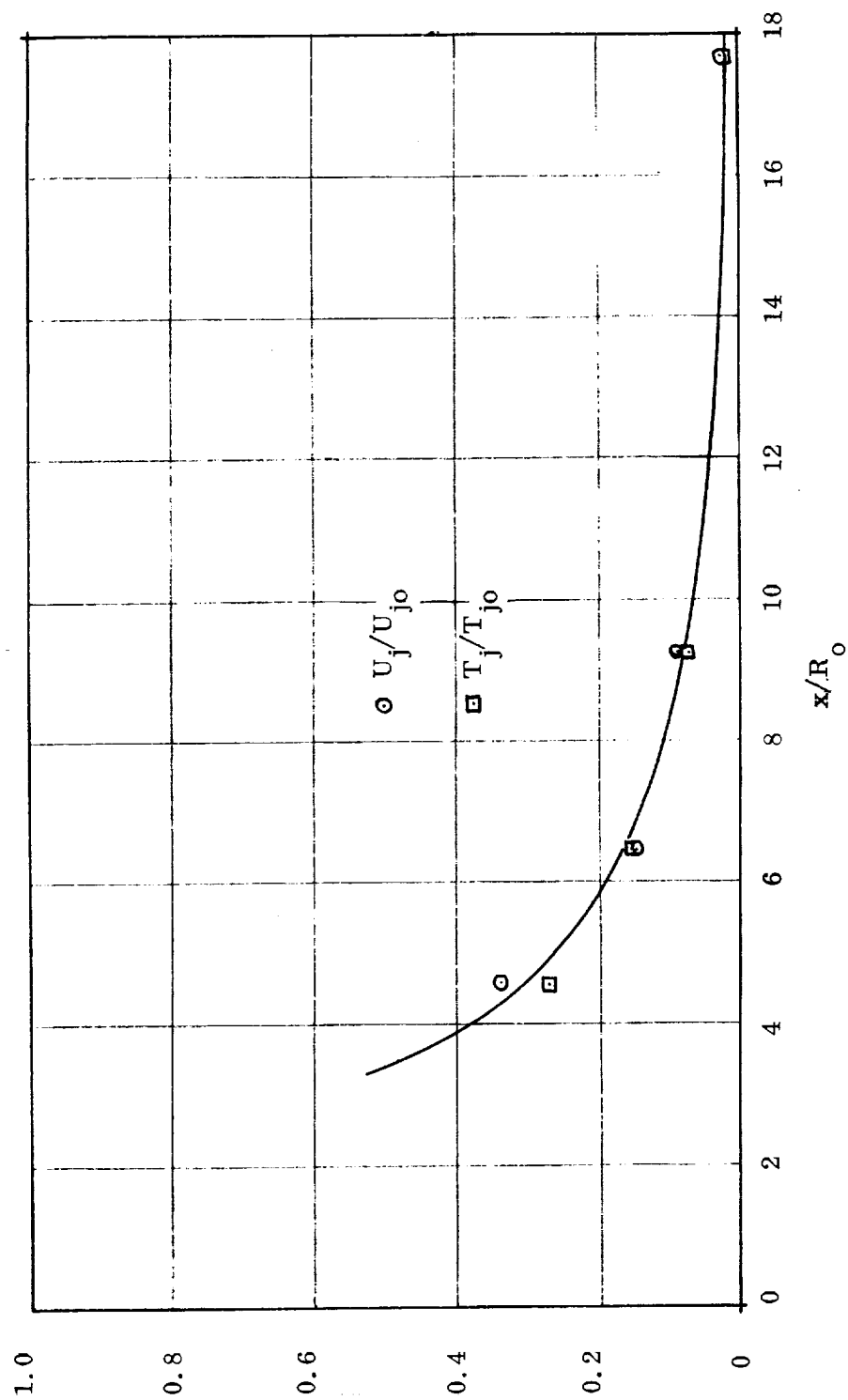


Figure 10. Variation of Centerline Temperature and Velocity along the Mixing Tube (Test Results)

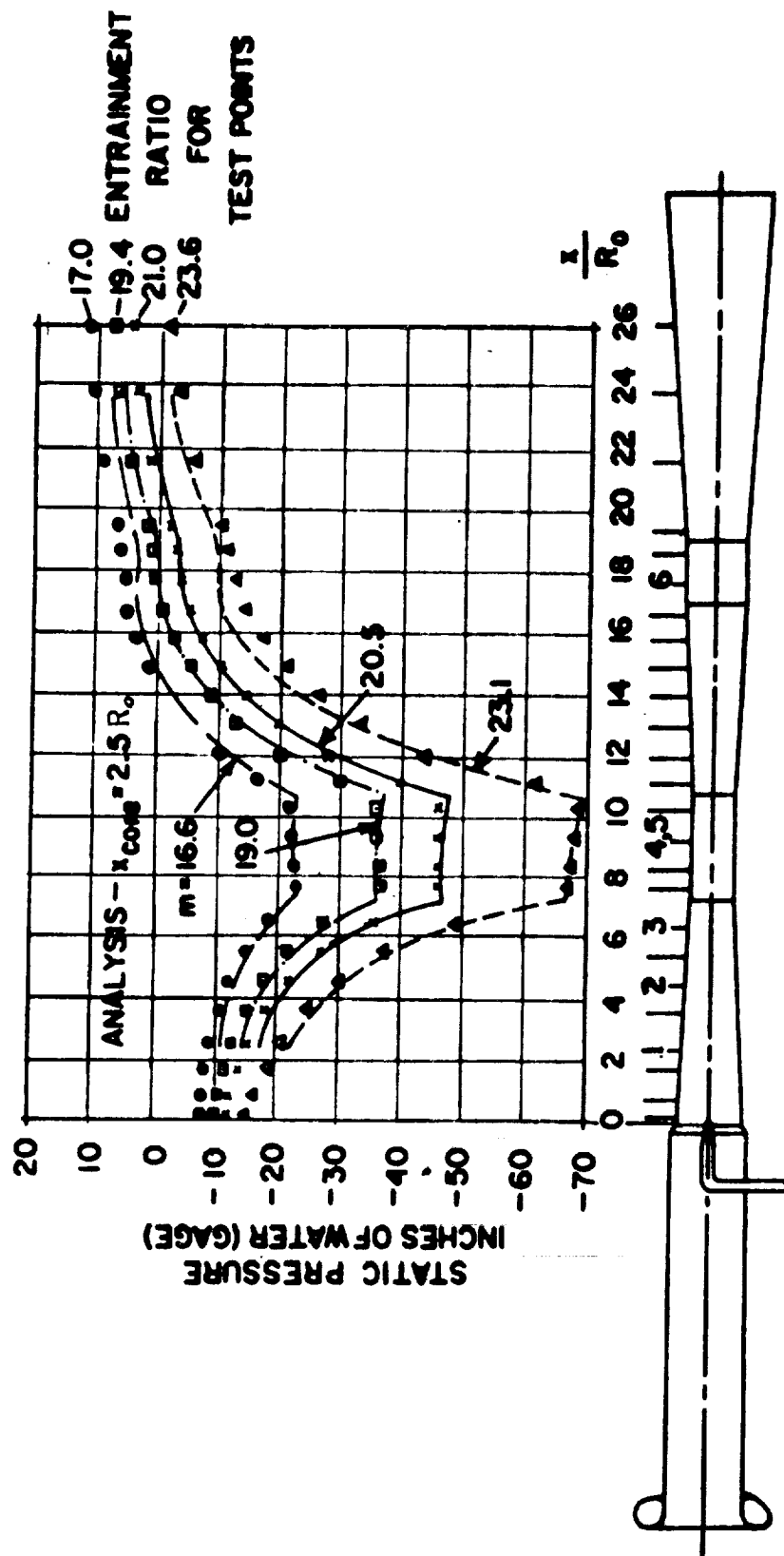


Figure 11 Comparison of Analytical and Experimental Mixing Tube Static Pressure Variations ($x_{core} = 2.5$, entrainment reduced by 2%)

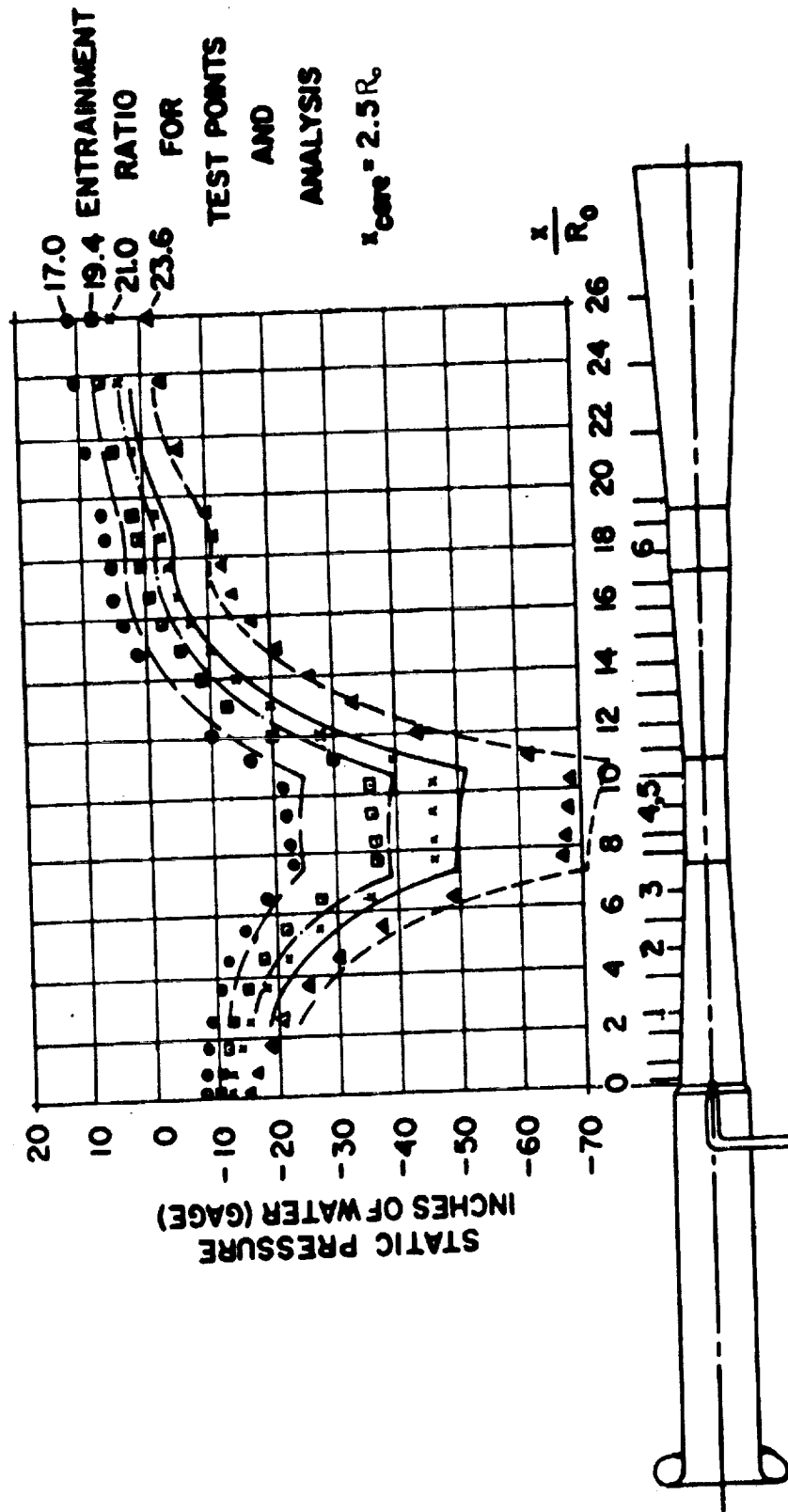


Figure 12 Comparison of Analytical and Experimental Mixing Tube Static Pressure Variations ($x_{core} = 2.5 R_0$, secondary flow from bellmouth calibration)

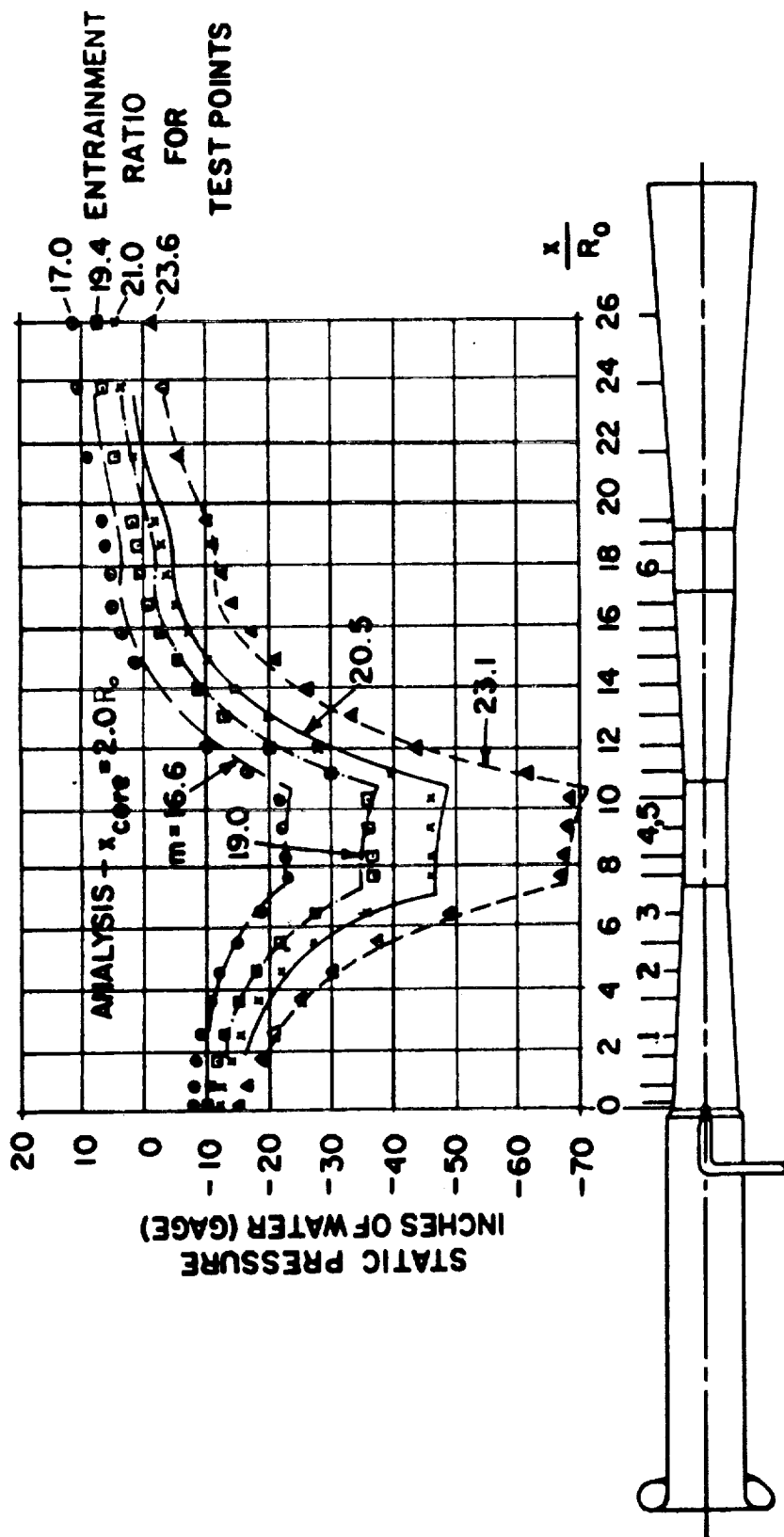


Figure 13 Comparison of Analytical and Experimental Mixing Tube Static Pressure Variations ($x_{core} = 2.0$, entrainment reduced by 2%)

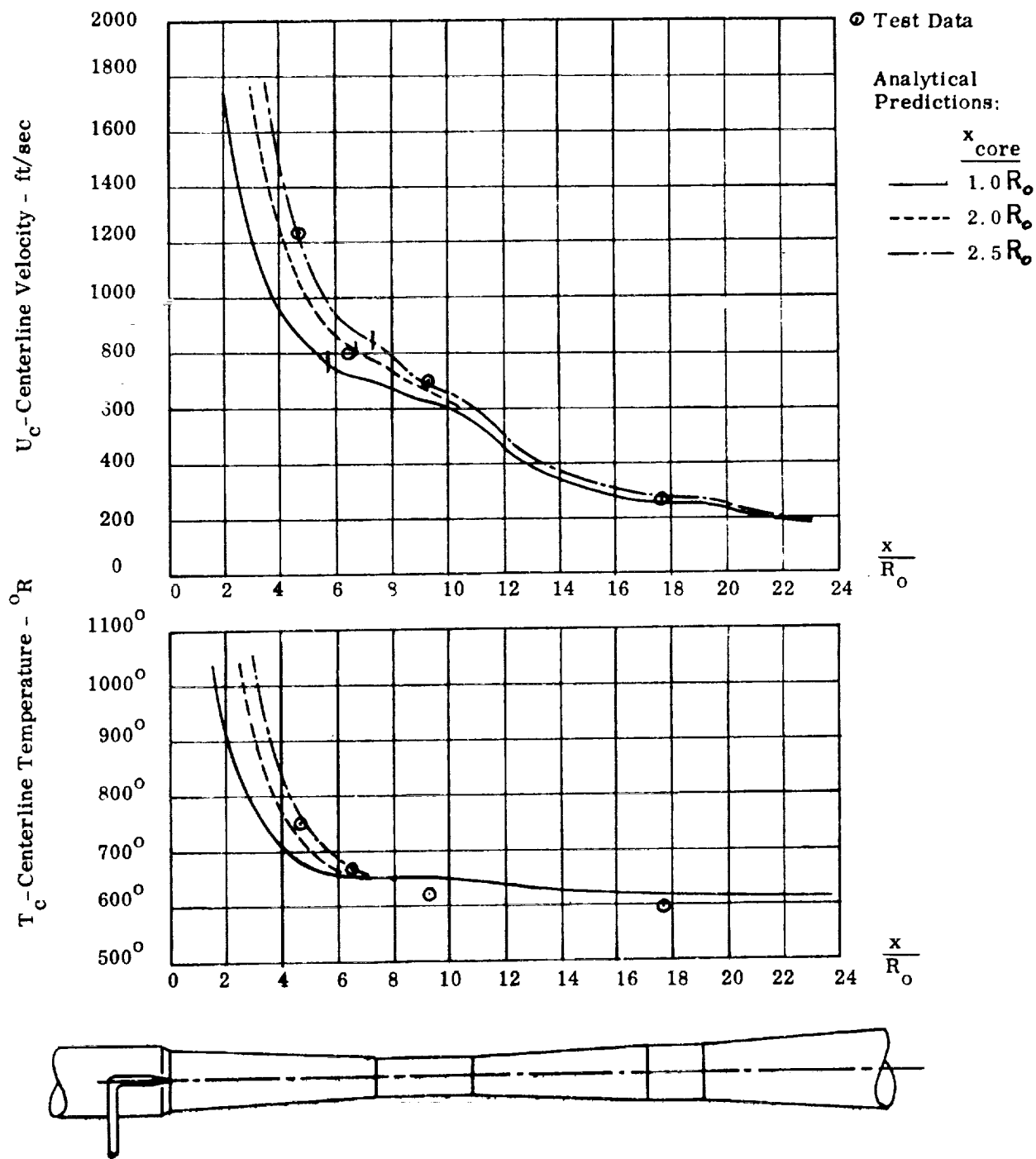


Figure 14 Comparison of Analytical and Experimental Values of Centerline Temperature and Velocity Along the Mixing Tube

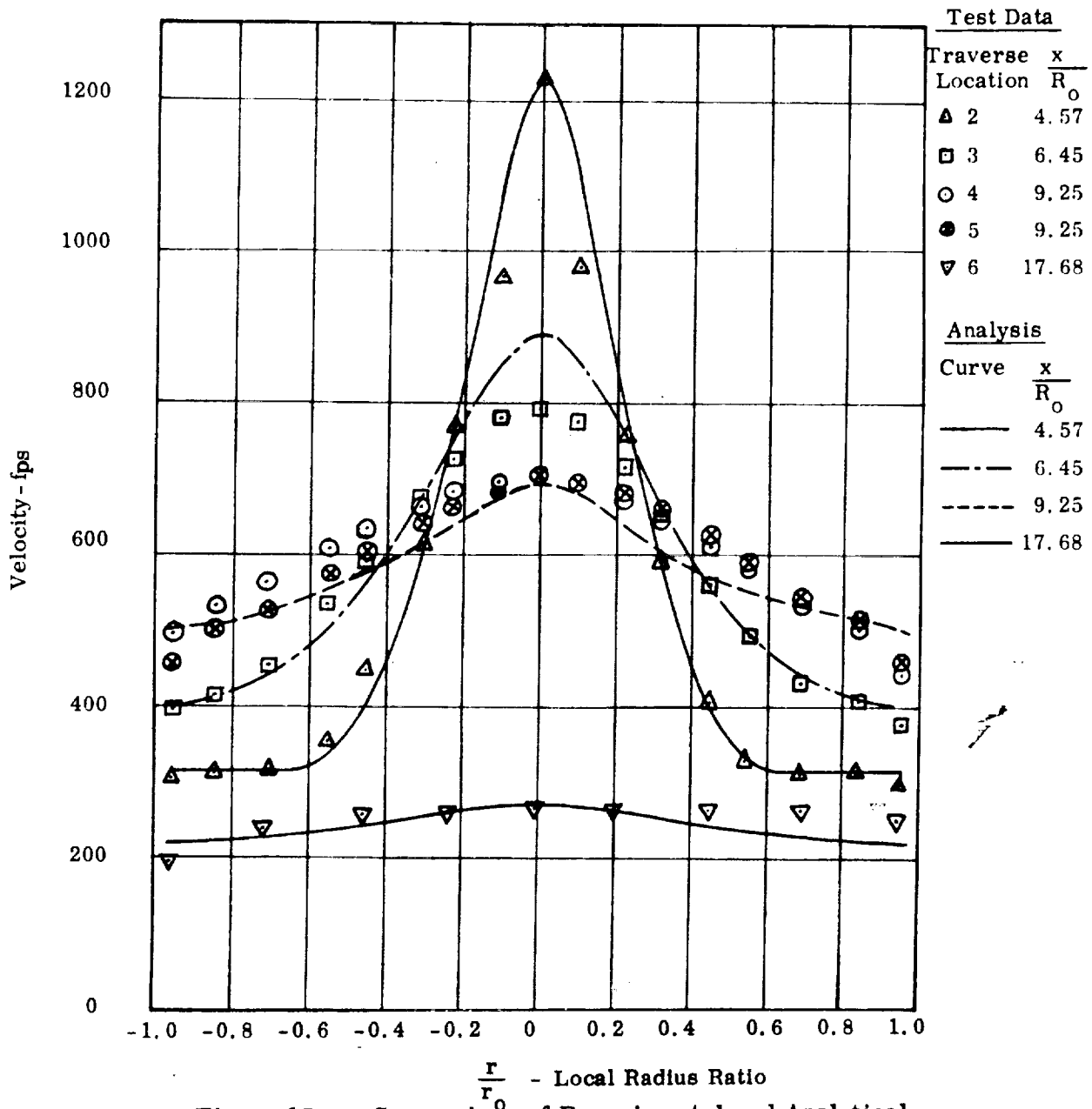


Figure 15 Comparison of Experimental and Analytical Velocity Profiles

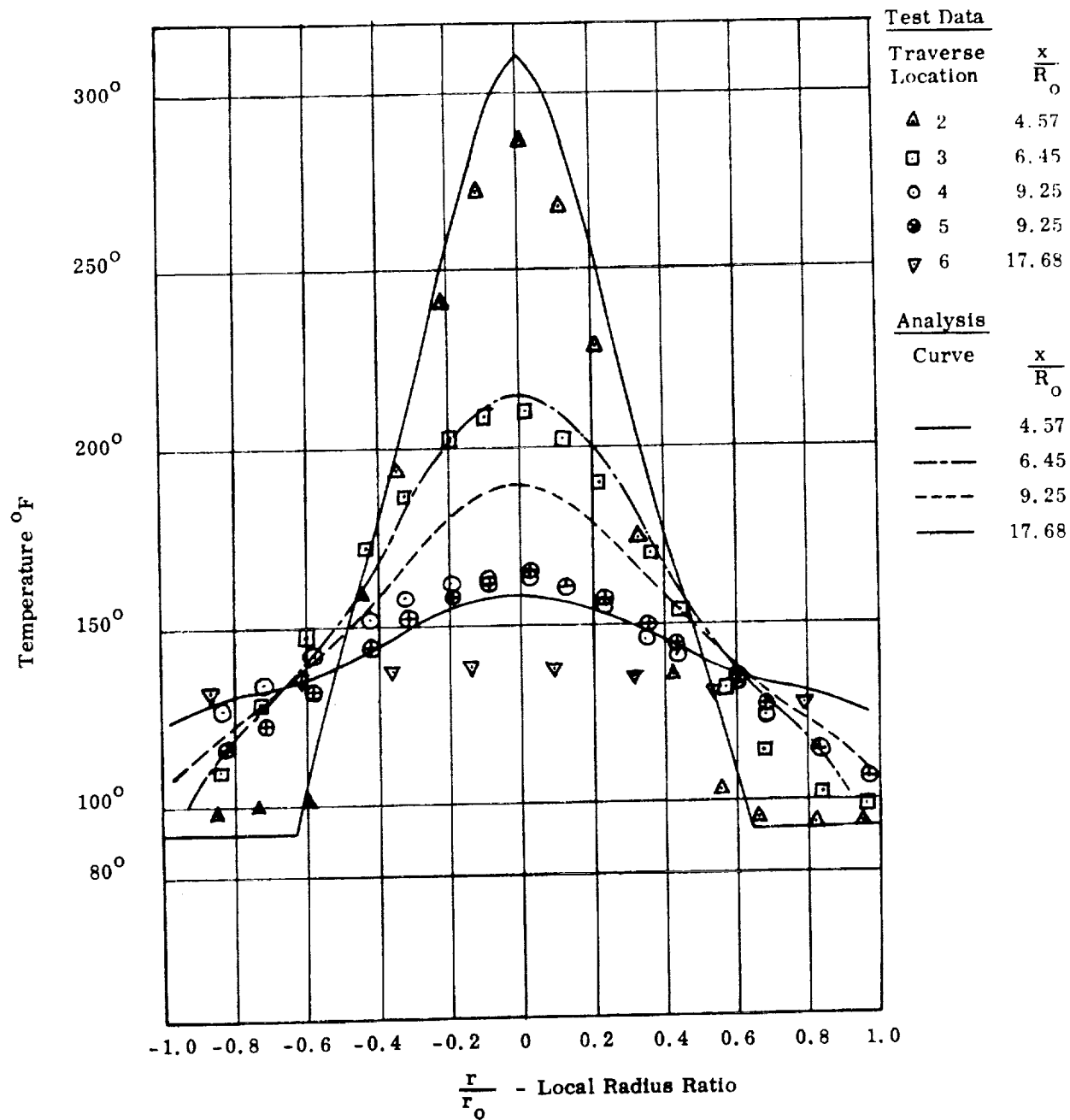


Figure 16 Comparison of Experimental and Analytical Temperature Profiles

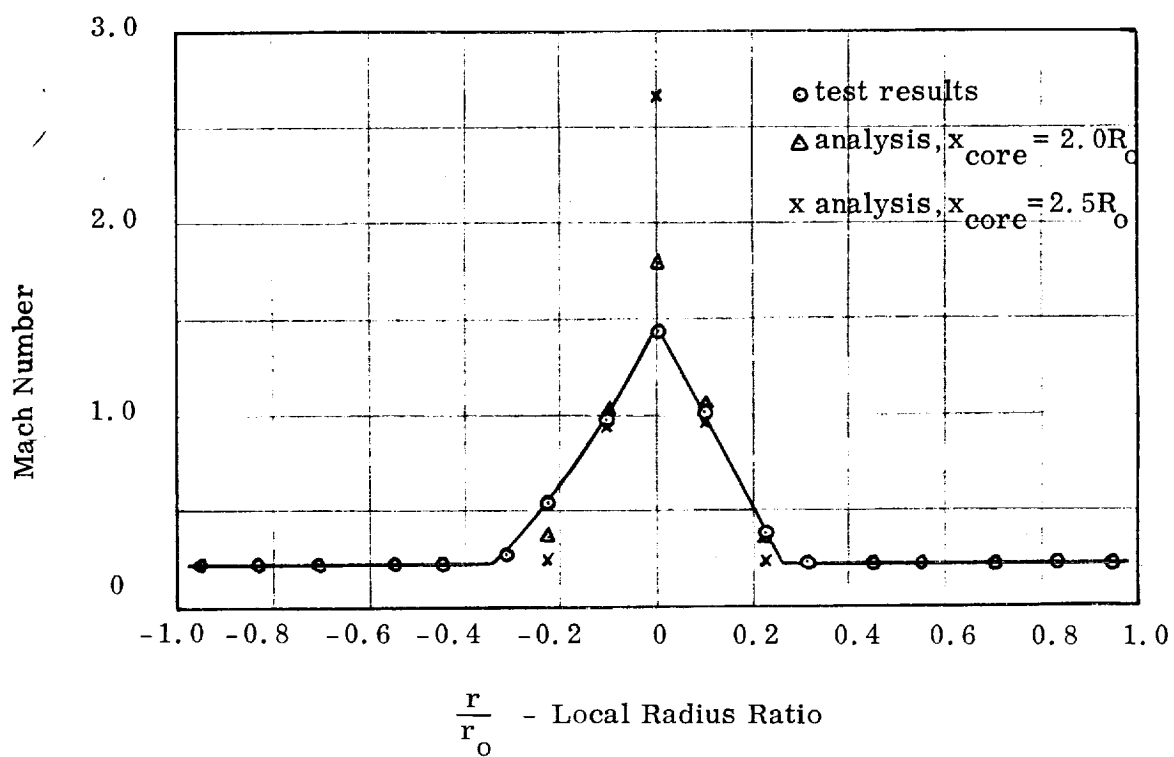


Figure 17. Comparison of "Measured" and Predicted Mach Number Profiles at Traverse Station 1, $\frac{x}{R_o} = 2.51$

